Algorithms for Passive Localization and Tracking

ALGORITHMS FOR PASSIVE LOCALIZATION AND TRACKING

by

THURAIAPPAH SATHYAN, B.Sc.Eng., M.A.Sc.

A Thesis

Submitted to the School of Graduate Studies

in Partial Fulfilment of the Requirements

for the Degree

Doctor of Philosophy

McMaster University

DOCTOR OF PHILOSOPHY (2008) MCMASTER UNIVERSITY

(Electrical and Computer Engineering) Hamilton, Ontario, Canada

TITLE: **Algorithms for Passive Localization and Tracking**

AUTHOR: Thuraiappah Sathyan

B.Sc.Eng.

University of Peradeniya

Peradeniya, Sri Lanka, 2001

M.A.Sc.

McMaster University

Hamilton, Ontario, Canada, 2003

SUPERVISOR: Dr. T. Kirubarajan

NUMBER OF PAGES: xv, 152

To Amma, Meesai, Vasee and Thiva

Abstract

This thesis considers passive localization and tracking. Here, *passive* refers to passive observations — the type of observations for which the full position estimate of the target cannot be obtained using a single measurement, like those are from a sonar. Hence, localizing or tracking targets based on these measurements calls for the use of multiple sensors. This poses a different set of challenges to tracking with passive observations as opposed to active observations where full target position is available from a single measurement.

We identify different issues that are related to passive localization and tracking and propose algorithmic solutions to these problems. We consider the angle of arrival (AOA), which is the passive measurement that is often considered in target tracking and time difference of arrival (TDOA) as representative passive measurements to illustrate our algorithms. Whereas, the AOA measurements from different sensors can be considered independent, TDOA measurements, on the other hand, are not independent. That is, they are correlated. We would, however, like to note that the proposed algorithms can be applied with straightforward, but simple, modifications to other types of passive measurements.

In particular, this thesis provides solutions to the following problems. First, it provides efficient and improved algorithms to the data association problem when

tracking with multiple passive synchronous sensors. These solutions are based on the assignment formulation. Whereas one of the algorithms proposed, the gated assignment algorithm, uses the validation gates to reduce the computational cost, the other is a new extension to the multidimensional assignment algorithm that associates the measurements directly to the tracks. This is called the $(S+1)$-D assignment-based data association, where S is the number of synchronous sensors available in the tracking system. An approximation to this new $(S+1)$-D algorithm is also presented.

In literature one finds algorithms to localize a single target using TDOA measurements. None of these algorithms considered the issues that might arise in tracking the localized targets. This thesis provides a framework to localize and track targets based on TDOA measurements. The localization algorithm uses a formulation based on the sensor-emitter geometry. This formulation is considered as a constrained optimization problem and two relaxation-based algorithms are provided to solve this optimization problem. The assignment-based data association provides an additional challenge because the TDOA measurements are correlated. This problem is identified and a solution is provided by modifying the calculation of the association cost.

Finally, this thesis also provides an efficient algorithm to form AOA mono tracks using the fast Fourier transform (FFT) and the assignment algorithm. Formation of the mono tracks is very useful in distributed tracking and is the well-known direction of arrival tracking problem in the signal processing community.

Acknowledgements

I would like to take this opportunity to thank all those who helped me in various ways during the preparation of this thesis. First, I would like to thank my supervisor, Dr. T. Kirubarajan, for his guidance and suggestions that helped me very much during my research. Next I would like to mention the valuable suggestions and advice of my supervisory committee, namely, Dr. S. Shirouspour, Prof. J. Reilly, and Dr. J. Peng. Thank you all.

My appreciation also goes to all the instructors in the ECE Department whose courses on various subjects helped me a lot in my research. The knowledge I gained from these courses greatly helped me understand the research papers and conduct my own research. Specially, I would like to mention Dr. T. Davidson for he helped me very much to pass the hardest course that I encountered at Mac — Engineering Optimization.

Special thanks goes to Dr. Abhijit Sinha — a post doctoral fellow at my laboratory — for all the help he extended. It was really a pleasure working with you, Abhijit. I would also like to thank my fellow students in my laboratory, not only for all the discussions that helped me a lot in my research, but also for the good times that we had. I felt being at home while with you guys.

Furthermore, I would like to thank all the administrative staff of the ECE Department. Specially, Cheryl Gies, the ever helpful graduate secretary. Also, thank you to Helen Jachna (the lady with money), Cosmin Coroiu and Terry Greenlay (the network guys).

Lastly, I would like to thank my family, Amma, Meesai, Vasee and Thiva, for without your love, encouragement, and continued support, I would not have achieved what I have achieved in my life. I am really proud to be a son, nephew, and a brother of yours.

Thank you again to all those who are mentioned here and for all those whom I might have forgot to mention.

List of Abbreviations

AOA	Angle of arrival
DOA	Direction of arrival
DTFT	Discrete-time Fourier transform
EKF	Extended Kalman filter
GNN	Global nearest neighbor
GPB	Generalized pseudo Bayesian
IMM	Interacting multiple model
JPDA	Joint probabilistic data association
JVC	Jonker, Volgenant, and Castanon
KF	Kalman filter
ML	Maximum likelihood
MLE	Maximum likelihood estimation
NN	Nearest neighbor
PDA	Probabilistic data association
pdf	Probability density function
QCQP	Quadratically constraint quadratic program
RMSE	Root mean square error
SDP	Semi-definite program

TDOA	Time difference of arrival
UKF	Unscented Kalman filter
ULA	Uniform linear array

Contents

List of Tables

List of Figures

Chapter 1

Introduction

Target tracking is an old problem. The origins of it can be traced to the eighteenth century. Primary interest in that period was astronomy where astronomers attempted to determine the orbits of the planets. Recent interest in tracking can be traced back to the mid twentieth century with applications such as ballistic missile defense and orbital vehicle tracking. These recent developments are fueled primarily by military applications, especially during the cold war era. Lately, some civilian applications of target tracking have become relatively important. These include air traffic control (due to the large growth in civilian aviation and the resulting traffic congestion near major airports [38, 68]) and highway vehicle surveillance (motivated by current interest in intelligent transportation systems [22, 56]).

The objective of target tracking is to collect sensor data and partition them into sets of observations or tracks that are produced by the same targets [12]. Once the partition has been made and confirmed, parameters of interest, which depends on the application, can be estimated for each track.

Modern target tracking systems traditionally used radars to observe the environment. Radar development is a matured field [90]. Radars operate by emitting specialized signals and form measurements from the signals that return after impinging targets. Since, radars use their own signal to obtain measurements they fall in the category of active sensors.

Passive sensors refer to the type of sensors that do not use any signals of their own. They listen to the environment for emissions from the targets and form their measurements from the signals received. Recent advances in computer technology have led to sophisticated signal processing methods that have greatly improved the capability of passive sensors [12]. Passive sensors include infrared search and track sensors, passive sonar [94], and time of arrival sensors. Localizing and tracking targets from passive sensor measurements has several important applications in many fields.

For example, electronic intelligence (ELINT), which includes all the aspects involved in remote sensing and processing of data from radars and other hostile sensors in order to obtain information about the capabilities of these sensors [98], uses passive sensors to achieve its objectives. In fact, electronic support measure (ESM) sensors that are a subset of ELINT provide passive measurements. Another important application is search and rescue operations. For example, the arrival times from a mobile phone at different base stations can be used to localize a phone in an emergency (E-911 service in North America) [80]. Further, in the mobile communications industry, localization of mobile terminals allows the provisioning of location-based services. Another potential application is the intelligent transportation systems [79].

Radars usually measure the range and azimuth of the targets in the environment. It is easy to localize a target with the range and azimuth measurements of radars. Various algorithms can then be used to track the localized targets. The passive sensors, on the other hand, usually do not measure the position of the targets directly. An example is the passive sonar, which measures the angle of arrival (AOA) of a target. Hence, it is not possible to localize a target from a single measurement. As a result, in order to localize a target one is required to employ multiple sensors. Use of multiple sensors adds a different set of challenges to the tracking algorithms.

1.1 Motivation

This thesis is concerned with algorithm development for localization and tracking with passive measurements, i.e., the type of measurements that do not provide the full target position in a single measurement. As discussed in the previous section, tracking using passive measurements has gained attention in recent years due to the advancements in signal processing techniques. Passive measurements are either used to complement radar measurements or are used exclusively to track targets. Since a single passive measurement would not localize a target (as is the case with a single radar measurement), tracking with passive measurements brings forward a different set of challenges to the tracking algorithms.

One of the important challenges is that since a single passive measurement does not provide the target position, in order to localize and track targets one typically needs to employ multiple sensors. Use of multiple sensors, as will be discussed later, complicates the all important data association problem. Further, it also brings forward challenges to the system designer in terms of the selection of an appropriate

tracking architecture.

Another challenge is in localizing a target from multiple passive sensor measurements. Typically, the relationship between the target position and a passive measurement is nonlinear. Hence, once the measurements that originated from a certain target are identified, estimating the position of the target (for example, maximum likelihood estimate (ML)) that caused these measurements usually results in a nonlinear optimization problem. This would result in a high computational cost. In addition, in order to get a close enough solution an initial estimate that is in the neighborhood of the actual solution is required. Such an initial solution is not available in practical scenarios.

Furthermore, when multiple sensors are used in the tracking system measurements from different sensors could be either correlated or uncorrelated. For example, whereas AOA measurements from different sensors can be considered uncorrelated, time difference of arrival (TDOA) measurements are typically correlated. This is because TDOA measurements are calculated with respect to a reference sensor and the presence of the common reference sensor measurement noise makes these measurements correlated. Whether the type of passive measurement is correlated or not presents different sets of challenges to the tracking system.

Due to the importance and recent interest in tracking targets with passive measurements, this thesis tries to solve some important challenges related to passive measurement tracking.

The single most important problem in any target tracking system is data association. The question of measurement origin uncertainty is answered by the data association step, that is, it identifies the measurements that have originated from a particular target. Except in the ideal case of tracking a single target with sensors

having unity detection probability and in an environment with no false returns, one always encounters the problem of data association. The complexity of the data association is influenced by the tracking scenario such as, whether single target or multitarget tracking, whether single sensor or multiple sensors are employed, whether the measurements are passive or active, or a combination of these and other issues. It is the hardest when tracking multiple targets using multiple synchronous[1] passive sensors [12].

This thesis considers the problem of data association in the multiple synchronous passive sensor tracking systems. It proposes two assignment-based algorithms that provide improved performance at a reduced computational cost compared to a previous algorithm. These improvements, both in performance and computational efficiency, are due to the fact that we consider the prior information of the targets that are being tracked in solving the data association. Besides, an approximation of one of the algorithms resulted in a much faster algorithm. We tested these algorithms on simulated, but realistic, scenarios with multiple synchronous AOA sensors and the results indicate the superior performance of these algorithms.

We also consider the problem of tracking using TDOA measurements. This study also serves as a representative example of tracking with correlated measurements. In the literature one could find several TDOA localization algorithms [17, 36, 41, 86, 92]. These algorithms considered localizing a single target in an ideal scenario, i.e., with no measurement origin uncertainty. Further, they did not consider tracking issues. It has to be noted that even to localize a target, in real-world scenarios, one needs to solve the data association problem.

[1]Here, synchronous sensors means that observation times of all the sensors are synchronized.

This thesis provides an algorithmic framework to localize and track multiple unknown numbers of targets using TDOAs. In this framework, we solve the problem of measurement origin uncertainty by using the assignment-based algorithms introduced in this thesis. One challenge posed by the TDOA measurements is that measurements from different sensors are correlated. The data association algorithms developed in this thesis are modified to account for the fact that the TDOA measurements are correlated. This framework is general in that it can be used with any type of correlated measurements (with certain simple modifications).

Localization of an emitter is required to initialize a track from passive sensor measurements. Typically, in order to localize a target from passive measurements one will find the ML estimate from the measurements from different sensors. The relationship between the target position and the passive measurements are typically nonlinear. Hence, the resulting ML estimation involves nonlinear search techniques. Such search techniques usually require a starting point that is close to the actual solution. In some cases, it may be possible to obtain a starting point. For example, when localizing an emitter in the two dimensional plane using AOA measurements, any two AOA measurements would intersect at a point and this point can be used as the starting point of the search algorithm.

With TDOA measurements, however, it is not possible to obtain such a starting point. This, combined with the fact that the ML TDOA localization results in a highly nonlinear function, makes it very difficult to find the ML estimate of the target position when using TDOA measurements. It is possible, however, to come up with a formulation based on the sensor-target geometry for the TDOA localization problem. We view this formulation as a nonconvex optimization problem and provide solutions based on semidefinite relaxation. The results are compared with

some of the other popular techniques found in literature.

This thesis also provides an efficient algorithm to form mono angle only tracks. Mono tracks refer to the tracks that consist of angles that originated from the same target. This is also the problem known as direction of arrival (DOA) tracking in the signal processing community. Formation of mono tracks is very important in distributed tracking systems. This is because instead of sending all the measurements from a sensor platform, which would require very high bandwidth, only the mono tracks can be sent to the central fusion center for further processing. The algorithm presented in this thesis, uses the discrete-time Fourier transform (DTFT) to form angle measurements from the response of a uniform linear array. The angle measurements thus obtained are associated using the multiframe association algorithm developed in this thesis to form mono tracks.

1.2 Contributions of the thesis

This thesis provides efficient and improved solutions to some of the challenging problems in passive localization and tracking. In the section, we summarize the contributions of this thesis briefly in the order of appearance.

- Data association is an important problem in target tracking. It presents additional challenges when tracking with passive sensors. This thesis provides two efficient and improved assignment-based algorithms to solve the data association problem. In addition, an approximation to one of the algorithms results in an extremely fast algorithm.

- This thesis also presents a framework to track an unknown number of targets using TDOA measurements. The framework proposed is general in that it

can be used with any correlated measurements with some straightforward modifications.

- The important problem of data association in the TDOA tracking framework provides an additional challenge because of the fact that the TDOA measurements are correlated. This issue is identified and solved by modifying the assignment-based association algorithms proposed in this thesis to account for the correlation between measurements from different sensors.

- Localizing using TDOA measurements is a difficult task due to the highly nonlinear nature of the TDOA equations. A formulation based on the sensor-emitter geometry results in a nonconvex optimization problem. This thesis presents two semidefinite programming techniques to solve the highly nonlinear TDOA equations.

- This thesis also presents a new efficient algorithm to form angle only tracks (i.e., mono tracks) from the signals received by a uniform linear array.

1.3 Organization of the thesis

This thesis is organized as follows. The next chapter provides an introduction to multitarget tracking. It identifies various functional units of a tracking system and gives a brief review of these units and popular algorithms that are used. It also discusses different tracking architectures for tracking with passive sensors.

Chapter 3 explains the multidimensional assignment-based algorithm that can

be used to solve the data association problem in synchronous passive sensor tracking systems. This chapter also identifies some problems with this solution, especially, computational issues. Chapter 4 proposes computationally efficient and improved assignment-based algorithms for passive sensor data association. The proposed algorithms can be used with any passive measurements. The effectiveness of these algorithms, however, is tested in simulated AOA tracking scenarios. Results of these simulations are provided in Chapter 5.

Chapter 6 considers the problem of tracking with time difference of arrival (TDOA) measurements. Various studies in literature have focused mainly on the problem of localizing a single emitter using TDOA. Tracking issues have not been considered in these studies. This chapter proposes an algorithmic framework to track multiple unknown numbers of emitters in practical scenarios. Chapter 7 proposes two solutions to solving the nonlinear TDOA equations. Solution to the TDOA equations is required in order to localize an emitter. These solutions are based on a geometry-based formulation of the problem.

Chapter 8 presents a new efficient algorithm to form angle only mono tracks using a uniform linear array. This algorithm uses fast Fourier transform (FFT) to get the angle of arrivals from the array response and uses assignment-based data association algorithm to form mono tracks.

Finally, Chapter 9 summarizes the thesis and provides directions for future work.

1.4 Terminology

We would like to clarify some of the terms that are used in various contexts in this thesis in order to avoid any confusion to the reader.

This thesis is about *passive* localization and tracking. Here, passive stands for passive measurements. This refers to the type of measurements for which the full position estimate of a target cannot be determined from a single measurement. For example, AOA and TDOA are passive measurements. *Active* measurements are the ones that allow one to determine the full target position from a single measurement (e.g., radar measurements). This terminology should not be confused with active and passive sensors. Active sensors emit signals and form measurements from the returns of these signals. Passive sensors, on the other hand, listens the environment and forms the measurements from the emission of the source. It has to be noted that most of the times passive sensors provide passive measurements[2].

Since with passive measurements the target position is not available from a single measurement, usually measurements from multiple sensors are required to get the position estimate of a target. We define localization as the process of obtaining the position estimate from multiple passive sensors. Tracking may refer to the continuous estimation of the positions of a target as it moves. Hence, tracking could simply be considered as localizing a target continuously. Tracking considered in this thesis, however, is more general than continuous localization. It could estimate quantities other than position (such as velocity and acceleration). As a result, it presents other challenges such as the measurement origin uncertainty.

Finally, we use AOA and TDOA to explain our algorithms. These quantities are typically measured by passive sensors. Since passive sensors listen to the emission of the targets to form measurements, we use the words emitter and source interchangeably with target.

[2]This need not be the case always. For example, active sonar could provides AOA measurements.

1.5 Related publications

The contents of this thesis were published at different conferences and journal articles at various times. The following are the publications related to this thesis.

Journal publications

- **T. Sathyan**, A. Sinha, and T.Kirubarajan, "Efficient Assignment-Based Algorithms for Data Association for Passive Multisensor Tracking", *IEEE Transactions on Aerospace and Electronic Systems, submitted,* Sep. 2007.

- **T. Sathyan**, A. Sinha, and T.Kirubarajan, "Passive Geolocation and Tracking of Multiple Unknown Number of Emitters", *IEEE Transactions on Aerospace and Electronic Systems*, Vol. 42, No. 2, pp. 740 – 750, Apr. 2006.

Conference publications

- **T. Sathyan**, A. Sinha, and T. Kirubarajan, "Computationally efficient assignment - based algorithms for data association for tracking with angle-only sensors", *Proc. SPIE Signal and Data Processing of Small Targets, presented,* San Diego, CA, Aug. 2007.

- **T. Sathyan** and T. Kirubarajan, "Two Solutions to the Localization Using Time Difference of Arrival Problem", *Proc. SPIE Signal Processing, Sensor Fusion, and Target Recognition XVI,* Vol. 6567, pp. 656704, Orlando, FL, Apr. 2007.

- **T. Sathyan**, A. Sinha, and T.Kirubarajan, "Passive Geolocation and Tracking of Multiple Unknown Number of Emitters", *Proc. SPIE Signal Processing, Sensor*

Fusion, and Target Recognition XIV, Vol. 5809, pp. 1 – 11, Orlando, FL, Apr. 2005.

- **T. Sathyan**, T. Kirubarajan, and A. Sinha, "Geolocation of Multiple Emitters in the Presence of Clutter", *Proc. SPIE Signal Processing, Sensor Fusion, and Target Recognition XIII*, Vol. 5429, pp. 66 – 76, Orlando, FL, Apr. 2004.

Chapter 2

Multiple Target Tracking

In this chapter we provide an introduction to tracking systems and elaborate on the issues of passive sensor tracking systems. Also we discuss various architectures for passive sensor tracking.

2.1 Generic tracking system

A generic high level block diagram of a tracking system is shown in Figure 2.1. It consists of sensors, signal processing unit, and tracking unit. Sensors scan the environment in which they operate and gather information from diverse sources. Traditionally, in tracking systems, the sensor is the radar. Radar development is a

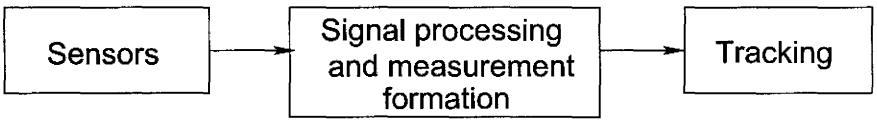

Figure 2.1: Generic tracking system.

matured field. Recent improvements, however, in sensor technology has resulted in a plethora of other sensors. This includes acoustic sensors such as active or passive sonar, infrared sensors, TV sensors, and imaging sensors. Modern tracking systems typically use multiple types of sensors to improve the tracking performance.

The output from the sensor is processed in the signal processing unit and measurements are formed. The type of measurement produced differs according to the sensor type. For example, if the sensor is radar the range and the azimuth constitute a measurement. Certain radars also measure the range-rate. Radar measurements are delivered to the tracking unit as a measurement vector. If the sensor is passive sonar, the measurement is typically the angle of arrival (AOA) of the signal, which is reported to the tracking unit as a scalar.

The tracking unit is the one that is responsible for estimating the parameters of interest of the targets in the region that is being monitored. This involves several important functions that are explained in the next section. A tracking unit is followed by a presentation logic that displays the output of this unit to the system user. It has to be noted that the tracking unit should be able to handle multiple types of sensors. Further, in distributed tracking systems the above system model may be replicated at different locations. In such systems, the tracking unit should also have the capabilities to provide and accept feedback to and from other tracking units to improve overall tracking performance.

This thesis is concerned with issues relating to the tracking unit. We now provide some details of the functionalities of the tracking unit.

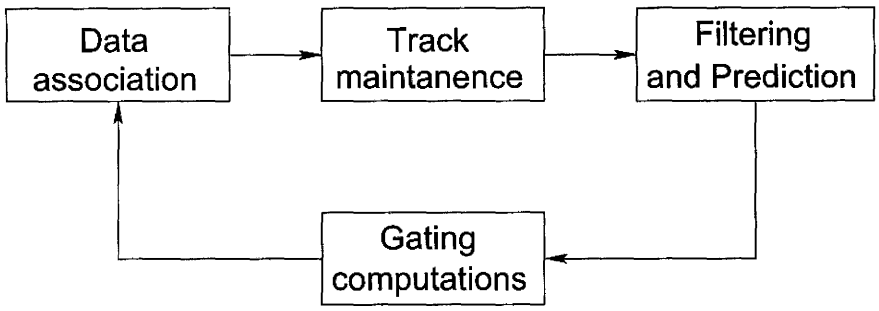

Figure 2.2: Tracking process.

2.2 Functional units of a tracking system

Figure 2.2 identifies the main functional units of a tracking system. It is assumed here that the tracks have already been initialized. The data association block takes the tracks from the previous scan and measurements from the current scan, and decides the origin of these measurements, i.e., decides from which target a given measurement originated. The data association problem is the most challenging task in target tracking. Track maintenance is responsible for making decisions such as initiation and deletion of the tracks. Once the observations are assigned to tracks the filtering process updates the tracks with the corresponding observations. It also predicts the tracks to the next scan, since predicted tracks are required in gating computations. Gating improves the efficiency and performance of data association algorithms. We will now describe these functional units in detail starting with filtering algorithms.

2.3 Filtering

Filtering is the process of estimating the state of a dynamic system. The reason for the use of the term "filter" is because the process amounts to obtaining the "best estimate" from the noisy observations amounts to "filtering out" the noise [6]. The state actually defines the parameters of interest. For example, an air-traffic controller would be interested in knowing the position and velocity of an airplane at any given time in order to provide instructions to the pilot. Hence, in this case position and velocity would constitute the state.

Filtering process is a well-studied field and one can find numerous algorithms in literature. Conventional tracking systems use the Kalman filter (KF) [46, 47] to update the tracks. The KF is the optimal estimator (in mean squared sense) for linear Gaussian stochastic systems and its performance would degrade if these assumptions are not met. Extended Kalman filter (EKF) can be used to account for nonlinearity to a certain extent [6]. When tracking with time difference of arrival (TDOA) measurements we, however, found that the unscented Kalman filter (UKF) [43, 95] gave a better performance in comparison to the EKF. Sequential Monte Carlo filters — best known as particle filters — promise to provide a better solution even in the case of nonlinear non Gaussian environments [1, 82]. The basic idea in the particle filter is to use a number of independent random variables called particles, sampled directly from the state space, to represent the posterior probability, and update the posterior by involving the new observations [39]. The computational cost of a particle filter could, however, be higher compared to KF or its variants.

Conventionally, from KF to particle filter, the development of the tracking filters assumed a single model for the target motion dynamics. When the targets start

to maneuver the performance of these filters invariably degrades. This is because characterizing the motion of a maneuvering target using a single motion model does not capture the actual nature of the maneuvers. In such cases, multiple model estimation techniques provide better performance. In the multiple model technique, several constituent filters (e.g., KF) tuned to different motion models are run in parallel. The outputs of these filters are probabilistically combined to get an estimate for the target state.

Several multiple model techniques are available in literature. These include: generalized pseudo-Bayesian estimator of first order (GPB1), GPB2, and the interacting multiple model (IMM) estimator. The IMM estimator gives the performance of the GPB2 at the computational cost of GPB1[1]. Hence, it is the one that is always used in modern systems. In this thesis, we used either the KF or the UKF (depending on whether the state-space model is linear or nonlinear) as the constituent filter of the IMM estimator to track the targets. We will now provide a brief description of these algorithms. A simulation study performed in [50] answers the question of when to use an IMM estimator over a KF.

2.3.1 The Kalman filter

The KF is the best linear minimum mean square error (LMMSE) filter, and is the optimal under linear Gaussian assumptions [6]. It assumes a single model for the state evolution (though it could be time-varying), and recursively updates the state based on the observations of current scan. Assume the following linear Gaussian

[1]Note that while the performance of the GPB2 is superior to that of GPB1, the computational cost of it is comparatively higher. In fact, if the target motion can be modeled using N motion models, the GPB1 and IMM requires N filters to run in parallel whereas the GPB2 requires N^2 filters.

model for the target motion

$$X^k = F^{k-1}X^{k-1} + v^k \tag{2.1}$$

In the above, X^k denotes the target state at time k and F^{k-1} is the state transition matrix that governs the state transition from time $k-1$ to k. v^k is the process noise that is assumed to be Gaussian distributed with zero mean and known covariance.

Measurements are assumed to be linear functions of the state and are modeled by

$$z^k = H^k X^k + w^k \tag{2.2}$$

where z^k is the measurement at time k and H^k is the measurement function. The measurement noise w^k is also assumed to be Gaussian distributed with zero mean and known covariance. The state and measurement models given by (2.1) and (2.2), respectively, describe a linear Gaussian stochastic system for which KF is the optimal estimator.

A single cycle of the KF starts with the state estimate $\hat{X}^{k-1}$ and the corresponding covariance P^{k-1} of the previous cycle, and updates them (using the measurement at time k) to the present cycle. Each cycle of the KF has two steps — prediction and update.

Prediction step

The state prediction at time k refers to applying the state function operator F^{k-1} to the previous state estimate $\hat{X}^{k-1}$ to obtain the predicted state $\hat{X}^{k|k-1}$. That is

$$\hat{X}^{k|k-1} = F^{k-1}\hat{X}^{k-1} \tag{2.3}$$

It is easy to show that the covariance associated with the state prediction error is given by

$$P^{k|k-1} = F^{k-1}P^{k-1}F^{k-1^T} + Q^k \tag{2.4}$$

where $Q^k = E\{v^k(v^k)^T\}$ is the process noise covariance matrix.

The predicted measurement at time k is obtained by applying the measurement function operator H to the predicted state, $\hat{X}^{k|k-1}$, i.e.,

$$\hat{z}^{k|k-1} = H^k\hat{X}^{k|k-1} \tag{2.5}$$

The measurement prediction error covariance is given by

$$S^k = H^kP^{k|k-1}H^{k^T} + R^k \tag{2.6}$$

where $R^k = E\{w^kw^{k^T}\}$ is the measurement noise covariance.

Update step

In this step, the current measurement z^k is used to update the state prediction and the associated covariance. According to the minimum mean square error (MMSE) criterion, at time k, the state estimate $\hat{X}^k$, based on measurements obtained up to time k, is the conditional mean. It can be shown [6] that the conditional mean can be calculated using

$$\hat{X}^k = \overline{X} + W^k\nu^k \tag{2.7}$$

where $\overline{X}$ is the prior (unconditional) mean, which is replaced by the state prediction $\hat{X}^{k|k-1}$, ν^k is the innovation at time k, which is defined as the measurement residual

$$\nu^k \triangleq \tilde{z}^{k|k-1} = z^k - \hat{z}^{k|k-1} \tag{2.8}$$

and W^k is the Kalman gain given by

$$W^k = P^{k|k-1} H^{k^T} \left(S^{k|k-1}\right)^{-1} \tag{2.9}$$

Hence, the state update equation will reduce to

$$\hat{X}^k = \hat{X}^{k|k-1} + P^{k|k-1} H^{k^T} \left(S^{k|k-1}\right)^{-1} \nu^k \tag{2.10}$$

The covariance associated with the updated state is

$$P^k = P^{k|k-1} - W^k S^{k|k-1} W^{k^T} \tag{2.11}$$

This completes one cycle of the KF.

2.3.2 The unscented Kalman filter

The KF assumes linear Gaussian state-space model and provides the optimal recursive state estimation in such a case. The performance of the KF would degrade or even the filter would diverge if the linear Gaussian assumption is not met. The EKF is an extension of the KF to handle nonlinear measurement process and/or nonlinear target dynamics. In the EKF the state is approximated by a Gaussian random

variable, and it is propagated through a first-order linear approximation[2] of the nonlinear state-space. This approximation may not be adequate for some nonlinear systems and as a result large errors could be introduced in the estimates. Or, in some cases the filter may diverge.

The UKF attempts to provide a solution to the approximation issues of the EKF. In the UKF, the state distribution is represented by a Gaussian random variable as in the EKF, but it is now specified using a minimal set of carefully chosen sample points [95]. These points are selected using the unscented transformation.

Consider the following nonlinear state-space model that describes the target dynamics and the measurement process.

$$\begin{aligned} X^k &= f^{k-1}(X^{k-1}) + v^k \\ z^k &= h^k(X^k) + w^k \end{aligned} \tag{2.12}$$

In the above equation $f(.)$ and $h(.)$ are the nonlinear state and measurement functions. Other quantities are similar to that defined in the pervious section. One cycle (from time $k-1$ to k) of the UKF starts with the mean $\hat{X}^{k-1}$ and covariance P^{k-1} of the state estimate from the previous cycle. Using the unscented transformation, a set of $2L+1$ *sigma points* are calculated as follows. (L denotes the dimension of the state.)

$$\begin{aligned} \mathcal{X}_0^{k-1} &= \hat{X}^{k-1} \\ \mathcal{X}_i^{k-1} &= \hat{X}^{k-1} + \sqrt{(L+\lambda)P^{k-1}} \quad i = 1, \ldots, L \\ \mathcal{X}_i^{k-1} &= \hat{X}^{k-1} - \sqrt{(L+\lambda)P^{k-1}} \quad i = L+1, \ldots, 2L \end{aligned} \tag{2.13}$$

[2]It is also possible to use a second-order linear approximation to propagate the state. This, however, would increase the computational cost, and may induce numerical instability because of the Hessian calculations required.

where $\lambda = \alpha^2(L + \kappa) - L$ is a scaling parameter. The constant α determines the spread of the sigma points around $\hat{X}^{k-1}$. The secondary scaling parameter κ is usually set to 0 or $3 - L$.

These sigma points are now propagated through the nonlinear state function to get the predicted sigma points. That is

$$\mathcal{X}_i^{k|k-1} = f^{k-1}(\mathcal{X}_i^{k-1}) \quad i = 0, 1, \ldots, 2L \tag{2.14}$$

The mean and covariance of the propagated sigma points are approximated using a weighted sample. These are given, respectively, by

$$\begin{aligned} \overline{\mathcal{X}}^{k|k-1} &= \sum_{i=0}^{2L} W_i^m \mathcal{X}_i^{k|k-1} \\ \mathcal{P}^{k|k-1} &= \sum_{i=0}^{2L} W_i^c \left(\overline{\mathcal{X}}^k - \mathcal{X}_i^{k|k-1}\right)\left(\overline{\mathcal{X}}^k - \mathcal{X}_i^{k|k-1}\right)^T \end{aligned} \tag{2.15}$$

where the weights are given by

$$\begin{aligned} W_0^m &= \frac{\lambda}{\lambda + L} \\ W_0^c &= \frac{\lambda}{\lambda + L} + (1 - \alpha^2 + \beta) \\ W_i^m &= W_i^c = \frac{1}{2(\lambda + L)} \quad i = 1, \ldots, 2L \end{aligned} \tag{2.16}$$

Based on this mean and covariance another set of sigma points are now redrawn.

$$\begin{aligned} \mathcal{X}_0^k &= \overline{\mathcal{X}}^{k|k-1} \\ \mathcal{X}_i^k &= \overline{\mathcal{X}}^{k|k-1} + \sqrt{(L + \lambda)\mathcal{P}^{k|k-1}} \quad i = 1, \ldots, L \\ \mathcal{X}_i^k &= \overline{\mathcal{X}}^{k|k-1} - \sqrt{(L + \lambda)\mathcal{P}^{k|k-1}} \quad i = L + 1, \ldots, 2L \end{aligned} \tag{2.17}$$

The newly redrawn sigma points are then propagated through the measurement equation.

$$z_i^{k|k-1} = h^k(\mathcal{X}_i^k) \quad i = 0, 1, \ldots, 2L \tag{2.18}$$

The mean of the predicted measurements $z_i^{k|k-1}$, $i = 0, 1, \ldots, L$ is approximated using the following weighted sum.

$$\overline{z}^k = \sum_{i=0}^{2L} W_i^m z_i^{k|k-1} \tag{2.19}$$

where the weights W_i^m are defined previously.

The gain of the filter is defined as

$$K = \mathcal{P}_{\mathcal{X}z}\mathcal{P}_{zz}^{-1} \tag{2.20}$$

where

$$\begin{aligned} \mathcal{P}_{zz} &= \sum_{i=0}^{2L} W_i^c \left(z_i^{k|k-1} - \overline{z}^k\right)\left(z_i^{k|k-1} - \overline{z}^k\right)^T \\ \mathcal{P}_{\mathcal{X}z} &= \sum_{i=0}^{2L} W_i^c \left(\mathcal{X}_i^k - \overline{\mathcal{X}}^k\right)\left(z_i^{k|k-1} - \overline{z}^k\right)^T \end{aligned} \tag{2.21}$$

The calculation of the updated state and covariance is similar to that of the KF. The updated state is given by

$$\hat{X}^k = \overline{\mathcal{X}}^{k|k-1} + K(z_k - \overline{z}^k) \tag{2.22}$$

and associated covariance is given by

$$P^k = \mathcal{P}^{k|k-1} + K\mathcal{P}_{zz}K^T \tag{2.23}$$

These are carried over to the next cycle.

2.3.3 The IMM estimator

The IMM estimator introduced in [15] has entrenched itself as the estimator of choice when it comes to tracking maneuvering targets. The effectiveness of the IMM estimator can be attributed to the fact that it assumes multiple models for the possible target state evolution. It then finds an overall estimate as a probabilistic combination (i.e., soft decision) of the individual filter estimates without making a hard decision as to which model is in effect at a particular time. Another important aspect of the IMM estimator is that the weights (or the mode probabilities) given to the individual filter estimates are calculated dynamically based on the likelihood function from the individual filters. In the KF or its variants, the input to the filter at time k is the estimate $\hat{X}^{k-1}$ at time $k-1$. In the IMM estimator, however, the input to each filter at time k is a probabilistic combination of the $(k-1)$th estimate of all the filters, thus accounting for all possible model transitions from time $k-1$ to time k.

One cycle of the IMM estimator and the corresponding mathematical expressions are presented next. For more details see [6]. It is assumed that there are N interacting filters running in parallel and that the Markov chain transition probability matrix is known[3].

[3]The IMM estimator is not very sensitive to errors in the assumed model transition probability values. In real large-scale tracking problems [96], where these probabilities or the KF parameters

Step 1: Mixing probability calculation

Each cycle of the IMM estimator starts with the estimates of the individual filters from the previous cycle. These N estimates are mixed probabilistically, giving N estimates that are the initial conditions for the N filters in the current cycle. The weights given in the mixing step are the mixing probabilities. The mixing probability $\mu_{i|j}^{k-1|k-1}$ is the probability that model M_i was in effect at time $k-1$ (previous cycle) given that model M_j is in effect at time k (current cycle) and all the measurements up to time $k-1$ (denoted by Z^{k-1}). That is

$$\begin{aligned}\mu_{i|j}^{k-1|k-1} &= P\left\{M_i^{k-1}|M_j^k, Z^{k-1}\right\} \\ &= \frac{1}{\bar{c}_j} P\left\{M_j^k|M_i^{k-1}, Z^{k-1}\right\} P\left\{M_i^{k-1}|Z^{k-1}\right\} \\ &= \frac{1}{\bar{c}_j} p_{ij}\mu_i^{k-1} \quad i,j = 1,2,\ldots,N\end{aligned} \tag{2.24}$$

where p_{ij} is the (i,j)th element of the Markov chain transition probability matrix. These mode transition probabilities are assumed to be time invariant and independent of the base state. In addition

$$\mu_i^{k-1} = P\left\{M_i^{k-1}|Z^{k-1}\right\} \tag{2.25}$$

is the probability that the state corresponds to model M_i at time $k-1$ termed mode probability and $\bar{c}_j$ is the normalizing constant given by

$$\bar{c}_j = \sum_{i=1}^{N} p_{ij}\mu_i^{k-1} \quad j = 1,2,\ldots,N \tag{2.26}$$

such as process noise variances are not known exactly, the IMM estimator has been proven to be very effective.

Step 2: Mixing

With the mixing probabilities as weights, estimates of all the filters at time $k-1$ are mixed to produce the initial estimates for each filter at time k:

$$\hat{X}_{0j}^{k-1} = \sum_{i=1}^{N} \hat{X}_i^{k-1} \mu_{i|j}^{k-1|k-1} \quad j = 1, 2, \ldots, N \tag{2.27}$$

where $\hat{X}_i^{k-1}$ is the estimate of the filter matched to model M_i at time $k-1$. The covariance associated with X_{0j}^{k-1}, $j = 1, 2, \ldots, N$ is given by

$$P_{0j}^{k-1} = \sum_{i=1}^{N} \mu_{i|j}^{k-1|k-1} \left[P_i^{k-1} + \left(\hat{X}_i^{k-1} - \hat{X}_{0j}^{k-1} \right) \left(\hat{X}_i^{k-1} - \hat{X}_{0j}^{k-1} \right)^T \right] \tag{2.28}$$

Step 3: Mode probability update

The initial conditions obtained in Step 2 and the measurement at time k are input to each filter. In addition to the updated state estimate and the associated covariance, each filter outputs its likelihood. The likelihood Λ_j^k of the filter matched to model M_j at time k is given by

$$\Lambda_j^k \triangleq p\left(z^k | M_j^k, Z^{k-1} \right) \quad j = 1, 2, \ldots, N \tag{2.29}$$

where z^k is the measurement at time k.

The updated mode probability is defined by

$$\mu_j^k \triangleq P\left\{ M_j^k | Z^k \right\} \tag{2.30}$$

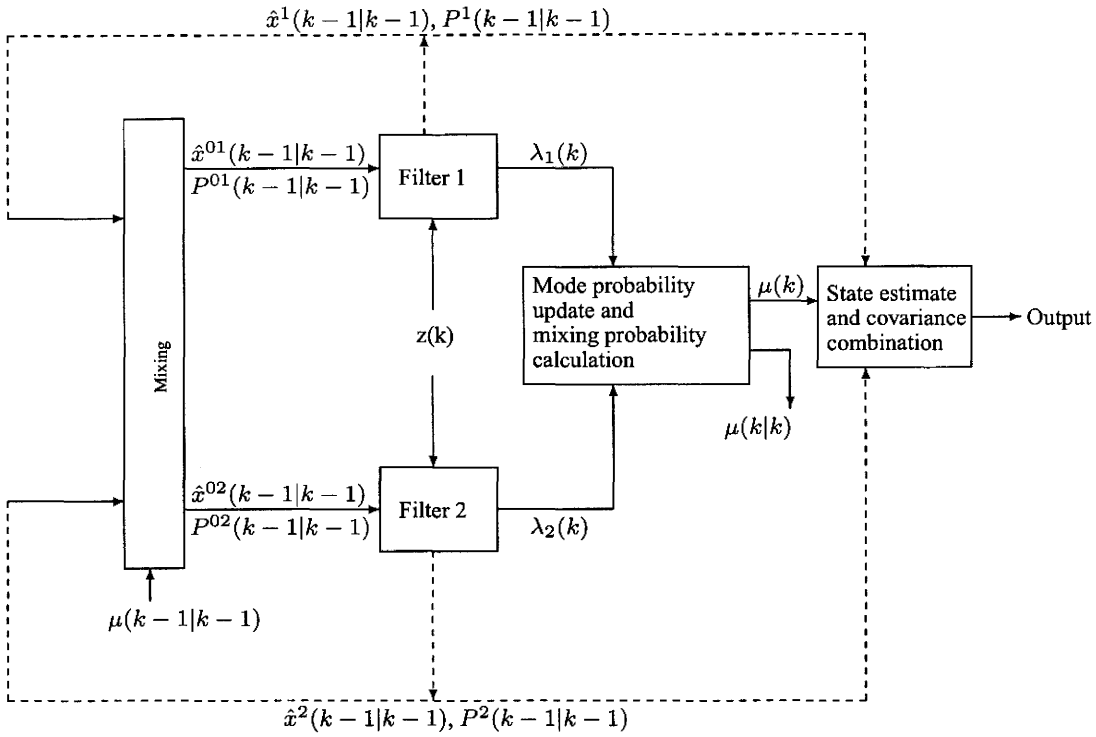

Figure 2.3: One cycle of the IMM estimator consisting of two filters.

It can be shown [6] that the mode probability can be updated using

$$\mu_j^k = \frac{1}{c}\Lambda_j^k \bar{c}_j \quad j = 1, 2, \ldots, N \tag{2.31}$$

where $\bar{c}_j$ is defined in (2.26), and the normalization constant c is given by

$$c = \sum_{j=1}^{N} \Lambda_j^k \bar{c}_j \tag{2.32}$$

Step 4: Overall estimate

The overall state estimate of the IMM estimator is calculated as a weighted sum of individual filter estimates (i.e., a Gaussian mixture)

$$\hat{X}^k = \sum_{j=1}^{N} \mu_j^k \hat{X}_j^k \tag{2.33}$$

and the covariance associated with the above estimate is given by

$$P^{k+1} = \sum_{j=1}^{N} \mu_j^k \left[P_j^k + \left(\hat{X}_j^k - \hat{X}^k \right) \left(\hat{X}_j^k - \hat{X}^k \right)^T \right] \tag{2.34}$$

Note that the above overall estimate is only for the purposes of the user of the IMM estimator. It does not affect the next cycle of the estimator. A block diagram of the IMM estimator consisting of two filters is given is Figure 2.3.

2.4 Gating computations

Gating is a technique that is used to eliminate the unlikely track-to-measurement pairings [12]. A gate is typically setup around the predicted measurement, and any observation that falls within the gate is considered for track update. How the observations that falls within the gate are used to update the track is dependent upon the data association technique used. All data association techniques, however, use gates to reduce the computational cost.

Let z^k denote the measurement vector at scan k. The measurement residual or

the innovation ν^k is given by

$$\nu^k = z^k - h\left(\hat{X}^{k|k-1}\right) \tag{2.35}$$

where $h(.)$ is the nonlinear measurement function. If the measurement function is linear then

$$\nu^k = z^k - H\hat{X}^{k|k-1} \tag{2.36}$$

where H is the measurement matrix. In either case, the residual covariance matrix S^k is defined by

$$S^k = HP^{k|k-1}H^T + R \tag{2.37}$$

There are two types of gates that are used commonly. They are the rectangular gate and the ellipsoidal gate.

2.4.1 Rectangular gate

This is probably the simplest gating technique that one could have. Let ν_l^k denote the lth element of the innovation vector. Then the gating requirement is said to be satisfied if all the elements of the innovation vector satisfy

$$|\nu_l^k| \leq K_{Gl}\sigma_r \tag{2.38}$$

where σ_r is the residual standard deviation as defined in terms of the measurement and prediction variances. That is

$$\sigma_r = \sqrt{\sigma_o^2 + \sigma_p^2} \tag{2.39}$$

K_{Gl} above denotes the gating coefficient and details about selecting an appropriate value for it is discussed in [11].

2.4.2 Ellipsoidal gate

A measurement is said to satisfy the ellipsoidal gate, if the following holds true:

$$\nu^{k^T} S^{k^{-1}} \nu^k \leq \tau \tag{2.40}$$

The gate threshold τ determines the probability with which the true measurement will be within the gate. The threshold τ is obtained using the chi-square distribution tables since the quadratic form that defines the gate is chi-squared distributed with the number of degrees of freedom equal to the dimension of the measurement.

2.5 Data association

Usually the sensors or the signal processing step does not identify the target from which a certain measurement originated. These units decide whether there is a detection and if so what is the corresponding value (in the measurement space) of the event that caused the detection. In order to update a track, however, one needs to know the measurement that originated from the target corresponding to that track. This is fulfilled by the data association step. That is, data association is the process that solves the important problem of measurement origin uncertainty.

Except in the ideal case of unity probability and no false alarms, which, of course, is not practical, one encounters the data association problem. In tracking

a single target in clutter with a non-unity probability of detection the data association can be considered *easy*. In such a case one needs to decide whether a given measurement originated from the target or a false alarm. In practical multitarget/multisensor tracking scenarios, the data association, however, becomes more challenging, since now the tracks start to compete for measurements.

The problem of data association was first identified in [89], and a number of algorithms have been developed to solve the data association problem. Details of various algorithms to solve the data association problem can be found in various books [3, 5, 11, 12, 31] and in numerous papers including the basic works [2, 30, 35, 81, 88, 89]. We will now briefly review some of the commonly used data association algorithms.

2.5.1 Nearest neighbor

The nearest neighbor (NN) method is the simplest data association algorithm one could have. It is also the one that provides worst performance. In this approach one selects the measurement that is closest to the predicted measurement. That is the innovation or the residual of all the measurements is calculated for a given track and the one with the smallest value is used to update that track. The performance of this algorithm may be acceptable in a single target tracking problem with low false alarm rate, or in multitarget tracking where the targets are well-separated and again with low false alarm rate. Due to its poor performance in realistic scenarios, this algorithm is not used in practice.

2.5.2 Global nearest neighbor

This is the most widely used algorithm for data association. It is similar to the NN technique in that it just maintains the single most likely hypothesis. The global nearest neighbor (GNN) algorithm, however, finds the measurement-to-track pairs such that the global cost of all the possible associations is minimized. The GNN technique is usually formulated as a two-dimensional (2-D) assignment problem. The resulting assignment-based data association has been demonstrated on large scale problems with hundreds of targets [96, 100].

Each track-to-measurement pair is assigned a cost, which typically is a generalized likelihood ratio. That is, the cost of assigning a track i to a measurement j — the assignment cost c_{ij} — is defined as

$$c_{ij} = \begin{cases} 0 & \text{if } i = 0 \text{ or } j = 0 \\ -\ln \frac{\Lambda(i,j)}{\Lambda(0,j)} & \text{if } -\ln(.) \leq 0 \\ \infty & \text{otherwise} \end{cases} \tag{2.41}$$

where $\Lambda(i,j)$ denotes the likelihood that measurement j came from the target corresponding to track i and $\Lambda(0,j)$ is the likelihood that the measurement came from none of the existing tracks, or in other words, it is a false alarm. The likelihood of false alarms is assumed to be uniformly probable in the surveillance region.

Track index 0 denotes a dummy track and measurement index 0 denotes a dummy measurement. They are used to account for the possibilities that a track may not have been detected in the current scan and a measurement could be a false alarm.

In order to reduce the computational load the assignment cost is calculated for only the measurement-track pairs that satisfy the gating requirements (discussed

before). The goal of the GNN technique is to find the most probable measurement-track pairs that minimize the global assignment cost such that a track is assigned at most to one measurement and a measurement is assigned to at most one track. This objective results in the following 2-D assignment problem. (It is assumed here that there are n_t number of tracks and n_m number of measurements are associated. Note also that n_t may not necessarily equal to n_m due to missed detections and false alarms.)

$$\begin{aligned} \min_{\rho_{ij}} \quad & \sum_{i=0}^{n_t} \sum_{j=0}^{n_m} c_{ij}\rho_{ij} \\ \text{subject to:} \quad & \sum_{i=0}^{n_t} \rho_{ij} = 1 \quad j = 1, 2, \ldots, n_m \\ & \sum_{j=0}^{n_m} \rho_{ij} = 1 \quad i = 1, 2, \ldots, n_t \end{aligned} \tag{2.42}$$

where ρ_{ij} is a binary variable such that

$$\rho_{ij} = \begin{cases} 1 & \text{if measurement-track pair } ij \text{ is included in the solution} \\ 0 & \text{otherwise} \end{cases} \tag{2.43}$$

The 2-D assignment problem can be solved optimally using various algorithms in (pseudo) polynomial time. Earliest assignment algorithms, such as the Hungarian method [53] were only applicable for square assignment problems (i.e., problems where $n_t = n_m$). The more advanced Munkers algorithm [58] is much faster and is applicable to rectangular problems. Newer, faster methods include Jonker, Volgenant, and Castanon (JVC) algorithm [42] as well as the auction algorithm [9]. In fact, comparison results of [45] appear to favor JVC and auction algorithms.

2.5.3 Multiscan data association

The above GNN approach assigns a single scan of data to the tracks. This may result in inaccurate associations if the targets' maneuver increases, since in such cases the predicted state may not be close to the actual target state. Better association performance can be obtained by associating the tracks with multiple scans of data rather than just a single scan.

Typically, multiscan data association is formulated as a discrete optimization problem. This idea was first proposed in [57], where the multiscan data association was considered as a 0-1 integer programming problem. Later works [25, 26, 66, 71, 72, 73, 74, 75] have extended and generalized this approach by mapping the multiscan data association problem to a generalized multidimensional assignment problem.

The multidimensional assignment formulation of the multiscan data association can be easily extended to combine a single scan, multisensor data. Combination of multisensor data is usually required in the passive sensor systems. These systems typically employ multiple sensors since passive sensors typically do not provide full position measurements. Hence, one needs to combine (associate the measurements from different sensors or measurement-to-measurement association) measurements from several sensors to get full position measurements. This thesis is concerned with passive sensor tracking and uses the multidimensional assignment formulation to solve the data association. Next chapter provides greater detail of how this is performed and identifies computational problems with this approach. Chapter 4 details computationally efficient assignment-based algorithms to solve the passive sensor data association problem.

2.5.4 Joint probabilistic data association

Before ending this chapter, we provide the basics of another technique that is commonly used to solve data association — the joint probabilistic data association (JPDA). The main difference of JPDA technique compared to the other data association solutions described earlier is that the JPDA algorithm is an *all-neighbors* approach as opposed to the *nearest neighbor* approach of other methods. That is in the nearest neighbor approaches a track is updated using only the measurement that is closest (defined in some sense) to that track. In the all-neighbors approach of JPDA all the measurements that fall within the gate of a track are used to update that track.

The all-neighbors approach to association was first proposed in [2] as probabilistic data association (PDA) under the assumption of a single target in clutter. Later results showed that PDA did not perform well in the presence of multiple targets and a modified method called joint PDA (JPDA) was derived to include the presence of multiple targets [3, 35].

In the PDA method, assume that there are N measurements within the gate of a track i. Then one could form $N+1$ hypotheses for that track. The first one (denoted $\mathcal{H}_0$) is that all the measurements are invalid, i.e., all the N measurements did not come from the target corresponding to this track. It can be shown [5] that the probability of this hypothesis is proportional to

$$p'_{i0} = \beta^N(1 - P_D P_G) \tag{2.44}$$

where P_D is the probability of detection and P_G is the probability that a correct return will fall within the track gate (typically $P_G \cong 1.0$). The extraneous return

is assumed to be Poisson distributed with density β. Similarly, probability of other hypotheses, namely jth measurement ($j = 1, 2, \ldots, N$) is valid and the rest are invalid is proportional to

$$p'_{ij} = \beta^{N-1} P_D P_G \frac{\exp(-0.5 d_{ij})}{P_G \sqrt{2\pi |S_i|}} \tag{2.45}$$

Therefore, the probabilities of these $N + 1$ hypotheses can be found using the normalization equation

$$p_{ij} = \frac{p'_{ij}}{\sum_{l=0}^{N} p'_{ij}} \quad j = 0, 1, \ldots, N \tag{2.46}$$

Using the values for p'_{ij} the following convenient form can be obtained for these probabilities.

$$p_{ij} = \begin{cases} \frac{b}{b + \sum_{l=1}^{N} \alpha_{il}} & j = 0 \\ \frac{\alpha_{ij}}{b + \sum_{l=1}^{N} \alpha_{il}} & j = 1, 2, \ldots, N \end{cases} \tag{2.47}$$

where

$$\begin{aligned} b &= (1 - P_D P_G) \beta \sqrt{2\pi |S_i|} \\ \alpha_{ij} &= P_D \exp(-0.5 d_{ij}^2) \end{aligned} \tag{2.48}$$

These probabilities are incorporated into a standard KF to update the track. The resulting filter is termed probabilistic data association filter. In the KF the prediction step would remain the same. As a result the calculation of the KF gain would remain the same. The measurement residual ν^k, for use in the update equation (2.10), is now calculated as a weighted sum of individual innovations weighted by the above

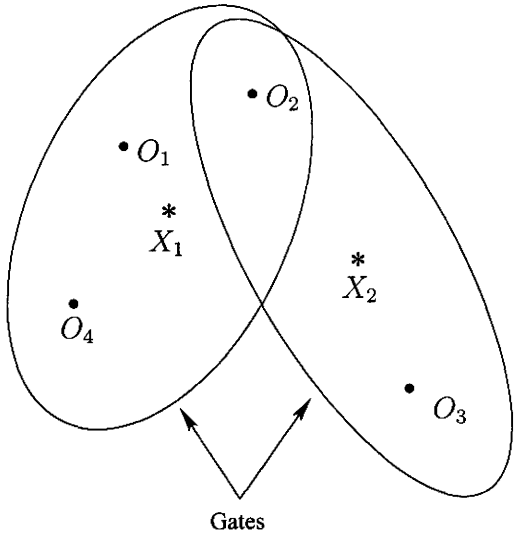

Figure 2.4: JPDA: tracks compete for observations.

probabilities. That is

$$\nu^k = \sum_{j=1}^{N} p_{ij} \nu_{ij}^k \tag{2.49}$$

where

$$\nu_{ij}^k = z_j^k - H X_i^{k|k-1} \tag{2.50}$$

It is possible to show that the covariance update equation is given by [5]

$$P_i^k = P_i^{k|k-1} - (1 - p_{i0}) W^k (S^k)^{-1} W^{K^T} + \tilde{P}^k \tag{2.51}$$

where $\tilde{P}^k$ is the weighted spread of innovation term given by

$$\tilde{P}_i^k = W^k \left[\sum_{i=1}^{N} p_{ij} \nu_{ij}^k \nu_{ij}^{k^T} - \nu^k \nu^{k^T} \right] W^{K^T} \tag{2.52}$$

The JPDA technique — the extension of PDA for multitarget scenario — is identical to the PDA except that the association probabilities are calculated over all observations and all tracks, and the calculation of these probabilities takes into account the fact that there are multiple targets present. The state estimation and covariance computation remain the same.

Consider the scenario depicted in Figure 2.4. There are two tracks whose validation gates are shown with centers at X_1 and X_2. There are four observations O_1, O_2, O_3, and O_4 within the validation gates of these tracks. The JPDA will compute a weighted residual for track X_1 based on observations O_1, O_2, and O_4 similar to the PDA weights. The weight given to O_2 will, however, be reduced to account for the fact that it is also present within the gate of track X_2. Similarly, when calculating the weighted residual for track X_2 (based on observations O_2 and O_3) the weight given for O_2 is reduced. Details of these weight calculations can be found in [5].

Several improvements to this basic JPDA have been proposed over the years. For example, to JPDA has been combined with the IMM estimator [4] and the resulting filter is denoted by IMMPDAF. The basic JPDA does not include explicit provision for track initiation or deletion. While several approaches have been proposed to handle these issues, the widely accepted ones are the IMMPDAF with "target" and "no target" modes [5], and the integrated PDA (IPDA) [60, 61, 62]. The basic JPDA has a tendency toward track coalescence for closely spaced targets [32]. In [33] a nearest neighbor PDA has been proposed to solve the track coalescence problem. A technique to select the hypotheses that could lead to track coalescence has been presented in [14]. Omitting these hypotheses from the probability calculations would reduce the coalescence problem.

A number of studies have addressed the implementation of the JPDA algorithm.

A cheap JPDA [34] has been proposed that calculates the probabilistic weighting factors approximately. Recently, a computationally efficient method to implement the exact JPDA has been proposed in [102]. Finally, JPDA logic has also been extended to handle multiple scan processing [28, 29, 83].

2.6 Multiple passive sensor system architectures

Four types of track initiation and maintenance architectures are identified for tracking with multiple passive sensors in [27]. A Type 1 system just uses data from each sensor to form mono tracks. No stereo tracks are formed[4]. Type 2 systems first form mono tracks from the sensor data. This step is followed by the formation of stereo tracks using track-to-track association of the mono tracks from different sensors. In distributed tracking systems, typically, mono tracks are formed at the local fusion nodes (called sensor level or local tracks) and the stereo tracks are formed at the central fusion node (called global tracks) from the mono tracks obtained from the various local fusion nodes. A variation of a Type 2 system could use feedback (from the global tracks) to aid the tracking at the local fusion nodes.

Type 3 systems first perform single scan, multiple-sensor observation association to form stereo tracks. Then the position measurements that are formed are input to the tracking system for multiscan data association. Hence in Type 3 systems sensor-to-sensor processing precedes scan-to-scan processing. Typically, this architecture is selected for centralized tracking. This architecture presents real computational

[4]A mono track means tracking just the measurements from the same target. No state estimation is performed. Stereo track refers to the tracks for which required quantities are estimated. For example, when tracking with angle only data, mono track refers to tracking the angles that have come from the same target (referred to as direction of arrival tracking in the signal processing community). A stereo track refers to the tracks for which position and velocity are estimated.

challenges in sensor-to-sensor processing. We describe this in the next chapter. Also we used this architecture to propose an algorithm to track multiple targets with time difference of arrival measurements.

Type 4 systems also use centralized processing. Observation-to-track processing is performed on each scan of data from each sensor as it becomes available. Triangulation is required to form initial stereo tracks and thereafter a nonlinear filter can be used to perform track update.

Chapter 3

Assignment-Based Data Association for Passive Sensor Tracking

In this chapter, we consider the data association problem in tracking systems that employ multiple synchronous passive sensors. This is the Type 3 track initiation and maintenance architecture as identified in [27]. We describe a solution based on the assignment-algorithm. This presentation is not specific to a particular type of passive measurement. It, however, assumes that the measurements obtained from various sensors are independent.

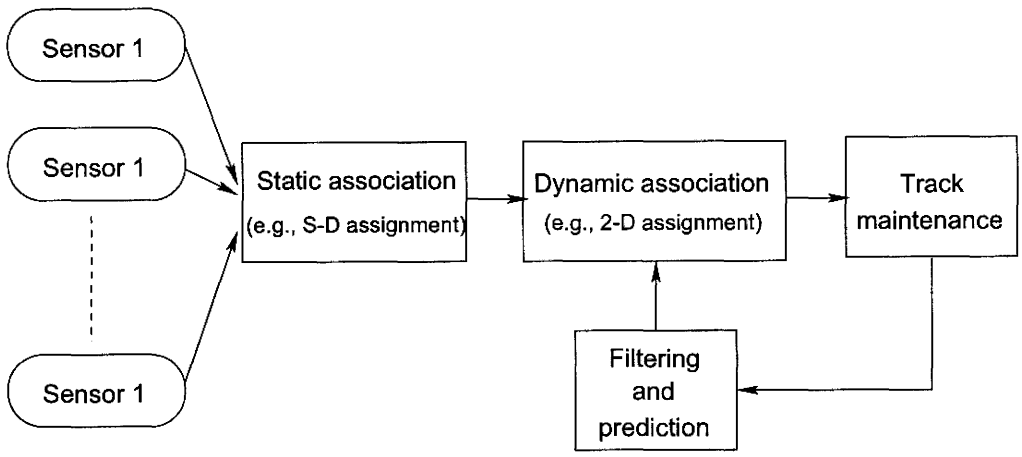

Figure 3.1: Block diagram.

3.1 Introduction

A high level block diagram of a centralized tracking system that uses multiple synchronous sensors is shown in Figure 3.1. In such systems, at every scan, one typically needs to solve two different data association problems: the measurement-to-measurement or static association and the measurement-to-track or dynamic association. Whereas the static association groups the measurements from different sensors that have originated from the same target, the dynamic association assigns the grouped (combined or composite) measurements to the tracks from the previous scan.

An assignment-based solution [67] views the static association as a multidimensional assignment and the dynamic association as a two dimensional assignment. If the tracking system has S sensors, in the measurement-to-measurement association step each feasible S-tuple of measurement (consisting one measurement from

each sensor) is assigned a cost (typically, a likelihood ratio) and then the set of S-tuples that minimize the global cost is found. This optimization is formulated as a multidimensional (S-dimensional or S-D) assignment as described in Section 3.2. Association of the S-tuple of measurements that are obtained from this step to the tracks from the previous scan is performed using a 2-D assignment.

As noted in Chapter 2 it is possible to find the optimal solution to the 2-D assignment problem using for example the auction algorithm. On the other hand, the S-D assignment can be shown to be NP-hard [70] and hence finding the optimal solution in polynomial time is impractical. Lagrangian relaxation-based techniques [26, 66, 67, 71, 76] have been proposed to find suboptimal solutions for applications that require real-time performance.

The formulation of the S-D assignment-based solution for the measurement-to-measurement association is provided in the next section. We then describe the 2-D assignment-based solution for the dynamic association. Note that the description provided here is brief and only the formulations of the data associations as assignment problems are provided. Interested readers are referred to [67] and the references therein for comprehensive treatment of these techniques.

3.2 S-D assignment algorithm for static association

In the measurement-to-measurement association, at each scan, S lists of measurements obtained from S synchronous sensors are available. The goal is to group the measurements that could have originated from the same (unknown) target. The

number of targets in the surveillance region is not known a priori. In the S-D assignment technique, each possible S-tuple[1] of measurement is assigned a cost and the set of S-tuples that minimizes the global assignment cost is found. Each S-tuple in the solution set signifies the measurements that originated from a single target.

Assume that at a given scan each sensor has generated n_s $(s = 1, 2, \ldots, S)$ measurements. It has to be noted that n_s need not be equal to the actual number of targets in the region due to missed detections and/or false alarms. A measurement in list s, i.e., from sensor s, is denoted by z_{si_s}, $i_s = 1, \ldots, n_s$. Since a single measurement could have originated from a real target or a false alarm, we can write

$$z_{si_s} = \begin{cases} h_s(X_p) + w_{si_s} & \text{if target originated} \\ \tilde{z}_{si_s} & \text{if false alarm} \end{cases} \tag{3.1}$$

where X_p is the unknown target state and $h_s(.)$ is the measurement function.

The measurement noise w_s is assumed to have a Gaussian distribution with zero mean and σ_s^2 variance, and conditionally independent across sensors. False measurements $\tilde{z}_{si_s}$ are assumed to be uniformly distributed in the field of view of the sensor. We would like to note that for notational convenience dependence of various quantities on time is not shown explicitly. Further, in order to incorporate possible missed detections a *dummy measurement* z_{s0} is added to each list of measurements.

An S-tuple of measurement $Z_{i_1 i_2 \ldots i_S}$, consisting one measurement from each list, is assigned a generalized log-likelihood cost $c_{i_1 i_2 \ldots i_S}$ defined by

$$c_{i_1 i_2 \ldots i_S} = -\ln \frac{p(Z_{i_1 i_2 \ldots i_S} | X_p)}{p(Z_{i_1 i_2 \ldots i_S} | p = \emptyset)} \tag{3.2}$$

[1] An S-tuple consists of one measurement taken from each sensor.

where $p(Z_{i_1 i_2 \ldots i_S}|X_p)$ denotes the likelihood that the S-tuple has originated from target p having state X_p and $p(Z_{i_1 i_2 \ldots i_S}|p = \emptyset)$ is the likelihood that all the measurements in the S-tuple are spurious. Since the measurements from different sensors are independent, the numerator in (3.2) is equal to the product of individual measurement likelihoods in the S-tuple. That is

$$p(Z_{i_1 i_2 \ldots i_S}|X_p) = \prod_{s=1}^{S} [1 - P_{D_s}]^{1-u(i_s)} \left[P_{D_s} p(z_{si_s}|X_p)\right]^{u(i_s)} \tag{3.3}$$

where P_{D_s} is the probability of detection of sensor s and $u(i_s)$ is a binary indicator function defined as

$$u(i_s) = \begin{cases} 0 & \text{if } i_s = 0 \\ 1 & \text{otherwise} \end{cases} \tag{3.4}$$

In the above likelihood, since the state of the target X_p is not known, it is replaced by its ML estimate [67]. That is

$$X_p = \arg\max_{X} \; p(Z_{i_1 i_2 \ldots i_S}|X) \tag{3.5}$$

Since the measurement noise is assumed to be Gaussian distributed, the conditional probability density function (pdf) $p(z_{si_s}|X_p)$ of a single measurement z_{si_s} is given by

$$p(z_{si_s}|X_p) = \mathcal{N}\left(z_{si_s}; h_s(X_p),\ \sigma_s^2\right) \tag{3.6}$$

where $\mathcal{N}(x; \mu, \Sigma)$ refers to the normal distribution of a random variable (vector) x having mean μ and variance (covariance matrix) Σ.

Since the false alarms are assumed uniformly distributed, the likelihood that all

the individual measurements in the S-tuple are from a spurious source is given by

$$p(Z_{i_1 i_2 \ldots i_s} | p = \emptyset) = \prod_{s=1}^{S} \left[\frac{1}{\psi_s}\right]^{u(i_s)} \tag{3.7}$$

where ψ_s is the volume of the field of view of sensor s.

Hence, the log-likelihood cost of assigning an S-tuple $(i_1, i_2, \ldots, i_S)$ to a target is given by

$$c_{i_1 i_2 \ldots i_s} = \sum_{s=1}^{S} [u(i_s) - 1] \ln (1 - P_{D_s}) - u(i_s) \ln \left(\frac{P_{D_s} \psi_s}{\sqrt{2\pi}\sigma_s}\right) + u(i_s) \frac{1}{2\sigma_s^2} [z_{si_s} - h_s(X_p)]^2 \tag{3.8}$$

The objective now is to find the most likely set of S-tuples such that each measurement is assigned to at most one target or declared false, and each target is assigned to at most one measurement from each sensor. This is formulated as the following generalized S-D assignment problem:

$$\begin{aligned}
\min_{\rho_{i_1 i_2 \ldots i_S}} \quad & \sum_{i_1=0}^{n_1} \sum_{i_2=0}^{n_2} \cdots \sum_{i_S=0}^{n_S} c_{i_1 i_2 \ldots i_S} \rho_{i_1 i_2 \ldots i_S} \\
\text{subject to:} \quad & \sum_{i_2=0}^{n_2} \sum_{i_3=0}^{n_3} \cdots \sum_{i_S=0}^{n_S} \rho_{i_1 i_2 \ldots i_S} = 1, \qquad i_1 = 1, 2, \ldots, n_1 \\
& \sum_{i_1=0}^{n_3} \sum_{i_3=0}^{n_3} \cdots \sum_{i_S=0}^{n_S} \rho_{i_1 i_2 \ldots i_S} = 1, \qquad i_2 = 1, 2, \ldots, n_2 \\
& \qquad \vdots \\
& \sum_{i_1=0}^{n_1} \sum_{i_2=0}^{n_1} \cdots \sum_{i_{S-1}=0}^{n_{S-1}} \rho_{i_1 i_2 \ldots i_S} = 1, \qquad i_S = 1, 2, \ldots, n_S
\end{aligned} \tag{3.9}$$

where $\rho_{i_1 i_2 \ldots i_S}$ is a binary variable such that

$$\rho_{i_1 i_2 \ldots i_S} = \begin{cases} 1 & \text{if } S\text{-tuple } \rho_{i_1 i_2 \ldots i_S} \text{ is included in the solution set} \\ 0 & \text{otherwise} \end{cases} \tag{3.10}$$

It has to be noted that there are no constraints on the dummy measurements and the use of them allows the association to be performed over the sets of all possible S-tuples. Note that an S-tuple in the association needs to have a certain number of measurements from a target in order for the state of the target to be observable.

The above generalized S-D assignment problem is NP-hard for $S \geq 3$ even under the assumptions of unity detection probability and no spurious measurements [66]. Hence, it is not possible to find the optimal solution in polynomial time. Therefore, it is necessary to seek suboptimal solutions for applications, such as target tracking, that require real-time performance.

Several Lagrangian relaxation-based solutions exist to find suboptimal solutions to the above assignment problem. For example, in [26] a suboptimal solution is obtained by using the fact that the 2-D assignment problem can be optimally solved in polynomial time. This algorithm uses Lagrangian multipliers and relaxes $(S-2)$ constraints simultaneously. The resulting 2-D assignment problem is then solved, for example, using the auction algorithm. Then, the Lagrangian multipliers are updated, which reimposes the constraints relaxed earlier. For more details see the references [26, 67].

3.3 2-D assignment for dynamic association

After performing the measurement-to-measurement association at a particular scan, one has a set of S-tuples of passive measurements. From each S-tuple in the solution set, we can obtain a set of full position estimates by finding the ML estimate of every S-tuple. The goal now is to use these full position estimates to update the tracks from the previous scan. Assuming that the tracks have been initialized, one is again faced with another data association problem — one needs to decide which track gets a given position estimate. In fact, there are three possibilities for the origin of the full position estimates. They are:

1. it could be the new position of an existing track
2. it could be a new target detected for the first time
3. it could be a clutter return

One could decide the (full position) measurement-to-track association by performing a 2-D assignment. In order to formulate the dynamic association as a 2-D assignment, assuming that the targets evolve according to known dynamic models, first the tracks from the previous scan are predicted to the current scan. The association between the elements of the two lists, namely, the predicted track information and the full position estimates can now be formulated as a 2-D assignment problem. (See Section 2.5.2 for details on 2-D assignment.) The assignment cost is now defined as

$$c_{i_1 i_2} = \begin{cases} 0 & \text{if } i_1 = 0 \text{ or } i_2 = 0 \\ -\ln \frac{\Lambda(i_1,i_2)}{\Lambda(0,i_2)} & \text{if } -\ln(.) \leq 0 \\ \infty & \text{otherwise} \end{cases} \tag{3.11}$$

where $\Lambda(i_1, i_2)$ denotes the likelihood that the full position estimate i_2 (the ML estimate of an S-tuple) came from the track i_1, and $\Lambda(0, i_2)$ is the likelihood that it came from none of the existing tracks, or in other words, it is a false alarm. The likelihood of false alarms is assumed to be uniformly probable in the surveillance region.

Once the solution to the 2-D assignment problem is obtained, the position estimate assigned to a track can be used to update that track[2]. Any of the tracks that are assigned to the dummy measurement means that the corresponding target is not detected in the current scan, or the target has moved out of the surveillance region. The position estimates that are assigned to the dummy track either correspond to a false alarm or suggest the birth of new tracks. It is up to the track maintenance phase to decide on how to handle these various cases.

3.4 Some issues

One of the important problems in using the S-D followed by 2-D assignment algorithm to solve the data association is passive synchronous multisensor tracking systems is that the resulting computational cost could be very high. One of the reasons is that the Lagrangian relaxation-based solution, being an iterative technique, requires considerable amount of computation to get a good solution. The primary bottleneck, however, is the cost associated with the construction of the assignment tree, that is, the calculation of the assignment cost of all the possible candidate associations. As noted earlier, the calculation of the assignment cost of a candidate association requires the ML estimate of the unknown target state, which in turn,

[2]If the target dynamics are linear then a Kalman filter [6] is sufficient to update the tracks, since the measurements are the positions of the target.

with passive measurements, requires nonlinear optimization. This results in huge computational requirement even in moderate scenarios.

There could be other factors, specific to the sensor type, that could also increase the computational burden further. For example, when tracking with angle only sensors in the two-dimensional plane, any two angle of arrival (AOA) measurements would intersect at a point. This implies that a target at that point is responsible for these two measurements. This is the well-known ghosting problem [5]. This means that with S AOA sensors any S-tuple that has two nondummy measurements is a candidate solution for the S-D assignment. This complicates the assignment tree building.

In fact, it has been proposed in [76] to consider only the candidates that are detected by the *majority* of the sensors to reduce the number of candidate associations. This technique, however, will only remove S-tuples whose dummy measurement count exceeding a given minimum. All the S-tuples that are made up of nondummy measurements alone are not affected. Hence, the resulting reduction in the number of branches that need to be built may not result in significant computational savings. It can be readily seen that when each sensor has reported n_s, $s = 1, 2, \ldots, S$, measurements at a given scan, without considering any of the branches that involve dummy measurements, one still needs to build

$$\prod_{s=1}^{S} n_s \tag{3.12}$$

number of branches, all of which require the costly MLE. This means that the number of candidate associations grows exponentially with the number of returns in each list.

Another related issue is the effects of MLE in the cost calculation. Most of the passive measurements are related to the target position through nonlinear functions. Hence, MLE problem often results in nonlinear optimization. Except in some special cases, obtaining the ML estimate requires gradient search over these nonlinear functions. Typically, nonlinear search techniques require good starting points in order to converge to the exact solution [10]. If such starting points are unavailable these search algorithms may converge to a local optimum, or worse they could diverge. Further, having a good starting point does not guarantee that the resulting solution will be accurate.

The error in the MLE of the target state could result in inaccurate assignment cost, which could lead to poor association performance. With some types of passive measurements it may be possible to get a good starting point. For example, as noted earlier, with AOA measurements any two angle measurements would intersect at a point, whose location can be found easily. This serves as a good starting point. For other types of passive measurements such a starting point may not be easily found.

In the next chapter, we present assignment-based data association algorithms that do not rely heavily on ML estimation. As a result, these algorithms give improved association results at substantially reduced computational cost.

Chapter 4

Efficient and Improved Data Association Algorithms

In this chapter we present two new efficient and improved assignment-based algorithms that solve the data association problem in passive synchronous multisensor tracking systems. As the simulation results (reported elsewhere in this thesis) suggests, the performance of these algorithms are better than that of the traditional S-D followed by 2-D technique described in the previous chapter, while providing significant computational savings.

The objective of the measurement-to-measurement association, as stated earlier, is to group the measurements that could have originated from the same target. In the solution based on the S-D assignment formulation only the measurement information from the current scan is used to achieve this objective. As such there is no way to reject a given S-tuple as not originated from a single target, unless the cost of the association is calculated and is found to be inconsistent [24]. As noted earlier, calculation of the assignment cost requires the costly ML estimation.

A clustering-based algorithm was proposed in [19] to reject improbable candidates. This algorithm, however, only uses the measurement information from the current scan, and one of the challenges, as noted in that paper, is to decide on the cluster size.

4.1 Gated S-D assignment-based algorithm

The gated S-D algorithm uses prior information and rejects improbable candidates without calculating the assignment cost. In particular, validation gates are setup based on the predicted track information for each track from the previous scan. Measurements from different sensors that fall within the validation gates of different tracks are identified. When calculating the cost of possible candidate associations, the S-tuples whose indices do not fall within the validation gate of a single track are not considered. This considerably reduces the number of candidate associations, especially, in high clutter environment. Once the association tree is formed we use the Lagrangian relaxation-based algorithm to solve the S-D assignment, and use the 2-D assignment, as described in the previous section, to associate the composite measurements to the tracks.

Let the state of target p at scan k is defined by $X_p^k = [x_p, \dot{x}_p, y_p, \dot{y}_p]^T$[1], where (x_p, y_p) denotes the position of the target and $(\dot{x}_p, \dot{y}_p)$ denotes the velocity components. Further, assume that target p evolves according to a known dynamic model

$$X_p^k = f_p^{k-1}(X_p^{k-1}) + v_p^{k-1} \tag{4.1}$$

[1]Note that in order to differentiate between predicted and updated tracks we use time indices for target states and their estimates.

where f_p^{k-1} is the state transition function which could be different for different targets and possibly time dependent, and v_p^{k-1} is the process noise, which is assumed to be Gaussian distributed with zero mean and associated covariance matrix Q_p^{k-1}.

It is assumed that each track is characterized by the mean and covariance of the estimate of that track. Let the mean and covariance of track p at scan k are denoted by $\hat{X}_p^k$ and P_p^k, respectively. Then the predicted state $\hat{X}_p^{k|k-1}$ and the associated covariance $P_p^{k|k-1}$ are given, respectively, by [6]

$$\hat{X}_p^{k|k-1} = f_p^k(\hat{X}_p^{k-1}) \tag{4.2}$$

and

$$P_p^{k|k-1} = F_p^k P_p^{k-1} F_p^{k^T} + Q_p^k \tag{4.3}$$

where F_p^k is the Jacobian of the state transition function evaluated at the predicted state $X = \hat{X}_p^{k|k-1}$. That is

$$F_p^k = \left. \frac{\partial f_p^{k-1}(X)}{\partial X} \right|_{X=\hat{X}_p^{k|k-1}} \tag{4.4}$$

For each track p and sensor s it is now possible to setup the validation gate defined by [6]

$$\nu_{ps}^k = \{z; (z - \hat{z}_{ps})^T (S_p^k)^{-1} (z - \hat{z}_{ps}) \leq \tau\} \tag{4.5}$$

In the above, τ is the threshold that decides the probability mass within the

validation gate. $\hat{z}_{ps}$ and S_p^k are the predicted measurement and the associated covariance, respectively. They are given by

$$\begin{aligned} \hat{z}_{ps} &= h_s(\hat{X}_p^{k|k-1}) \\ S_p^k &= \tilde{h}_s P_p^{k|k-1} \tilde{h}_s^T + \sigma_s^2 \end{aligned} \tag{4.6}$$

where

$$\tilde{h}_s = \left. \frac{\partial h_s(X)}{\partial X} \right|_{X=\hat{X}_p^{k|k-1}} \tag{4.7}$$

It is now straightforward to identify all the measurements z from sensor s that falls within the validation region of track p. Let the indices of these measurements be grouped in a set I_{ps}. To all the index sets I_{ps} the dummy measurement index is added. When building the assignment tree an S-tuple is checked against the measurement index sets of all the tracks and the S-tuple is considered a candidate solution only if all the indices in the S-tuple satisfy the validation gate requirement. This means that all the indices of an S-tuple need to be within the validation gate of at least one of the tracks.

To illustrate this gated assignment consider the simple scenario depicted in Fig. 4.1. There are two tracks T_1 and T_2 with their validation gates shown and there are two sensors. One of the sensors reports two measurements (1_1 and 1_2) and the other reports three measurements (2_1, 2_2, and 2_3). One can construct the following four index sets (since there are two tracks and two sensors): $I_{11} = \{1_0, 1_1\}$, $I_{12} = \{2_0\}$, $I_{21} = \{1_0, 1_2\}$, and $I_{22} = \{2_0, 2_1, 2_2\}$. Note that dummy measurement (1_0 and 2_0) is part of all the index sets, and the third measurement of second sensor 2_3 is not part of any of the sets since it does not fall within the validation gates of any of the two tracks. During the construction of the assignment tree only the branches

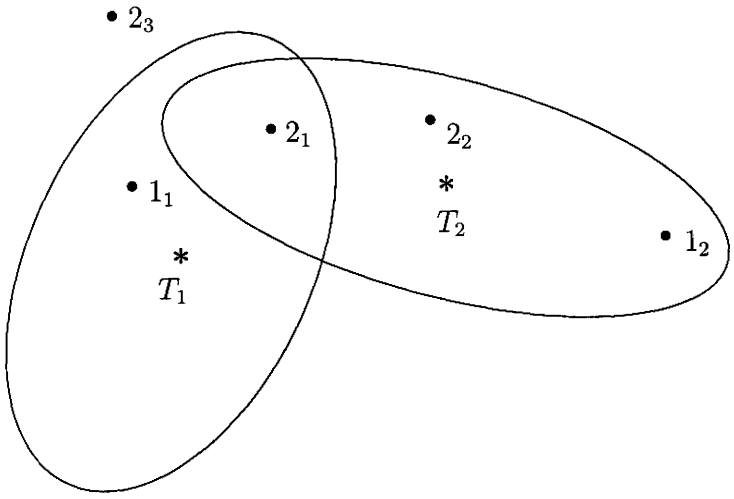

Figure 4.1: Illustration of gated assignment.

connecting (1_1,2_1), (1_2,2_1), and (1_2,2_2) are built. In the standard S-D assignment one needs to build six branches. The savings increases substantially as the number of sensors and tracks increases.

It has to be noted that it is difficult to characterize how many candidate solutions that this approach will eliminate, since it depends on how many measurements end up in the validation gate of a given track. This is dependent purely on the scenario such as target spacing and clutter, and sensor parameters such as detection probability and measurement noise variance. Further, it is hard to predict analytically the performance of this algorithm in comparison to the S-D followed by 2-D approach. We performed extensive Monte Carlo simulations to study various issues and the results are presented in the next chapter.

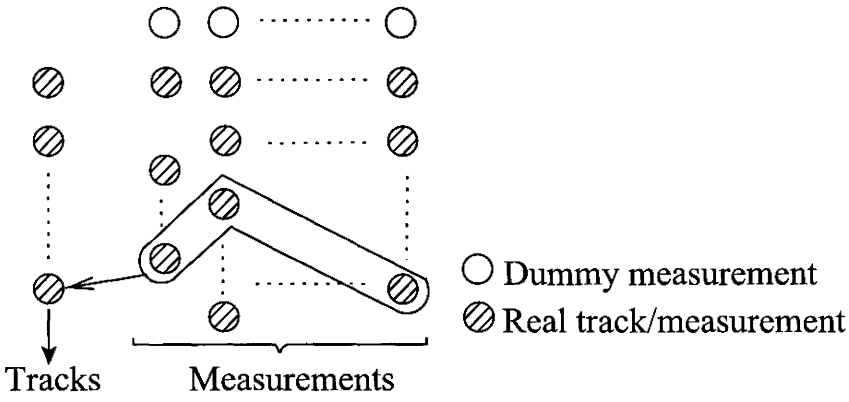

Figure 4.2: $(S+1)$-D data association.

4.2 $(S+1)$-D assignment-based algorithm

The S-D followed by 2-D technique or the gated assignment of the previous section, as discussed earlier, are two step algorithms. In this section, we present an algorithm that performs the data association with multiple passive sensors in a single step. We consider this single step algorithm as an $(S+1)$-D assignment, where the first dimension is the predicted track information and the rest of the S dimensions are the lists of measurements from the sensors as shown in Figure 4.2. It has to be noted that there are no dummy tracks in the track list, i.e., this algorithm assigns the measurements to tracks that have already been established.

We define the cost of assigning an S-tuple of measurement $(i_1, i_2, \ldots, i_S)$ to a track p, i.e., the cost of an $(S+1)$-tuple $(p, i_1, i_2, \ldots, i_S)$ as

$$c_{pi_1i_2\cdots i_S} = -\ln \frac{p(Z_{i_1i_2\cdots i_S}|X_p)}{p(Z_{i_1i_2\cdots i_S}|p=\emptyset)} \tag{4.8}$$

The only difference between the cost defined above and the cost of an S-tuple in

the assignment-based measurement-to-measurement association (defined in (3.2)) is that since we are trying to assign the S-tuple of measurements to already established tracks, instead of assuming the target state is unknown we use the track information that we have. The advantage of the $(S+1)$-D assignment for data association is that it eliminates the need for the costly ML estimation of the unknown target state altogether. The resulting algorithm is computationally efficient.

Since the measurement noises are assumed to be independent, one could think of calculating the measurement likelihood $p(Z_{i_1 i_2 \cdots i_S}|X_p)$ as in (3.3) with X_p replaced appropriately by the track information. Usually the track information that one would have is the predicted state $\hat{X}_p^{k|k-1}$. The assignment cost calculated using (3.8) with X_p replaced by $\hat{X}_p^{k|k-1}$, however, would only be an approximation. This is because the measurements in the S-tuple are conditionally independent only if the track information is known exactly. We, however, are using the predicted state, and due to the effect of common process noise in the predicted track information, the S-tuple of measurements are no longer conditionally independent. Hence, $p(Z_{i_1 i_2 \cdots i_S}|X_p^{k|k-1})$ cannot be calculated as a product of the likelihoods of the individual measurements (similar to (3.3)). We will now explain how this cost can be calculated.

The measurements in the $(S+1)$-tuple $(z_{i_1}, z_{i_2}, \ldots, z_{i_S})$ are used to form an S-dimensional vector of measurements[2]. With the individual measurement equation given in (3.1), and since we are assuming that all the measurements originated from a single target, we can write the vector of measurements as

$$z = H(X_p) + v \tag{4.9}$$

[2]When there are dummy measurements in the S-tuple, they are not included in the vector of measurements formed. As a result, the dimension of the vector could be less than S.

where

$$z = \begin{bmatrix} z_{i_1} \\ z_{i_2} \\ \vdots \\ z_{i_S} \end{bmatrix} \qquad H(X_p) = \begin{bmatrix} h_1(X_p) \\ h_2(X_p) \\ \vdots \\ h_S(X_p) \end{bmatrix} \qquad v = \begin{bmatrix} v_{i_1} \\ v_{i_2} \\ \cdots \\ v_{i_S} \end{bmatrix} \tag{4.10}$$

Typically, with passive measurements, $H(X_p)$ is nonlinear and hence, we approximate (4.9) using the Taylor series expansion around $\hat{X}_p$ (actually, around $\hat{X}_p^{k|k-1}$, the predicted state). We will then have

$$z = H(\hat{X}_p) + H_X(X_p - \hat{X}_p) + v \tag{4.11}$$

where

$$H_X = \left.\frac{\partial H(X_p)}{\partial X_p}\right|_{X_p=\hat{X}_p} \tag{4.12}$$

is the Jacobian of $H(X_p)$ evaluated at $X_p = \hat{X}_p$.

Since the measurement noises are assumed to be Gaussian distributed, the vector of measurements z forms a joint Gaussian process, and the conditional mean and covariance can be approximated using the linearized equation (4.11). The mean $\overline{z}$ and the covariance S are given by

$$\overline{z} = H(\hat{X}_p) \tag{4.13}$$

and

$$S = H_X P_p^{k|k-1} H_X^T + R \tag{4.14}$$

respectively, where $R = \text{diag}(\sigma_1, \sigma_2, \ldots, \sigma_S)$ is the covariance matrix of measurement noise vector v. We can now write the measurement likelihood in (4.8) as

$$p(z_{i_1 i_2 \ldots i_S} | X_p) = p(z|\hat{X}_p) \prod_{s=1}^{S} P_{D_s}^{u(i_s)} [1 - P_{D_s}]^{(1-u(i_s))} \tag{4.15}$$

where

$$p(z|\hat{X}_p) = \frac{1}{\sqrt{|2\pi S|}} \exp\left((z - \overline{z})^T S^{-1} (z - \overline{z})\right) \tag{4.16}$$

Hence, the $(S+1)$-D assignment cost $c_{pi_1 i_2 \ldots i_S}$ is given by

$$c_{pi_1 i_2 \ldots i_s} = -\ln p(z|\hat{X}_p) + \sum_{s=1}^{S} [u(i_s) - 1] \ln(1 - P_{D_s}) - u(i_s) \ln(P_{D_s} \psi_s) \tag{4.17}$$

With the cost defined as above we can now formulate the $(S+1)$-D association as an $(S+1)$-D assignment problem. This will be similar to the formulation given in (3.9) with $(S+1)$ dimensions. The Lagrangian relaxation-based algorithm can now be used to find the best set of $(S+1)$-tuples that minimizes the global assignment cost. Once a solution to the $(S+1)$-D assignment problem is obtained, the tracks (the first element in an $(S+1)$-tuple) can be updated with the measurements (rest of the elements in that $(S+1)$-tuple) to which they are assigned using a nonlinear filter such as the extended Kalman filter [6] or the unscented Kalman filter [95].

The computational requirement of the $(S+1)$-D assignment can further be reduced by a gating procedure similar to that described in the previous section. As described in the previous section validation gates of all the tracks are first formed. And an $(S+1)$-tuple is considered a candidate solution if and only if all the S measurements of the $(S+1)$-tuple falls within the validation gates of the track in that $(S+1)$-tuple.

4.3 An approximation to $(S+1)$-D assignment algorithm

We will now show that when measurements from various sensors are independent and when the predicted target states are accurate (for example in scenarios where target maneuver is low), the $(S+1)$-D algorithm can be approximated by a set of S two-dimensional assignment algorithms. The resulting data association algorithm is much faster than the other algorithms described.

Before describing the approximation, we would like to note the following regarding the assignment cost calculation of the S-D assignment technique. The assignment cost defined in (3.2), can be calculated using (3.8) for angle of arrival sensors if and only if the (unknown) target state X_p is known exactly. Since the target state is not known, the ML estimate of the S-tuple of measurement was found and used in the cost calculation [66]. The conditional likelihood of the S-tuple given the ML estimate of the target state, however, cannot be calculated as the product of the individual likelihoods (similar to (3.3)). This is because the ML estimate will be erroneous (due to measurement noise) and the common error in the ML estimate will make the individual conditional densities dependent. Hence, the cost calculated using (3.8) with an ML estimate of the target state is, at best, an approximation of the true likelihood ratio cost.

We will make a similar approximation to the $(S+1)$-D assignment cost, which results in an extremely fast algorithm. Consider the $(S+1)$-D assignment cost defined in (4.8). Since the track information one has is typically the predicted state, we used that to calculate the cost using (4.17). We now assume that the track predictions are accurate (i.e., $P_p^{k|k-1}$ is small). In such a case, if we neglect the

cross correlation introduced by the predicted state (i.e., we neglect the off-diagonal elements of S), we can approximate the numerator of the assignment cost (4.15) as

$$p(z_{i_1 i_2 \cdots i_S}|X_p) \approx \prod_{s=1}^{S} p(z_{i_s}|X_p) \tag{4.18}$$

where $p(z_{i_s}|X_p) = 1 - P_{D_s}$, if the index i_s corresponds to a dummy measurement, or

$$p(z_{i_s}|X_p) = P_{D_s}\mathcal{N}\left(z_{i_s}; h_s(\hat{X}_p), \tilde{h}_s(\hat{X}_p)P_p^{k|k-1}\tilde{h}_s(\hat{X}_p)^T\right) \tag{4.19}$$

if the index i_s refers to a nondummy measurement z_{i_s}. Hence, the assignment cost is now given by

$$c_{pi_1 i_2 \cdots i_S} = \sum_{s=1}^{S} -\ln \frac{\Lambda(z_{i_s}|X_p)}{\Lambda(z_{i_s}|p = \emptyset)} \tag{4.20}$$

The above means that the cost of the $(S+1)$-tuple decomposes as the sum of the costs of assigning individual measurements to the track. It can easily be shown (see Appendix) that when the assignment cost decomposes as above, the solution to the $(S+1)$-D problem is equivalent to solving S individual 2-D assignments. This means that we can assign the measurements from different sensors to the track list separately. All the measurements from different sensors that are assigned to a given track can then be used to update that track using a nonlinear filter.

4.4 Improving the data association accuracy

The data association accuracy of all the algorithms presented in this chapter and the previous chapter, can be improved albeit at a higher computational cost by ranked m-best solutions as opposed to considering the best solution. With an appropriate modification to the assignment tree, a series of modified copies of the initial

problem are solved to obtain solutions ranked based on the global cost.

The utility of calculating the ranked solutions was first recognized for 2-D assignment problem and various other classical optimization problems in [59]. This algorithm has been later improved by various researchers. For applications to target tracking please see [20, 21, 23, 76, 77]. We, however, did not consider the ranked solution in our simulations.

Chapter 5

Performance Evaluation: Angle Only Tracking

This chapter provides the results of the simulations that are conducted to evaluate the performance of the assignment algorithms presented in the pervious chapters. We consider the angle of arrival (AOA) measurements as the representative passive measurements. This is because it is the one that has received much attention in tracking literature.

We would like to note that even though the solution to the data association, i.e., performing the S-D assignment for static association and a 2-D assignment for dynamic association, is mentioned in the literature as a possible solution to the passive multiple synchronous sensor data association, to our knowledge, no study has been done to evaluate the tracking performance of this solution. Hence, our study also serves as a base line for this solution.

5.1 Scenario description

Simulation results are presented for two different scenarios. The ground truth of the first scenario consists of three targets flying in a parallel formation. In the second scenario there are two crossing targets. The ground truth of these two scenarios during a sample run is shown in Figure 5.1.

5.1.1 Target motion

True target motion is generated using the nearly constant velocity motion model. This type of motion is described by a constant white noise accelaration model as [6]

$$X^k = F_{CV} X^{k-1} + \Gamma_{CV} v^{k-1} \tag{5.1}$$

where X^k is the state of the target at time k, F is the state transition matrix and Γ_{CV} is the process noise gain matrix. They are given by

$$F_{CV} = \begin{bmatrix} 1 & T & 0 & 0 \\ 0 & 1 & 0 & 0 \\ 0 & 0 & 1 & T \\ 0 & 0 & 0 & 1 \end{bmatrix} \qquad \Gamma_{CV} = \begin{bmatrix} \frac{1}{2}T^2 & 0 \\ T & 0 \\ 0 & \frac{1}{2}T^2 \\ 0 & T \end{bmatrix} \tag{5.2}$$

v^{k-1} is a two dimensional, independent joint zero mean Gaussian process noise. That is v is distributed as $\mathcal{N}(0, Q)$, where $Q = \mathrm{diag}(q_x, q_y)$. In the simulations, q_x and q_y are assumed equal. The process noise covariance matrix $\tilde{Q}$ is given by

$$\tilde{Q} = \Gamma Q \Gamma' \tag{5.3}$$

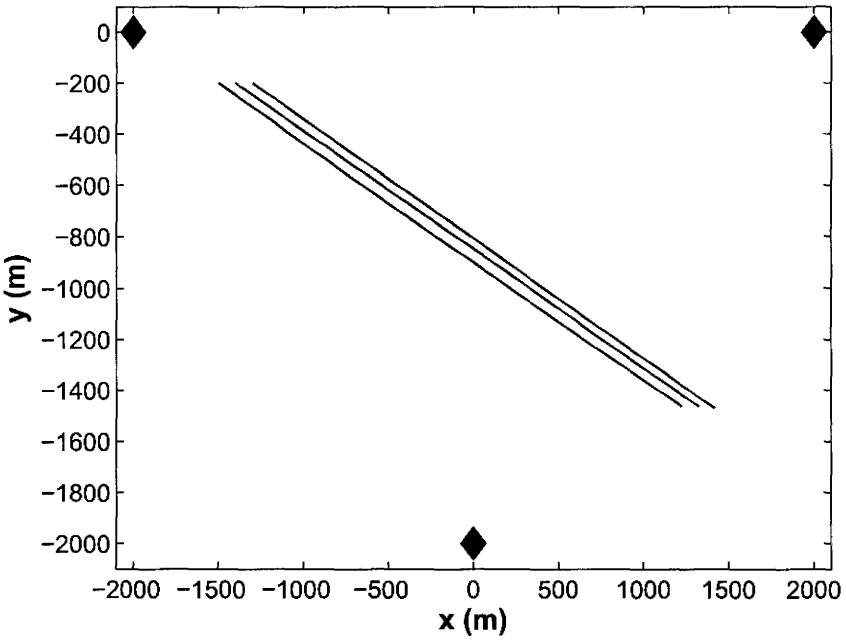

(a) Parallel formation

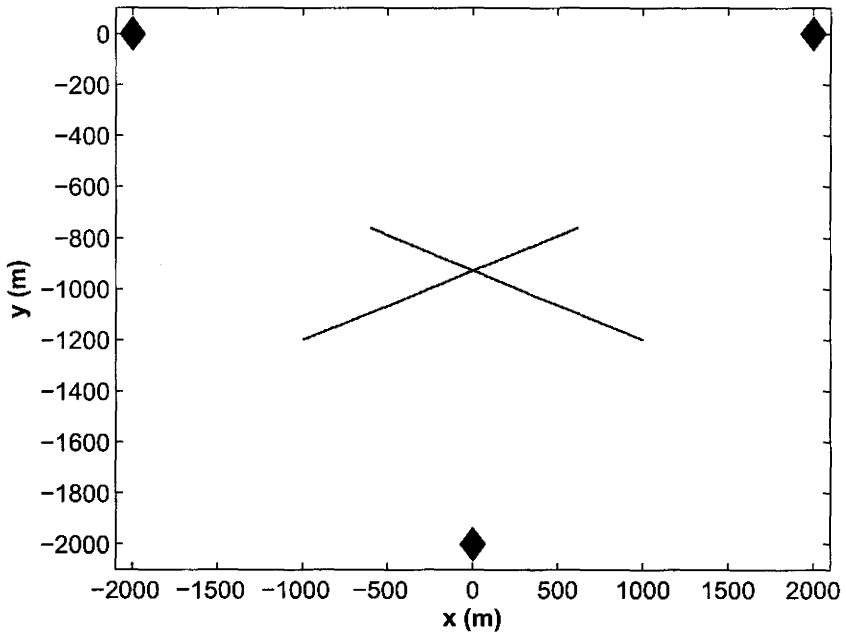

(b) Crossing targets

Figure 5.1: Ground truth in the simulations.

In the first scenario the three targets start at (-1500,-200)m, (-1400,-200)m, and (-1300,-200)m, and maintain a constant speed of 30m/s throughout the simulation at 105° from the vertical axis[1]. In the second scenario, one target starts at (-1000,-1200)m and the other at (1000,-1200)m. Both targets maintain a constant speed of 60km/hr. Whereas the course of the first target was 75° from the vertical axis, that for the second target was $-75°$.

5.1.2 Measurements

In both scenarios, targets are tracked using three fixed AOA sensors located at the circumference of a circle with a radius of 2000m. Since the sensors measure AOAs, the measurements are generated using the following model

$$z = \arctan\left(\frac{y_t - y_s}{x_t - x_s}\right) + w \tag{5.4}$$

where (x_t, y_t) denotes the true target positions at a given time and (x_s, y_s) denotes that of the sensors. It is assumed that there is no uncertainty in the sensor positions. w denotes the measurement noise, which is assumed to be Gaussian distributed. The following parameters are assumed the same for all the sensors.

- The field of view (FOV) of all the sensors is assumed to be 180°.
- Measurement noise of all the sensors have a zero mean and a standard deviation of σ_θ.
- The probability of detection P_{D_s} for each sensor is assumed to be 0.9.

[1]Positive angles are measured clockwise.

- The number of false alarms is assumed to be Poisson distributed with a rate of 0.8/radian, and the false alarms are assumed to be uniformly distributed in the surveillance region.

Since the false alarm rate is 0.8/radian and the FOV is π radians, on average, there will be 2.5 false measurements for each sensor at a given scan. False alarms are generated such that their spatial distribution is uniform, i.e., false alarm position (x,y) has the following distribution: $\mathcal{U}[x; -2000, 2000]$ and $\mathcal{U}[y; -2000, 0]$. Here $\mathcal{U}[\alpha; a, b]$ means variable α is uniformly distributed between a and b.

5.1.3 Tracker

Since the target dynamics are linear, in both the S-D 2-D and gated S-D 2-D assignment techniques, the Kalman filter is used to update the tracks using the composite position measurements. Further, since the covariance of the composite measurements is not known, following [67], we used the Cramer-Rao lower bound [93] as the measurement noise covariance in the KF.

For the $(S+1)$-D association algorithm and its approximation, all the measurements associated to a track are formed into a measurement vector. This measurement vector is used to update the tracks. It has to be noted that even though the motion model is linear, since the vector of AOA measurement are nonlinear, a UKF [95] is used to update the track in both these algorithms.

It also has to be noted that since the algorithms proposed in this thesis do not handle track initiation[2], in the simulations we did not consider track initialization. Hence, if an algorithm loses a track it is considered lost track for the remaining

[2]As discussed perviously, track initialization can be performed in these algorithms by pooling the measurements that are not associated with any of the tracks and by performing an S-D assignment

scans. We do not try to reinitialize it.

The simulations were written in MATLAB, and since the CPU times are compared to measure efficiency, care was taken to make sure that all the algorithms use the same code as much as possible. For example, multidimensional assignment code was the same for all algorithms. The assignment tree building code was also the same except the assignment cost calculation part, which is dependent on the algorithm. Also, the gated assignment has a separate function before the tree building to perform gating.

5.2 Performance metrics

Before presenting the results of the simulations, we would like to define the performance metrics that are used to compare these algorithms. For a detailed description of these metrics the reader is referred to [84].

Completeness history

This refers to the ratio between the real objects that should be tracked (i.e., the number of targets in the ground truth) and the number of declared tracks that are held as declared tracks. In order to calculate the completeness history, at each time step, a unique gated assignment is carried out between the targets at that time step (obtained from the ground truth) and the tracks as reported by the tracker in that time step. This will yield three quantities:

1. Number of valid tracks: if a target is assigned to a track then the number of valid tracks is increased by one.

2. Number of missed tracks: if a target is not assigned to a track then this number is increased by one.

3. Number of extra tracks: all the tracks that are not assigned to a target are considered extra tracks.

The completeness history is the ratio between the number of valid tracks and the true number of targets. This is averaged over all Monte Carlo runs at each time step. Note also that the fraction of missed targets is equal to one minus the completeness history.

Mean cumulative swap of tracks

This metric and the one described next (the mean cumulative broken tracks) determines the performance of the trackers in terms of track continuity, that is, how capable a tracker is in maintaining the initialized tracks.

Mean cumulative swap of tracks (MCST) refers to the number of track swaps that has happened at each time step. If a certain target is assigned to a certain track in the last N scans and if that target is assigned to another track in the current scan then the number of swaps of that track is increased by one. For each real object the number of swaps is computed at each time step and averaged over all Monte Carlo runs. It is also possible to average the MCST over all the real targets.

Mean cumulative broken tracks

Mean cumulative broken tracks (MCBT) refers to the average number of track breaks during the simulations. After performing the gated assignment between the real objects and the declared tracks at a given scan, if a target is assigned to a track

during the last N scans, and if that target is not assigned to any of the declared tracks in the current scan then the MCBT of that target at the corresponding scan in incremented by one. The results are averaged over all the Monte Carlo runs and over all the real object at each scan.

Tracking accuracy

How accurate the tracker tracks the targets is measured by means of the root mean squared error (RMSE) in position and velocity estimates. At each scan of each Monte Carlo run, after performing the unique gated assignment, if a target is assigned to a declared track then it is considered in the mean square error calculations. The RMSE is calculated at each time step and is averaged over all the Monte Carlo runs and over all the targets. Note that if a target is not assigned to a declared track at a given time scan in a given Monte Carlo run then it is not considered in the calculation of the RMSE. Note that in the simulations we did not perform initialization after a track is lost. Hence, if a track is lost at a given scan, the target corresponding to that track may not get any assignments in the remainder of the scans and hence it will not be considered in the RMSE calculations any further.

5.3 Results

In this section we provide the results of the simulations conducted for the two scenarios described above.

Table 5.1: Association accuracy in the first scenario

Method	Association accuracy (%)		
	$\sigma_\theta = 0.5°$	$\sigma_\theta = 1°$	$\sigma_\theta = 2°$
S-D 2-D	57.46	47.80	43.22
Gated S-D 2-D	90.99	71.96	56.87
$(S+1)$-D	92.23	79.68	70.48
Approx. $(S+1)$-D	92.65	85.78	75.69

5.3.1 First scenario

First we compare the association accuracy of various algorithms described in this paper. The association accuracy is calculated as follows. The 3-tuple of measurements that are assigned to different tracks at each time step are identified. Since there are three targets and three sensors, there will be nine true measurement-to-track pairs (or three true 3-tuples). The maximal set of assignments between the true 3-tuples and the assigned 3-tuples are found. The number of correct associations is summed in each time step and over all Monte Carlo runs. Table 5.1 gives association accuracy as the measurement noise standard deviation is varied.

As can be seen the S-D 2-D assignment gives the worst performance in terms of association accuracy. This is largely because of the huge number of false candidate associations it has to process and that it relies on the ML estimate to calculate the association cost without using any prior information.

Next we compare the efficiency of these algorithms in terms of average processor times. The results are presented in Table 5.2. As can be seen from the table, the proposed algorithms not only provided improved association accuracy, but also at a reduced computational cost. It has to be noted that although the $(S+1)$-D algorithm eliminates all the costly ML estimation, its computational load is slightly higher than that of the gated assignment. This is because the $(S+1)$-D assignment has an

Table 5.2: Average processor time for single data association step

Method	CPU time (s)
S-D 2-D	1.4545
Gated S-D 2-D	0.2608
$(S+1)$-D	0.3860
Approx. $(S+1)$-D	0.0091

additional dimension and hence the assignment tree will be larger than that of the gated assignment.

The RMSE performance of the tracking algorithms that use the various data associations is shown in Figure 5.2. The proposed algorithms are outperforming the standard S-D 2-D algorithm. This is due to the fact that the proposed algorithms use prior information to eliminate several unnecessary association hypotheses. The performance of the gated assignment algorithm did suffer due to the fact that it uses the ML estimation to get the measurements.

The completeness history is compared in Figure 5.3. Note that both the $(S+1)$-D algorithm and its approximation has a completeness history of unity in this scenario. This means that these algorithms had no missed tracks throughout the simulations. The gated assignment also has better completeness history ratio compared with the S-D 2-D algorithm. Further, the $(S+1)$-D and its approximation do not have any broken tracks as seen from the MCBT metric shown in Figure 5.5. For the S-D 2-D algorithm, towards the end of the simulation, only half of the targets that should be tracked are held as declared tracks. All the algorithms exhibit track swaps as one would expect since targets are flying in a parallel formation throughout the simulation duration. The performance of the $(S+1)$-D algorithm and its approximation again give better performance.

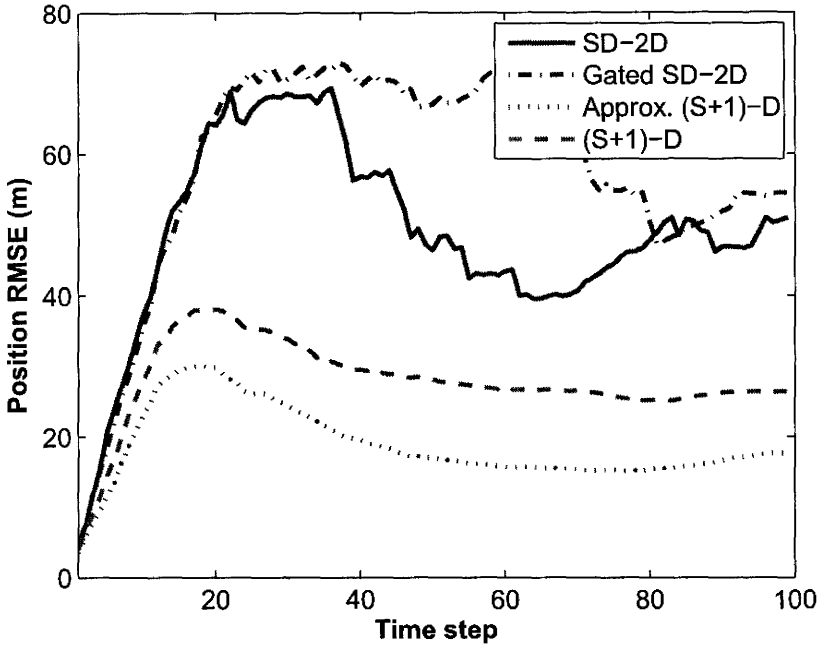

(a) Position RMSE

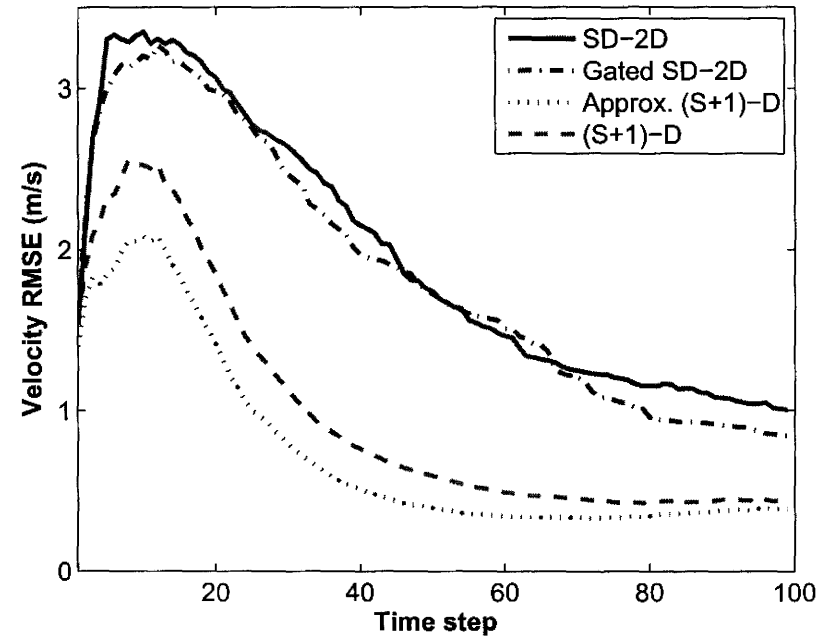

(b) Velocity RMSE

Figure 5.2: Comparison of accuracies. $\sigma_\theta = 1°$.

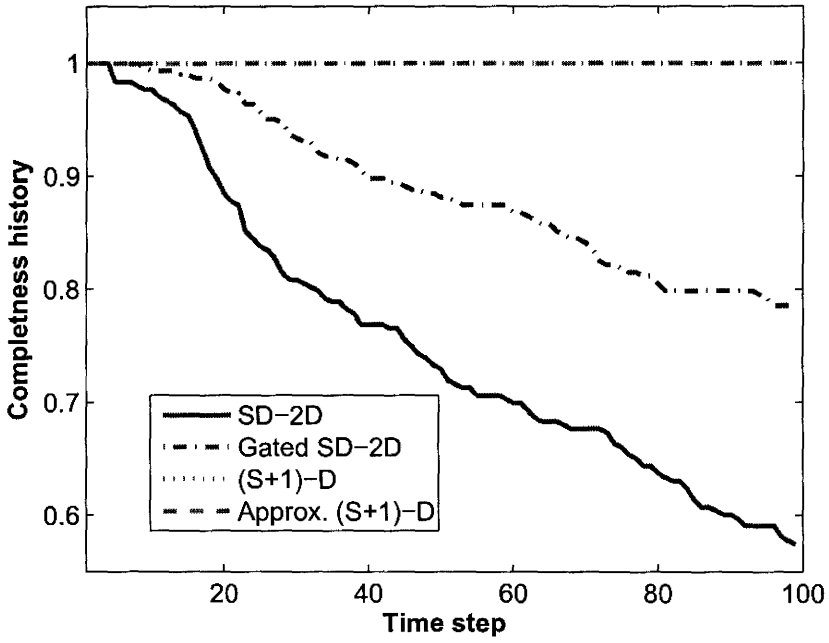

Figure 5.3: Completeness history. $\sigma_\theta = 1°$.

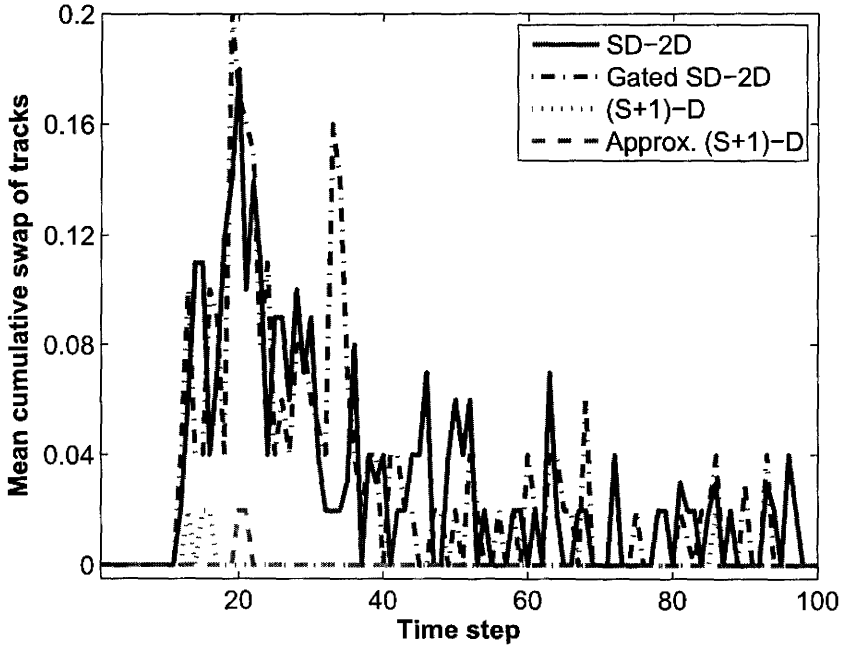

Figure 5.4: Mean cumulative swap of tracks. $\sigma_\theta = 1°$.

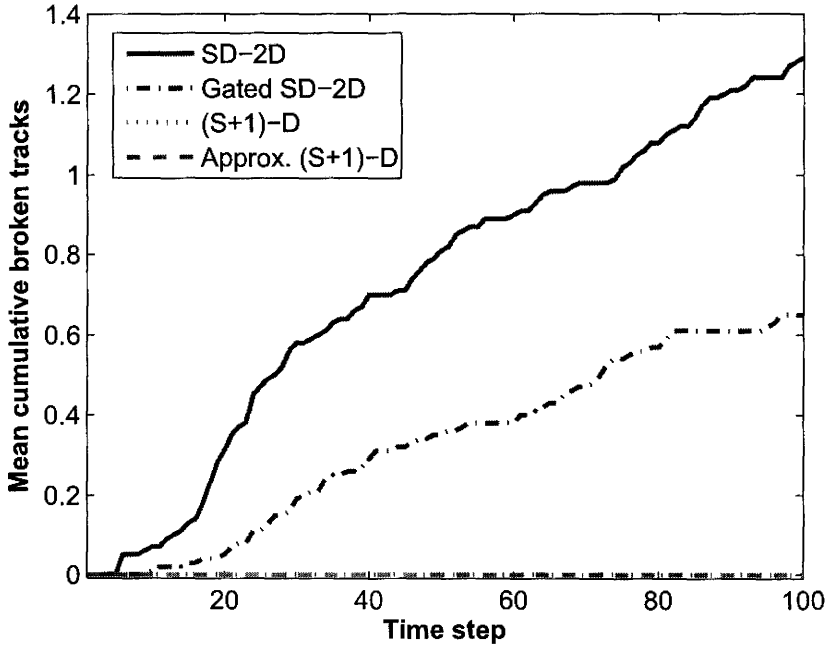

Figure 5.5: Mean cumulative broken tracks. $\sigma_\theta = 1°$.

Table 5.3: Association accuracy in the second scenario

Method	Association accuracy (%)		
	$\sigma_\theta = 0.5°$	$\sigma_\theta = 1°$	$\sigma_\theta = 2°$
S-D 2-D	59.19	46.73	45.46
Gated S-D 2-D	91.02	88.05	80.99
$(S+1)$-D	92.18	89.04	82.23
Approx. $(S+1)$-D	93.6	87.15	82.65

5.3.2 Second scenario

The same performance metrics are computed for the crossing target scenario depicted in 5.1. Table 5.3 compares the association accuracy for various algorithms. Again the $(S+1)$-D assignment algorithm and its approximation gives better data association accuracy. Note also that the association accuracy of all the algorithms are improved considered to the first scenario. This is due to the fact that in this scenario data association is relatively easy, because the targets are well separated before and after the changeover point.

The computation times are compared in Table 5.4. Figure 5.6 shows the RMSE performance of the algorithms considered. Notice that all the algorithms show a spike in the velocity RMSE plot around the point where targets cross. This is because of the potential track swaps that occur near the target crossing point.

Figures 5.7, 5.8, and 5.9 presents the completeness history, MCST and MCBT. All the algorithms show track swaps near the crossing points. The gated assignment algorithm, the $(S+1)$-D algorithm and its approximation, were all able to recover from these track swaps and maintained the tracks continuously. This is evident from Figure 5.9. The S-D 2-D algorithm, on the other hand, loses the tracks more than 25% of the time after the crossing point.

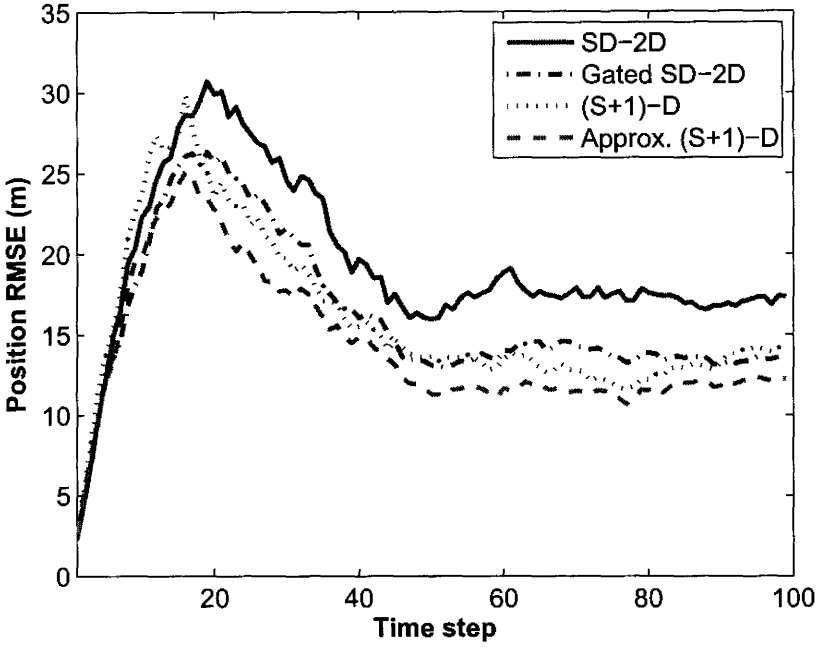

(a) Position RMSE

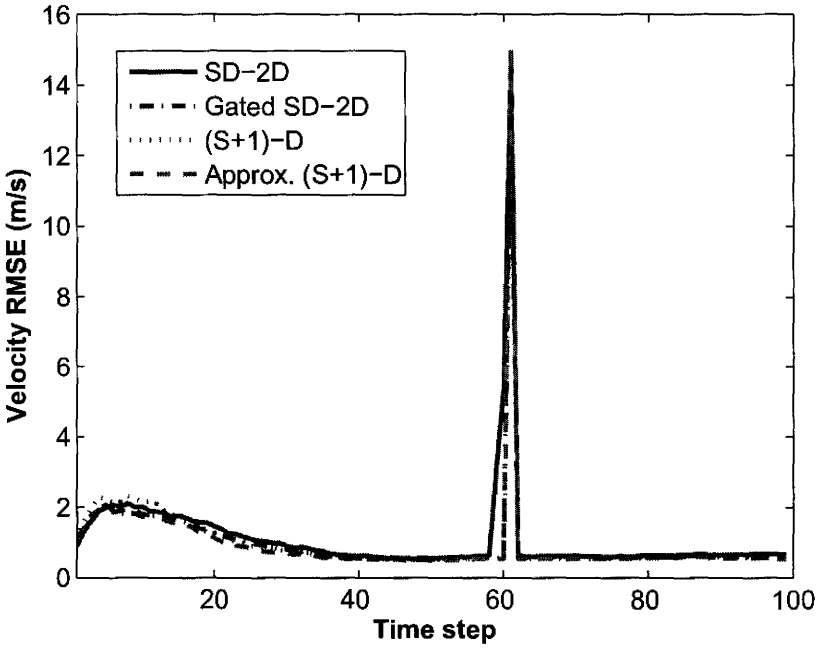

(b) Velocity RMSE

Figure 5.6: Comparison of accuracies. $\sigma_\theta = 1°$.

Table 5.4: Average processor time for single data association step

Method	CPU time (s)
S-D 2-D	1.0297
Gated S-D 2-D	0.0630
$(S+1)$-D	0.0893
Approx. $(S+1)$-D	0.0065

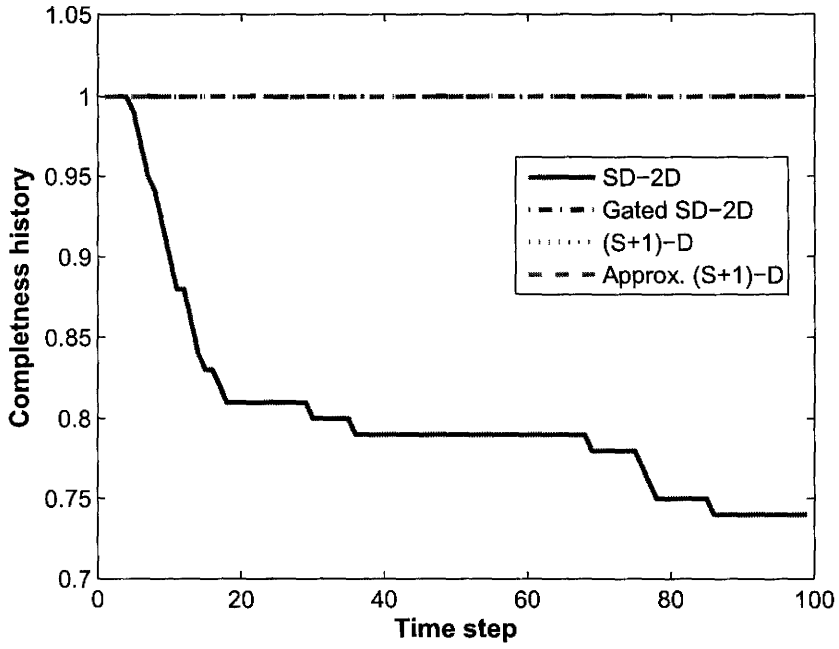

Figure 5.7: Completeness history. $\sigma_\theta = 1°$.

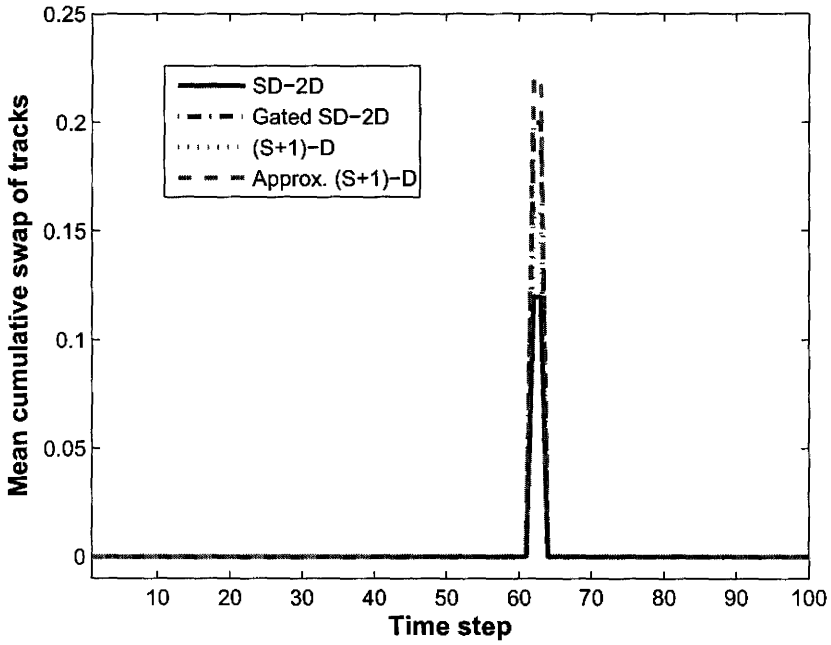

Figure 5.8: Mean cumulative swap of tracks. $\sigma_\theta = 1°$.

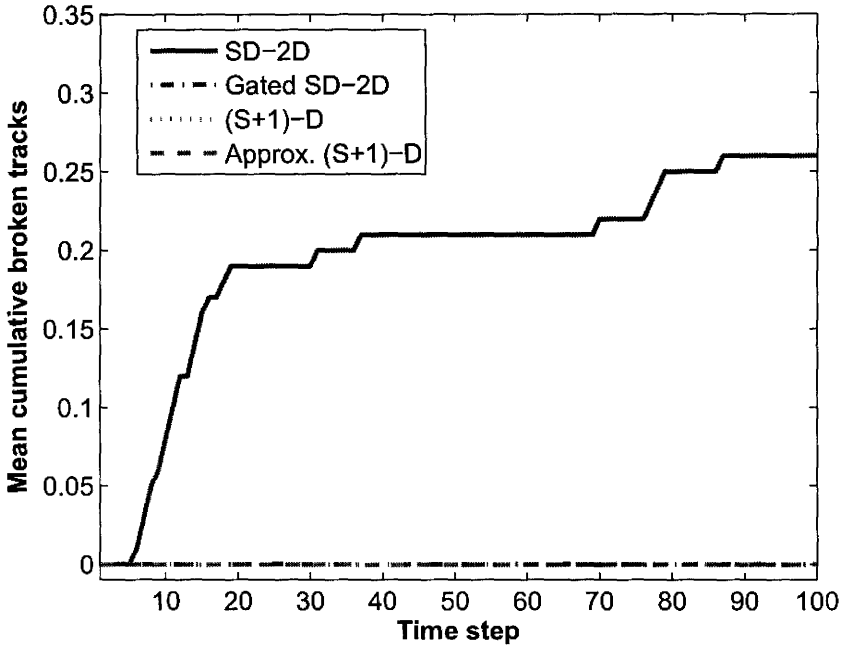

Figure 5.9: Mean cumulative broken tracks. $\sigma_\theta = 1°$.

Chapter 6

Multitarget Tracking using TDOA Measurements

In this and the next chapters we consider the problem of localizing and tracking multiple targets using time difference of arrival (TDOA) measurements. In the TDOA technique, in order to localize an emitter, a set of nonlinear equations that relate the TDOA measurements with the unknown source and known receiver locations is solved. Solving the set of TDOA equations, however, in view of the nonlinearity, is a non-trivial task. Various researchers have considered this problem and have proposed iterative [36, 92] or closed form solutions [17, 41, 86, 91]. These solution techniques have been proposed under idealistic assumptions, i.e., all the detections are from a single emitter and all the sensors detected the emitter.

The problem of multitarget localization using TDOA has been considered in [63] and [97]. The approach of [63] is to perform the multitarget localization in two separate steps: first obtaining the TDOA measurements of different targets and then solving them to localize the emitters. In particular, [63] obtained the optimum (in

the maximum likelihood (ML) sense) time delay vector in a multitarget scenario. Since the computational complexity of the optimum processor is prohibitively high, a suboptimal post correlation processor (PCP) has also been proposed. The multitarget ML position estimator proposed in [97] combines the two steps into a single step. These two methods assumed that the number of targets is known a priori and that the emissions from all the targets are zero-mean Gaussian processes with known spectral densities. These assumptions restrict their applicability considerably in most practical scenarios. In addition, these two techniques did not consider the tracking issues.

The objective of this work is to develop a localization and tracking framework that could be used in realistic scenarios (consisting of multiple emitters, with missed detections and false measurements). The important challenge in real-world scenarios is the data association problem. We modify the assignment-based algorithms developed in this thesis to solve the data association problem. A technique to localize the emitter (i.e., to solve the nonlinear TDOA equations) has also been developed. This is described in Chapter 7.

6.1 Overview of the proposed algorithm

The block diagram of the proposed localization and tracking framework is given in Figure 6.1. This framework is suitable for a centralized architecture. The first step in the proposed algorithm is to obtain the TDOA measurements. Typically, the TDOA measurement of an emitter between two sensors is obtained by the generalized cross-correlation (GCC) process [51]. The GCC process, however, was formulated under a single target assumption and in the presence of multiple targets there exists

multiple peaks in the cross-correlation function, resulting in performance degradation [63]. Further, the bandwidth requirement of the GCC technique is high since during each observation interval signals from different sensors are to be transmitted to a central location for processing. Compression of the signals while reducing the bandwidth requirement may result in the distortion of the signals. This may, however, lead to erroneous TDOA measurements.

In this work, we assume that the observations are in the form of time of arrival (TOA) measurements[1], from which TDOA estimates are obtained. This reduces the bandwidth requirement considerably, because at each time step only the TOA values are transmitted to the central location instead of the whole received signal.

Once the TOAs from all the sensors corresponding to a given scan are received at the central location, they are associated with the track list using the $(S+1)$-D association algorithm. Any track that receives an S-tuple of TOA measurement is updated with that set of measurements. The tracks that did not receive any measurements are just predicted to the next time scan. The tracks that did not receive any measurements for a given maximum number of scans are deleted. All the measurements that are not assigned to any of the tracks are identified and an S-D assignment is performed to identify any new targets. If the S-D algorithm has resulted in S-tuple of measurements then they are solved to obtain position estimates of the potential new targets.

In order to reduce the bandwidth requirements we assumed that the TDOAs are obtained by measuring the TOAs. The TOA measurement typically contains the unknown time of emission and hence the S-D or $(S+1)$-D algorithms, as described

[1]Note that this assumption is not restrictive. It will become clear later that the proposed framework can be used if the TDOA measurements are available directly (through GCC procedure or any other techniques).

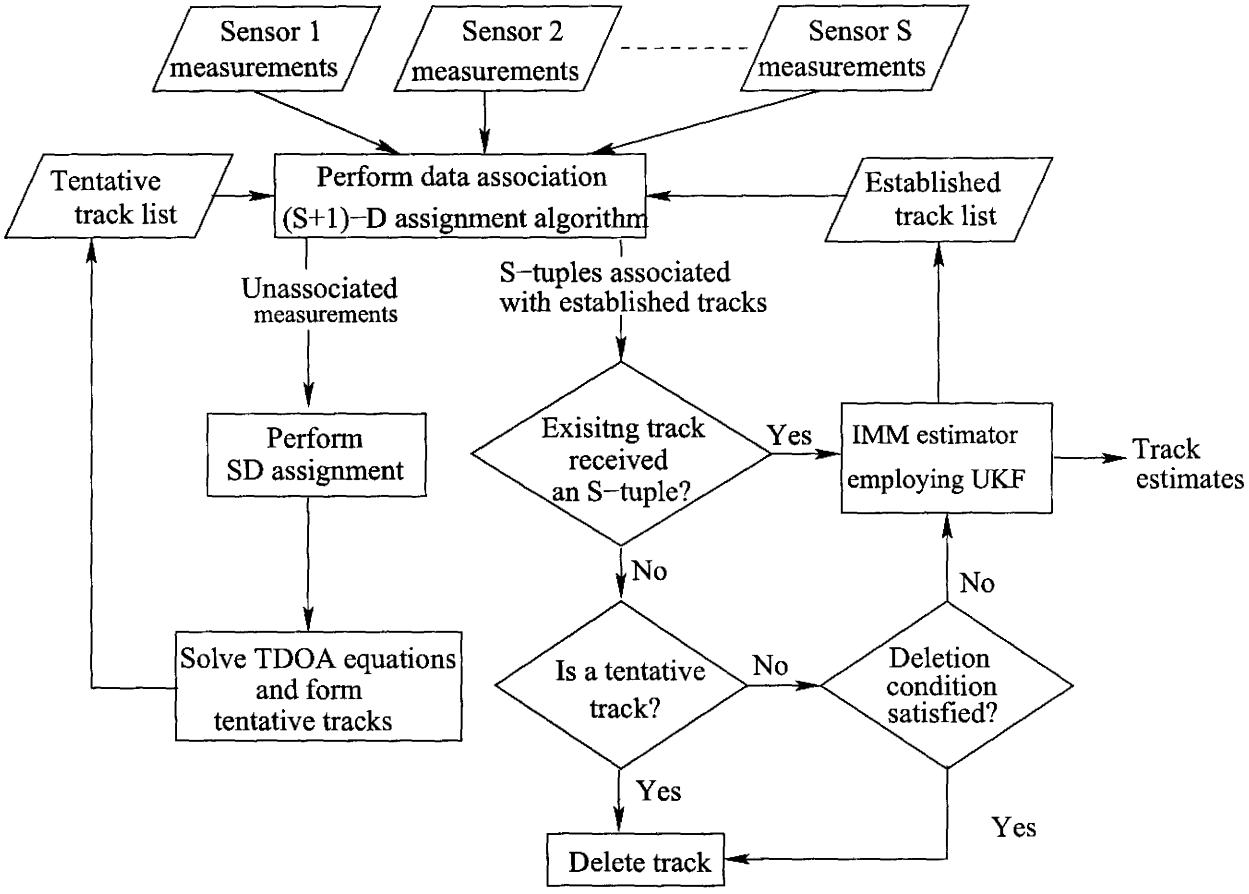

Figure 6.1: Block diagram of the proposed diagram.

in the previous chapters, cannot be directly applied to solve the data association. We will now explain how the assignment-based techniques can be used to solve the data association problem in tracking with TDOA measurements.

6.2 S-D assignment for correlated measurements

Assume that there are S TOA sensors and in a given scan each sensor has generated n_s, $s = 1, 2, \ldots, S$, measurements. We denote a single measurement in the list s by z_{si_s}, $i_s = 0, 1, \ldots, n_s$. This single TDOA measurement is given by

$$z_{si_s} = t_{em} + \frac{\|H(X_p - X_s)\|}{c} + v_{si_s} \tag{6.1}$$

In the above X_p as defined previously is the target state and X_s is the known sensor state. t_{em} is the time of emission, c is speed of propagation of the emission, and H is matrix that selects the position components from the state. In the two dimensional case it is given by

$$H = \begin{bmatrix} 1 & 0 & 0 & 0 \\ 0 & 0 & 1 & 0 \end{bmatrix} \tag{6.2}$$

We also assume that the TOA measurement noise v_{si_s} is Gaussian distributed with zero mean and variance σ_s^2, and independent from other sensors. Since these assumptions are similar to that was made in Chapter 3, one might think that in order to calculate the log-likelihood assignment cost defined in (3.2) one can use (3.3) with

$$p(z_{si_s}|X_p) = \mathcal{N}\left(z_{si_s}; t_{em} + \frac{\|X_p - X_s\|}{c}, \sigma_i^2\right) \tag{6.3}$$

It, however, is not possible to evaluate the pdf in (6.3) since typically the time of emission t_{em} is unknown (at least in uncooperative environments). Hence, the S-D assignment algorithm cannot be used directly to perform the data association. To overcome this problem, for each S-tuple of TOA measurement we define a cost based on TDOA, which is independent of t_{em}.

We can write the following measurement equation for a TDOA measurement $z_{i_s i_1}$ obtained from two TOA measurements z_{i_s} and z_{i_1}

$$\begin{aligned} z_{i_s i_1} &= z_{i_s} - z_{i_1} \\ &= \frac{\|H(X_p - X_s)\|}{c} - \frac{\|H(X_p - X_1)\|}{c} + v_{i_s i_1} \end{aligned} \tag{6.4}$$

where $v_{i_s i_1} = v_{i_s} - v_{i_1}$ is the TDOA measurement noise. It is easy to show that $v_{i_s i_1}$ will have a Gaussian distribution with zero mean and variance $\sigma_s^2 + \sigma_1^2$. Therefore, the conditional pdf of a single TDOA measurement $z_{i_s i_1}$ is given by

$$p(z_{i_s i_1}|X_p) = \mathcal{N}\left(z_{i_s i_1}; \frac{\|H(X_p - X_s)\|}{c} - \frac{\|H(X_p - X_1)\|}{c}, \sigma_{s1}^2\right) \tag{6.5}$$

Note that this pdf is not dependent on the unknown emission time t_{em} and hence, can be evaluated even in uncooperative environments. Therefore, we define the assignment cost of an S-tuple of TOA using the TDOA likelihood as follows. One sensor with a non-dummy measurement from the S-tuple of TOA is considered as the reference sensor (let it be denoted by 1). By subtracting the TOA measurement of the reference sensor from all the other non-dummy TOA measurements in the S-tuple, at most $(S-1)^2$ TDOA values (i.e., $z_{i_s i_1}$, $s = 2, 3, \ldots, S$) can be obtained.

Even with the TDOA likelihood defined in (6.5) the assignment cost cannot be

[2]Due to miss detections the number of TDOAs could be less than $(S-1)$.

evaluated using (3.3). This is because the $(S-1)$ TDOA measurements obtained from the S-tuple of TOA are all affected by the common measurement noise of the reference sensor (i.e., v_{i_1}) and hence are not independent. Therefore, it is required to account for the correlation in the calculation of the cost. In order to account for correlation, we follow an approach that is similar to the one used in the $(S+1)$-D assignment cost definition.

The $(S-1)$ TDOA measurements thus obtained from an S-tuple of TOA constitute a correlated joint-Gaussian process. We can stack all the TDOA measurements into a vector and obtain the following.

$$z = H(X_p) + v \tag{6.6}$$

where

$$z = \begin{bmatrix} z_{i_2 i_1} \\ z_{i_3 i_1} \\ \vdots \\ z_{i_S i_1} \end{bmatrix} \qquad H(X) = \begin{bmatrix} h_2(X_p) \\ h_3(X_p) \\ \vdots \\ h_S(X_p) \end{bmatrix} \qquad v = \begin{bmatrix} v_{i_2 i_1} \\ v_{i_3 i_1} \\ \vdots \\ v_{i_S i_1} \end{bmatrix} \tag{6.7}$$

From this the conditional pdf of the joint-Gaussian process can be obtained as

$$p(z|X_p) = \mathcal{N}(z; H(X_p), R) \tag{6.8}$$

where for an $(S-1)$-dimensional z it is easy to show that

$$R = E[vv'] = \begin{bmatrix} \sigma_2^2 + \sigma_1^1 & \sigma_1^2 & \dots & \sigma_1^2 \\ \sigma_1^2 & \sigma_3^2 + \sigma_1^2 & \dots & \sigma_1^2 \\ \vdots & \vdots & \dots & \vdots \\ \sigma_1^1 & \sigma_1^2 & \dots & \sigma_S^2 + \sigma_1^2 \end{bmatrix} \tag{6.9}$$

When z has fewer than $(S-1)$ TDOAs due to missed detection by one or more sensors, rows and columns corresponding to those sensors are removed from R.

The likelihood of the $(S-1)$-tuple TDOA obtained from the S-tuple of TOA measurement can now be expressed as

$$p(Z_{i_1 i_2 \dots i_S} | X_p) = p(z|X_p) \prod_{s=1}^{S} [1 - P_{D_s}]^{1-u(i_s)} P_{D_s}^{u(i_s)} \tag{6.10}$$

where $u(i_s)$ is the indicator function defined in (3.4).

With the assumption that the false alarms are uniformly probable in the surveillance region, we can define the following assignment cost for the S-tuple of TOA measurement.

$$\begin{aligned} c_{i_1 i_2 \dots i_s} &= -\ln \frac{p(\Delta t|X_p) \prod_{i=1}^{S} [1 - P_{D_s}]^{1-u(i_s)} P_{D_s}^{u(i_s)}}{\prod_{s=1}^{S} \left[\frac{1}{\psi_s}\right]^{u(i_s)}} \\ &= -\ln p(\Delta t|X_p) + \sum_{i=1}^{S} \{(u(i_s) - 1) \ln (1 - P_{D_s}) + u(i_s) \ln (P_{D_s} \psi_s)\} \end{aligned} \tag{6.11}$$

We would like to note that the above assignment cost even though is specifically obtained for TDOA measurements is valid for any type of correlated measurements for which assignment-based data association is sought.

6.3 $(S+1)$-D assignment for correlated measurements

We would like to note here that the $(S+1)$-D assignment-based algorithm to solve the data association problem, described in Section 4.2, would not require any changes. This is because there was no assumption made as to the independence of the measurements in developing that algorithm. It, however, has to be noted that the approximation of the $(S+1)$-D assignment algorithm will not be good choice with correlated measurements. This is because the measurement noise covariance matrix R is no longer diagonal. Hence, neglecting the off-diagonal elements of (4.14) could result in incorrect approximation.

6.4 Simulations

Simulations are performed to demonstrate the performance of the proposed framework. A local North-East-Up (NEU) coordinate framework is chosen, with the xy plane as the earth surface where the emitters lie. TOA sensors are assumed to be mounted on unmanned aerial vehicles (UAVs) flying in a parallel formation at a fixed altitude with constant velocity.

6.4.1 Scenario Description

Two different scenarios are used in the simulations: the first scenario considered fixed number of targets throughout the simulation duration, while in the second scenario the number of targets is varied.

In both the scenarios UAVs, used as sensor platforms, fly at a constant altitude of 6000m. The UAVs move at a constant speed of 100m/s, and then make a 180°

coordinated turn with a turn rate of 2rad/s. They then proceed with constant speed for the reminder of the simulation period. It is assumed that the UAV positions are known exactly at each time step, i.e., there is no process noise in their motion. Further, it is assumed that the footprint of each UAV covers the entire surveillance region.

True motions of the sources in the first scenario are illustrated in Figure 6.2(a). There are five emitters — a stationary emitter, three constant velocity emitters, and an emitter that performs a coordinated turn. The constant velocity target motion is generated using (5.1). The coordinated motion is generated using the following model.

$$X^k = F_{CT} X^{k-1} + \Gamma v^{k-1} \tag{6.12}$$

where

$$F_{CT} = \begin{bmatrix} 1 & \frac{\sin \Omega^j_{k-1} T}{\Omega^j_{k-1}} & 0 & -\frac{1-\cos \Omega^j_{k-1} T}{\Omega^j_{k-1}} & 0 \\ 0 & \cos \Omega^j_{k-1} T & 0 & -\sin \Omega^j_{k-1} T & 0 \\ 0 & \frac{1-\cos \Omega^j_{k-1} T}{\Omega^j_{k-1}} & 1 & \frac{\sin \Omega^j_{k-1} T}{\Omega^j_{k-1}} & 0 \\ 0 & \sin \Omega^j_{k-1} T & 0 & \cos \Omega^j_{k-1} T & 0 \\ 0 & 0 & 0 & 0 & 1 \end{bmatrix} \tag{6.13}$$

and

$$\Gamma_{CT} = \begin{bmatrix} \frac{T^3 l_1}{3} & \frac{T^2 l_1}{2} & 0 & 0 & 0 \\ \frac{T^2 l_1}{2} & T l_1 & 0 & 0 & 0 \\ 0 & 0 & \frac{T^3 l_1}{3} & \frac{T^2 l_1}{2} & 0 \\ 0 & 0 & \frac{T^2 l_1}{2} & T l_1 & 0 \\ 0 & 0 & 0 & 0 & T l_2 \end{bmatrix} \tag{6.14}$$

Note now that the state is augmented with the turn rate. In the second scenario the same sources are considered and to vary the number of sources they are

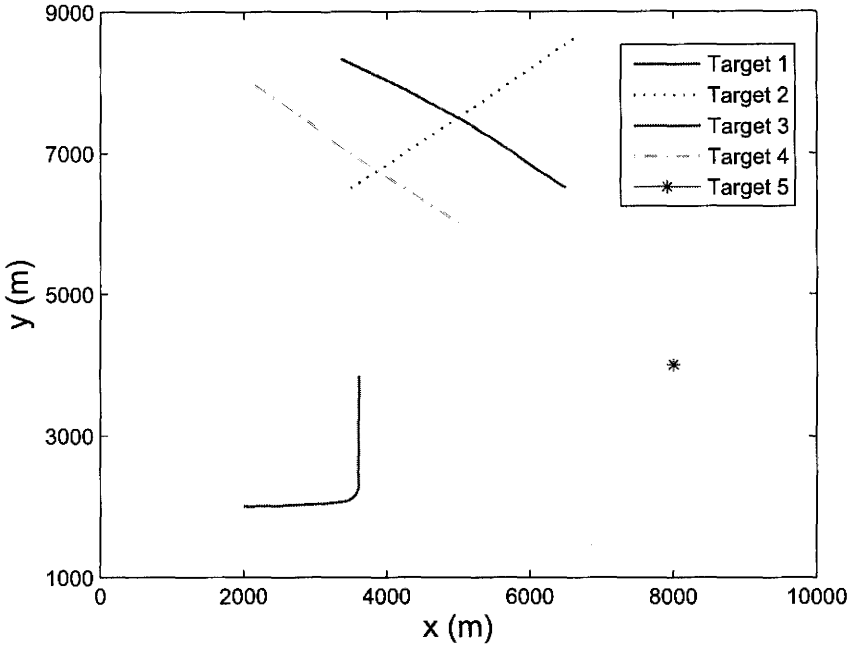

(a) True target motion in scenario 1

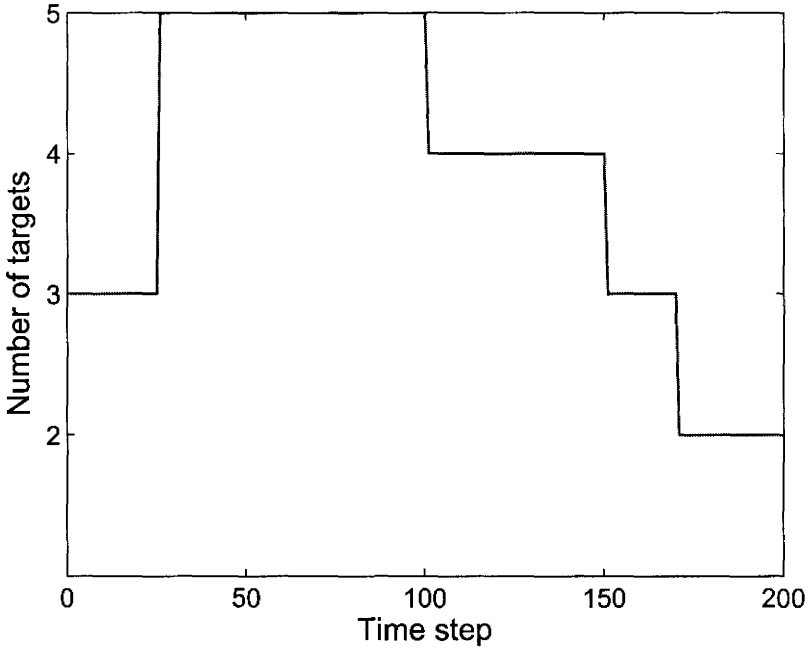

(b) Variation of number of targets in scenario 2

Figure 6.2: Simulation scenarios.

assumed to emit at different time intervals. Figure 6.2(b) shows the number of sources in the surveillance region at each time step.

Some other parameters used in the simulations include:

- Probability of detection P_{D_s} of 0.9 is assumed for all the sensors.
- The number of false measurements is assumed to be Poisson distributed with an average of two false measurements per sensor per scan. And the false measurements are assumed to be uniformly distributed over the surveillance region.
- For the targets, process noise variance in velocity is $0.01\text{m}^2/\text{s}^4$. For turn rate it is $0.0001\text{rad}^2/\text{s}^2$.

An IMM estimator consisting of two fixed models, namely, a constant velocity model and a coordinated turn model, is used to track the targets. A fixed Markov chain state transition probability matrix [6] of

$$[p_{ij}] = \begin{bmatrix} 0.95 & 0.05 \\ 0.05 & 0.95 \end{bmatrix} \tag{6.15}$$

is used in the IMM estimator to model the state transitions.

6.4.2 Simulation Results

The position and velocity root mean square errors (RMSE) are calculated at each time step and averaged over 50 Monte Carlo runs. Figure 6.3 and Figure 6.4 show the RMSE variation for different targets in the first and second scenarios. In both cases the measurement noise standard deviation is 1ns. The RMS errors in both

Table 6.1: Comparison of execution times

Algorithm	Execution Time (s)	
	Scenario 1	Scenario 2
Algorithm 1	10119.8	2669.5
Algorithm 2	3503.1	801.7

scenarios are higher when targets perform maneuvers. The fixed target gives the smallest RMS errors. The spikes in the velocity RMSE for the second scenario corresponds to the times at which new targets appeared in the surveillance region. This is because targets are initialized with the velocity components of the state set to zero.

Figure 6.5 gives the effect of measurement noise on the performance of the proposed method. In this figure, the RMS errors at each time step averaged over all the targets and over 50 Monte Carlo runs are plotted. As one would expect, the RMS errors in position and velocity decrease with improved measurement accuracy.

Table 6.1 presents the average execution times for the two scenarios considered. The execution times are based on a MATLAB 7 implementation on an Intel Pentium 3.0GHz personal computer with 512MB memory. Algorithm 1 refers to the TDOA tracking algorithm that uses the S-D followed by 2D for data association and Algorithm 2 refers to the TDOA tracking algorithm that uses the $(S+1)$-D algorithm for data association. As it can be seen from the table, the proposed method, on average, executes nearly three times faster — a significant reduction in computation.

Figure 6.6 compares the performance of the two algorithms in terms of RMS errors. One can conclude from this figure that the $(S+1)$-D algorithm is not only efficient but also results in better tracking accuracy in comparison to the S-D followed by 2-D technique.

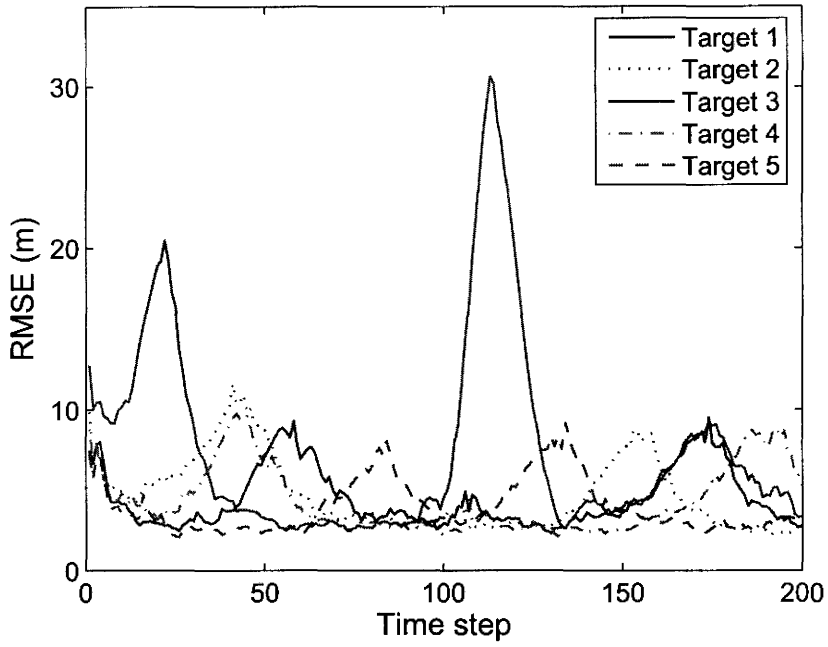

(a) Position RMSE

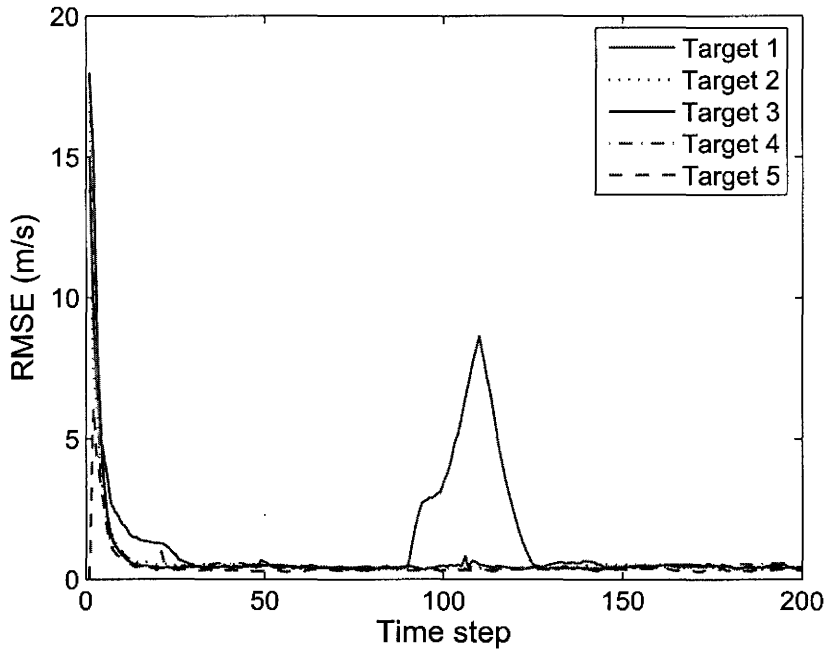

(b) Velocity RMSE (m/s)

Figure 6.3: Position and Velocity RMSE in the first scenario. $\sigma_s = 1$ns.

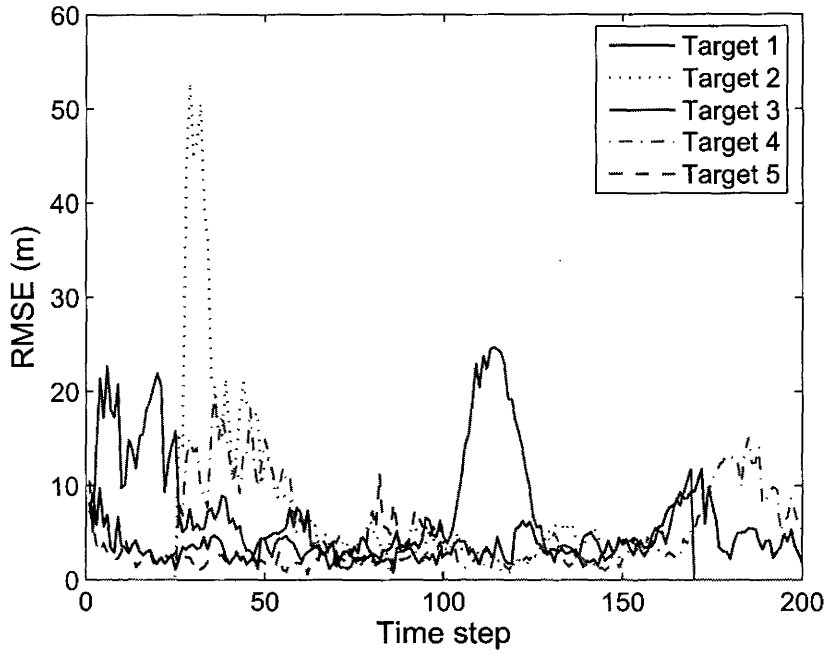

(a) Position RMSE

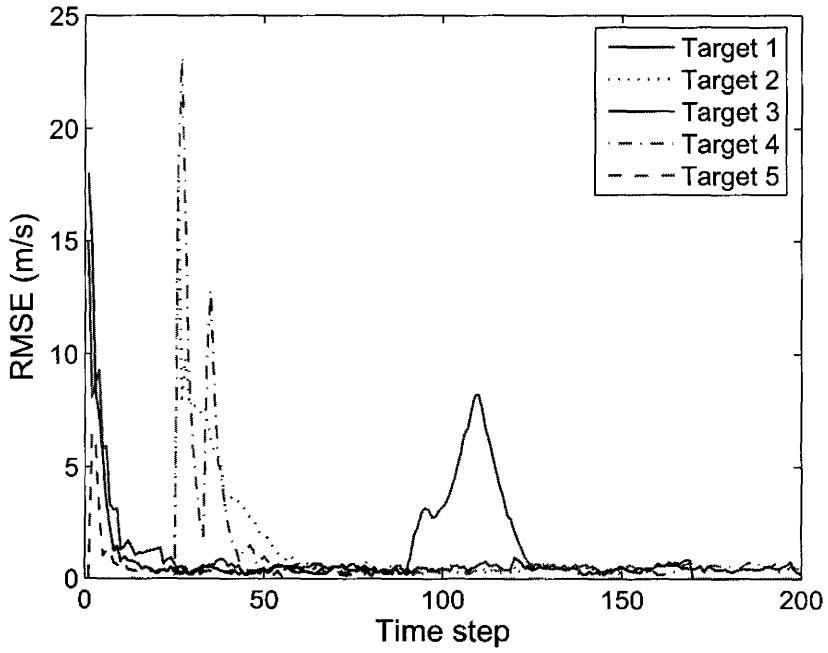

(b) Velocity RMSE (m/s)

Figure 6.4: Position and velocity RMSE in the second scenario. $\sigma_s = 1$ns.

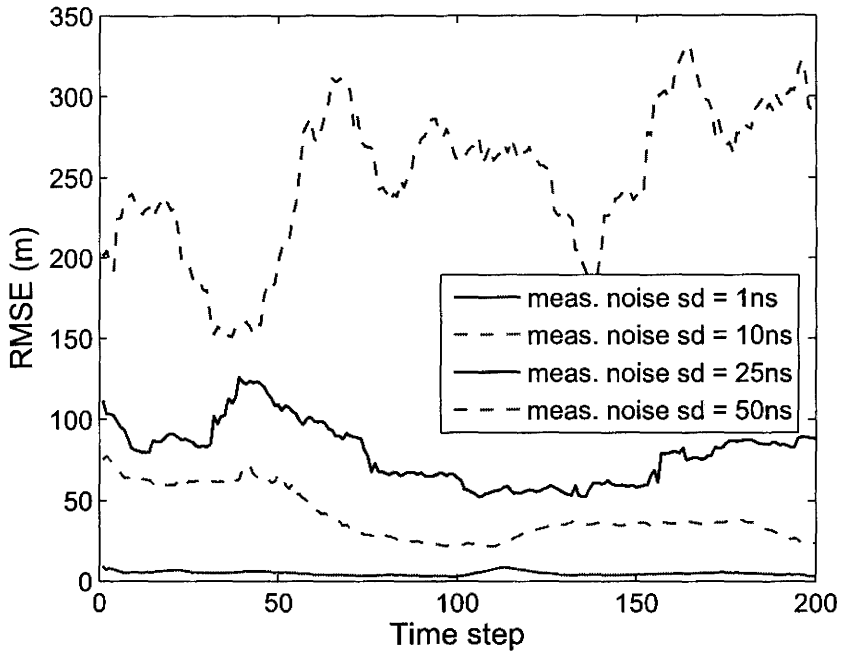

(a) Position RMSE

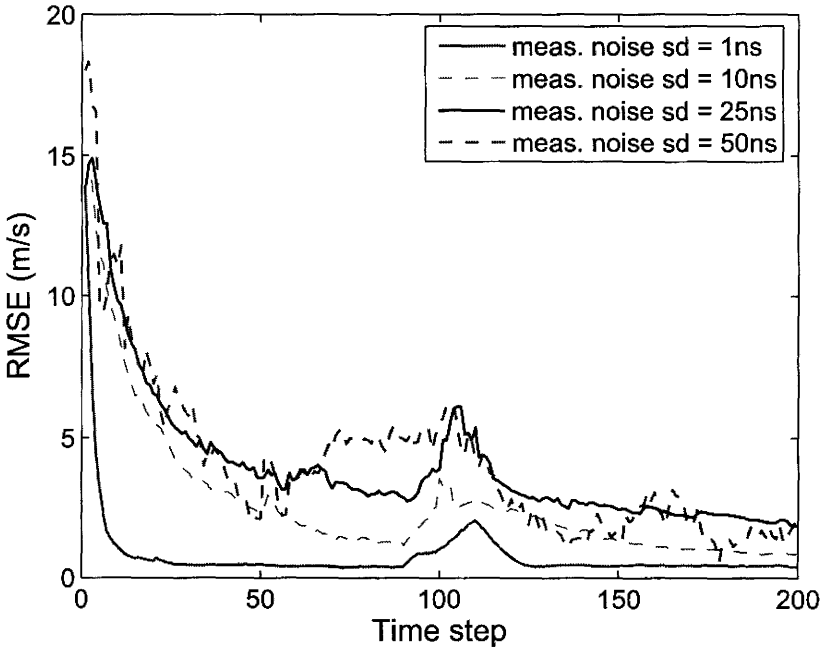

(b) Velocity RMSE (m/s)

Figure 6.5: Position and velocity RMSEs averaged over all the targets in the first scenario for different measurement noise standard deviations.

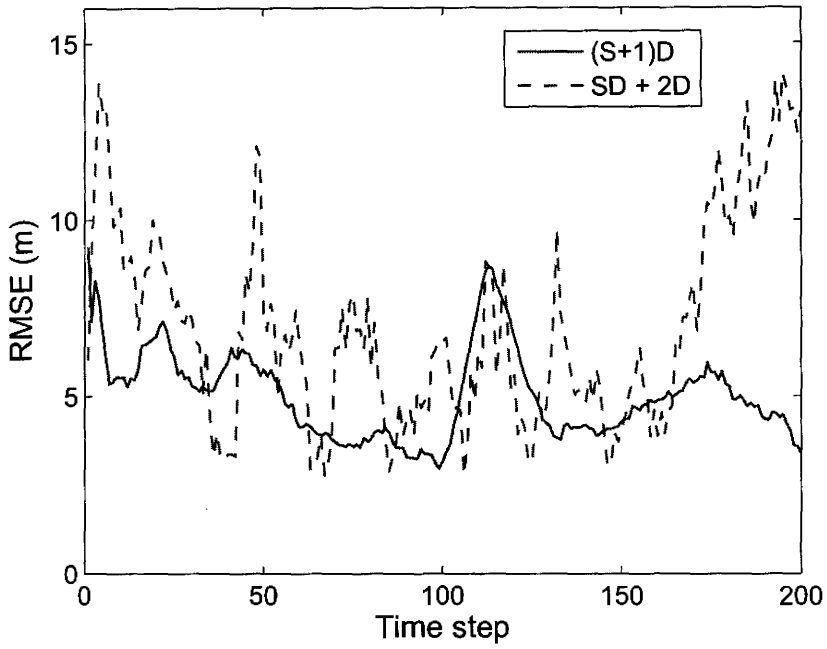

(a) Position RMSE

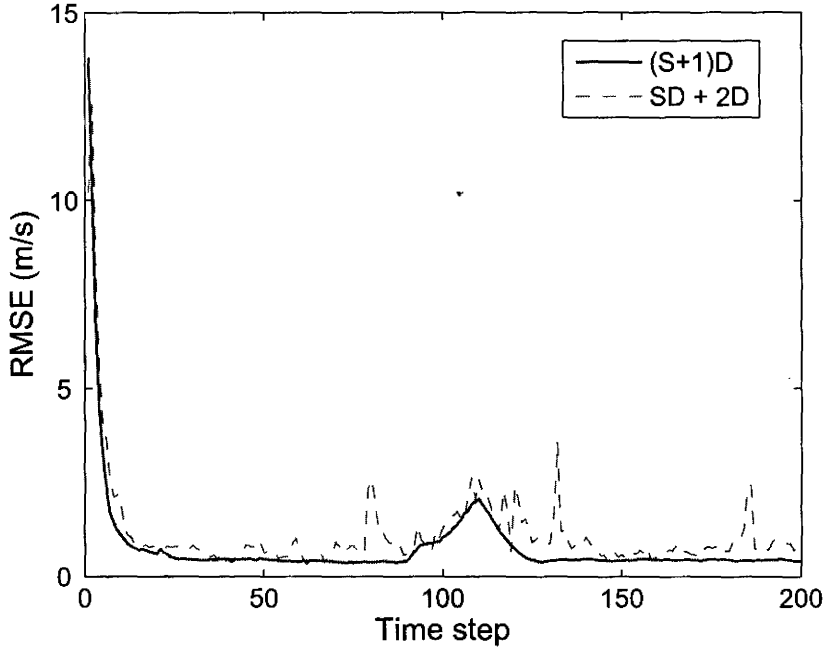

(b) Velocity RMSE (m/s)

Figure 6.6: Position and velocity RMSE averaged over all 5 targets in the first scenario for the S-D + 2-D and $(S+1)$-D data association algorithms.

Chapter 7

TDOA Localization

In this chapter we consider the problem of localizing an emitter from the TDOA measurements. As described earlier, by localization we mean estimating the emitter location using a set of TDOA measurements obtained from various sensors. The assumption here is that there is no measurement origin uncertainty in the set of measurements. That is, all the measurements one have came from the same emitter. As explained in the previous chapter, localization is only required for track initialization in the TDOA tracking framework developed. Once a track has been initialized it can be updated using a nonlinear filter.

In the localization problem, we again assume that several spatially separated sensors measure the TOAs. These TOA measurements are relative to the time of emission, which is not known in an uncooperative environment. Thus, TDOAs are formed from these TOA measurements, which eliminates the unknown emission time. A TDOA measurement relates the unknown emitter position and the known sensor positions. A set of TDOA measurements could then be used to localize the emitter.

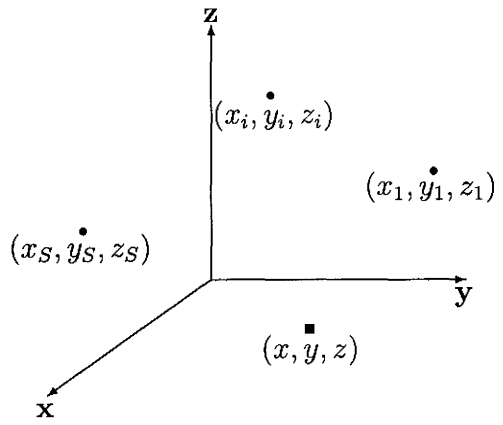

Figure 7.1: Localization scenario.

We first discuss the maximum likelihood estimation (MLE) of the target localization using TDOA measurements and the problems associated with using the MLE technique in practical scenarios. We then describe a formulation based on the sensor-target geometry that will result in another set of equations that can then be solved to localize the emitter.

The geometry-based formulation has been considered perviously in [17, 41, 91]. The solution techniques presented in these papers solved the problem by invoking least squares principles. We view the problem of solving this set of equations as a minimization of a quadratically constrained quadratic program (QCQP). Unfortunately, even though the objective function of this problem is convex, the constraint set is nonconvex. As a result, the QCQP is not easily solvable. We propose two relaxation based techniques to obtain an approximate solution to this formulation.

7.1 Background

Consider the localization problem of an emitter at an unknown location (x, y, z) by a set of S TOA sensors whose known locations are (x_s, y_s, z_s), $s = 1, \ldots, S$. This scenario is illustrated in Figure 7.1. The time t_s at which sensor s receives the emission is given by

$$t_s = t_{em} + \frac{\|H(X - X_s)\|}{c} + v_s \tag{7.1}$$

This equation is the same as that defined in (6.1) and hence, the definitions and assumptions about various quantities remain the same. Note, however, that we now have omitted the index indicating the emitter, since the consideration here is the localization of a single emitter only. Further, since we will only be dealing with the position components of the state of the emitter and sensors to simplify the notation we denote it by Y. That is for the emitter $Y = HX$ and for sensor s, $Y_s = HX_s$.

The unknown emission time can be eliminated by considering the TDOA between two sensors. We consider one of the S sensors as the reference sensor (denoted by 1) and form $(S - 1)$ TDOA measurements. They are then given by

$$\tau_{s1} = h_s(Y) + v_{s1} \qquad s = 2, \ldots, S \tag{7.2}$$

where the measurement function $h_s(Y)$ is actually

$$h_s(Y) = \frac{\|Y - Y_s\|}{c} - \frac{\|Y - Y_1\|}{c} \tag{7.3}$$

To localize an emitter, once the TDOA measurements from the same emitter are identified (say after the data-association step), one can use the set of equations

given in (7.2). We next consider different techniques to localize the emitter.

7.2 Maximum likelihood TDOA localization

In this section, we describe the ML localization of an emitter and the problems associated with it. To obtain the ML estimate first all the $(S-1)$ TDOA equations of (7.2) are stacked to form an $(S-1)$-dimensional vector of TDOAs. This can be written as

$$\tau = H(Y) + v \tag{7.4}$$

where

$$\tau = \begin{bmatrix} \tau_{21} \\ \tau_{31} \\ \vdots \\ \tau_{S1} \end{bmatrix} \qquad H(X) = \begin{bmatrix} h_2(Y) \\ h_3(Y) \\ \vdots \\ h_S(Y) \end{bmatrix} \qquad v = \begin{bmatrix} v_{21} \\ v_{31} \\ \vdots \\ v_{S1} \end{bmatrix} \tag{7.5}$$

Since vector v forms an $(S-1)$-dimensional jointly-Gaussian correlated process, we can write the likelihood function as

$$p(\tau|X) = \frac{1}{\sqrt{|2\pi R|}} \exp\left\{-0.5\,(\tau - H(Y))^T\, R^{-1}\,(\tau - H(Y))\right\} \tag{7.6}$$

where R is the TDOA noise covariance matrix defined in (6.9).

Therefore, the ML estimate of the position vector Y is given by solving the following minimization problem

$$\arg\min_{Y} (\tau - H(Y))^T R^{-1} (\tau - H(Y)) \tag{7.7}$$

The above is a nonlinear and nonconvex minimization problem and there exists

no algorithm to always find the global minimum. The only option one has is to use a global decent algorithm. Any such algorithm, however, would require an initial point close enough to the solution to avoid local minima or divergence. Such an initial point is not obtainable in practical scenarios. Further, the computational cost of the global search algorithms may also be high. Hence, the ML localization of an emitter from TDOA measurements is typically not practical. In the next section we consider a TDOA localization formulation that uses the sensor-emitter geometry.

7.3 Formulation based on the sensor-emitter geometry

Consider the scenario depicted in Figure 7.1. There are S TOA sensors and without loss of generality, we assume that the sensor located at the origin (denoted by 1) as the reference sensor.

If we denote the distance between the emitter and the reference sensor by D_1, then we have

$$D_1 = \|Y\| \tag{7.8}$$

Further, denote the distance between the emitter and the sth ($s = 2, \ldots, S$) sensor by D_s. Then

$$D_s = \|Y - Y_s\| \tag{7.9}$$

Using these definitions, the difference in the distances between the reference sensor and the sth sensor, and the reference sensor and the emitter (or, the range

difference) is given by

$$d_{s1} = D_s - D_1 \qquad s = 2, \ldots, S \tag{7.10}$$

Note that the range difference d_{s1} is proportional to both the TDOA measurement between sensor s and the reference sensor (i.e., τ_{s1}) and the speed of propagation c, that is

$$d_{s1} = c\tau_{s1} \tag{7.11}$$

Eliminating D_s from (7.9) and (7.10), we will get

$$(D_1 + d_{s1})^2 = \|Y - Y_s\|^2 \tag{7.12}$$

Expanding both sides of the above equation and making the substitution $D_1^2 = Y^T Y$ (from (7.8)) and rearranging the terms results in

$$Y_s^T Y + d_{s1} D_1 - \frac{1}{2}(Y_s^T Y_s - d_{s1}^2) = 0 \tag{7.13}$$

Since the TDOAs are not measured precisely (and hence, the range difference d_{s1} is imprecise), an *equation error* is introduced to the above equation [91]. That is

$$e_s = Y_s^T Y + d_{s1} D_1 - \frac{1}{2}(Y_s^T Y_s - d_{s1}^2) \tag{7.14}$$

where e_s is the equation error of the sth sensor. We stack all the $(S-1)$ equation errors and write it in the following matrix form.

$$e = A\theta - b \tag{7.15}$$

In the above error equation

$$e = \begin{bmatrix} e_2 \\ e_3 \\ \vdots \\ e_S \end{bmatrix} \quad \theta = \begin{bmatrix} x \\ y \\ z \\ D_1 \end{bmatrix} \quad A = \begin{bmatrix} x_2 & y_2 & z_2 & d_{21} \\ x_3 & y_3 & z_3 & d_{31} \\ \vdots & \vdots & \vdots & \vdots \\ x_S & y_S & z_S & d_{S1} \end{bmatrix} \quad b = \frac{1}{2} \begin{bmatrix} Y_2^T Y_2 - d_{21}^2 \\ Y_3^T Y_3 - d_{31}^2 \\ \vdots \\ Y_S^T Y_S - d_{S1}^2 \end{bmatrix} \tag{7.16}$$

It would be tempting to think that in order to localize the emitter one needs find the least squares solution — that is the θ that minimizes the sum of the square of the equation errors (i.e., $\|e\|^2$) — of (7.15). It is important to note that such a solution assumes that the elements of the unknown θ are independent. In the above formulation this is not the case since $Y = [x, y, z]^T$ and D_1 are related by (7.8). We need to explicitly incorporate this relationship between the elements of θ while minimizing $\|e\|^2$. That is we can localize the emitter by solving the following constrained optimization problem.

$$\begin{aligned} &\arg\min_{\theta} \quad \|e\|^2 \\ &\text{subject to} \quad \theta^T B \theta = 0 \end{aligned} \tag{7.17}$$

where

$$B = \begin{bmatrix} 1 & 0 & 0 & 0 \\ 0 & 1 & 0 & 0 \\ 0 & 0 & 1 & 0 \\ 0 & 0 & 0 & -1 \end{bmatrix} \tag{7.18}$$

By substituting for e from (7.15), we will get the following.

$$\begin{aligned} \arg\min_{\theta} \quad & \theta^T A^T A\theta - 2\theta^T A^T b + b^T b \\ \text{subject to} \quad & \theta^T B\,\theta = 0 \end{aligned} \tag{7.19}$$

This is clearly a QCQP [16]. The objective function is quadratic and convex (provided that $A^T A$ is positive semidefinite). The feasible set defined by the constraint is, however, not a convex set. Therefore, the QCQP in (7.19) is not a convex QCQP. In the following we describe two relaxation-based methods to solve the above QCQP and comment on their solution accuracy.

7.4 Solutions to the TDOA QCQP

In this section we explain in detail two techniques to solve the localization formulation in (7.19). Both these techniques relax the original QCQP and solve the relaxed problems. From the solutions of these relaxed problems a solution to the original problem are found.

7.4.1 Relaxation based on the equivalent rank one problem

In this method we perform a direct relaxation of (7.19). The relaxation thus obtained is a semidefinite program (SDP) and hence is convex. There are several algorithms and software implementations that exist to obtain the optimal solution to the SDP [16]. Once the optimal solution to the relaxed SDP is found, we obtain a solution to the localization problem using a randomization technique.

In particular, we can rewrite (7.19) as

$$\begin{aligned} \arg\min_{\tilde{\theta}} \quad & \tilde{\theta}^T B \tilde{\theta} \\ \text{subject to} \quad & \tilde{\theta}^T \Lambda \tilde{\theta} = 0 \end{aligned} \tag{7.20}$$

where

$$\tilde{\theta} = \begin{bmatrix} \theta \\ 1 \end{bmatrix} \quad \tilde{A} = \begin{bmatrix} A^T A & A^T b \\ b^T A & b^T b \end{bmatrix} \quad \tilde{B} = \begin{bmatrix} B & 0 \\ 0 & 0 \end{bmatrix} \tag{7.21}$$

By defining a new variable $\Psi = \tilde{\theta}\tilde{\theta}^T$ and noting that for any square matrix Y

$$\tilde{\theta}^T Y \tilde{\theta} = \text{tr}(Y \tilde{\theta}\tilde{\theta}^T) \tag{7.22}$$

where tr(.) denotes the trace of a matrix, we can transform the above problem to the following:

$$\begin{aligned} \arg\min_{\Psi} \quad & \text{tr}(\tilde{A}\Psi) \\ \text{subject to} \quad & \text{tr}(\tilde{B}\Psi) = 0 \\ & \Psi = \tilde{\theta}\tilde{\theta}^T \\ & \Psi_{[4,4]} = 1 \end{aligned} \tag{7.23}$$

This problem is difficult to solve due to the rank one constraint, namely

$$\Psi = \tilde{\theta}\tilde{\theta}^T \tag{7.24}$$

If, however, this constraint is relaxed, we will end up with the following problem:

$$\begin{aligned} \arg\min_{\Psi} \quad & \mathrm{tr}(\tilde{A}\Psi) \\ \text{subject to} \quad & \mathrm{tr}(\tilde{B}\Psi) = 0 \\ & \Psi_{[4,4]} = 1 \\ & \Psi \succcurlyeq 0 \end{aligned} \tag{7.25}$$

This clearly is an SDP [16] and can be solved using off-the-shelf software. If the optimal solution to this relaxed problem (let it be Ψ^*) satisfies the rank one constraint, that is, if

$$\Psi^* = \tilde{\theta}^*(\tilde{\theta}^*)^T \tag{7.26}$$

then θ^* — consisting of the first three elements of $\tilde{\theta}^*$ — is the optimal solution to the localization problem given in (7.19). If the optimal solution does not satisfy the rank one constraint then randomization techniques can be used to obtain a solution to (7.19). We used the following randomization algorithm to get a solution when the rank one constraint was not satisfied by the optimal solution to the relaxed problem.

1. The size of Ψ^* is 4×4. From this the 3×3 matrix corresponding to the first two rows and columns is extracted and a new matrix is formed. Let this matrix be Ψ_2^*.

2. The Cholesky factor of the matrix Ψ_2^* is computed. That is

$$\Psi_2^* = LL^T \tag{7.27}$$

3. A number of candidate solutions $\hat{\theta}$ to the localization problem are generated using

$$\hat{\theta} = \begin{bmatrix} L^T u \\ \|L^T u\| \end{bmatrix} \tag{7.28}$$

where u is a unit normal random vector.

4. Out of all these candidate solutions the one that minimizes

$$(A\hat{\theta} - b)^T (A\hat{\theta} - b) \tag{7.29}$$

is selected as the estimate to the localization problem.

It has to be noted that there is, however, no guarantee that the solution thus obtained using randomization will be closer to the optimal solution. In our extensive simulation study we found that the solution obtained using the above randomization was closer to the true emitter location.

7.4.2 Lagrangian dual-based solution

The Lagrangian function of the constraint optimization problem posed in (7.19) is given by

$$L(\theta, \nu) = (A\theta - b)^T (A\theta - b) + \nu \theta^T B \theta \tag{7.30}$$

where ν — a scalar — is the Lagrange multiplier. We can simplify the Lagrangian function to

$$L(\theta, \nu) = 2(A^T A + \nu\Sigma) - 2b^T A\theta + b^T b \tag{7.31}$$

The Lagrangian dual function is infimum of the Lagrangian function with respect

to the primal variable θ. That is

$$g(\nu) = \inf_{\theta} L(\theta, \nu) \tag{7.32}$$

A necessary condition for the minimization of the Lagrangian is

$$\frac{\partial L(\theta, \nu)}{\partial \theta} = 0 \tag{7.33}$$

For the above Lagrangian function applying this condition yields

$$2(A^T A + \nu\Sigma)\theta - 2A^T b = 0 \tag{7.34}$$

Therefore, the primal variable that minimizes the Lagrangian function is given by

$$\theta_{min} = (A^T A + \nu\Sigma)^{-1} A^T b \quad \text{provided} \quad A^T A + \nu B \succcurlyeq 0 \tag{7.35}$$

The Lagrangian dual function of QCQP in (7.19) can then be shown to be

$$g(\nu) = \begin{cases} b^T b - b^T A(A^T A + \nu B)^{\dagger} A^T b & A^T A + \nu B \succcurlyeq 0 \\ -\infty & \text{otherwise} \end{cases} \tag{7.36}$$

The Lagrangian dual problem is the maximization of the dual function over the Lagrangian multiplier. That is

$$\max_{\nu} g(\nu) \tag{7.37}$$

Hence, using (7.36) we can write the dual problem of (7.19) as

$$\begin{aligned} \max_{\nu} \quad & b^T b - b^T A(A^T A + \nu B)^\dagger A^T b \\ \text{subject to} \quad & A^T A + \nu B \succcurlyeq 0 \end{aligned} \tag{7.38}$$

This dual problem can be easily transformed to the following problem.

$$\begin{aligned} \max_{\nu,t} \quad & t \\ \text{subject to} \quad & t \leq b^T b - b^T A(A^T A + \nu B)^\dagger A^T b \\ & A^T A + \nu B \succcurlyeq 0 \end{aligned} \tag{7.39}$$

After rearranging the terms in the above form of the dual problem, we will get

$$\begin{aligned} \max_{\nu,t} \quad & t \\ \text{subject to} \quad & (b^T b - t) - b^T A(A^T A + \nu \Sigma)^\dagger A^T b \geq 0 \\ & A^T A + \nu B \succcurlyeq 0 \end{aligned} \tag{7.40}$$

Applying the Schur complement [101] to the above formulation we will get the following.

$$\begin{aligned} \max_{\nu,t} \quad & t \\ \text{subject to} \quad & \begin{bmatrix} A^T A + \nu \Sigma & A^T b \\ b^T A & (b^T b - t) \end{bmatrix} \succcurlyeq 0 \\ & A^T A + \nu B \succcurlyeq 0 \end{aligned} \tag{7.41}$$

Hence, the problem in (7.41) is equivalent to the dual problem and also it clearly is an SDP. Once an optimal solution to the dual problem is obtained (let it be ν^*),

we can find the θ that minimizes the Lagrangian function (let it be θ^*) by

$$\theta^* = (A^T A + \nu^* B)^{-1} A^T b \tag{7.42}$$

This θ^* is a solution for the primal problem if it is primal feasible. Further, this would be the optimal solution to the primal problem if strong duality — i.e., the optimum values of the primal and dual are the same — holds. If θ^* is not primal feasible then we need to resort to some heuristics to generate approximate primal solutions to the primal problem.

It has to be noted, however, that in our simulations, for all the scenarios considered, the θ^* thus obtained was primal feasible (or, within acceptable numerical tolerances). We think that this is because for the problem in (7.19) strong duality holds. We, however, still have not proved it analytically.

7.5 Simulations

This section presents simulation results on the performance of the proposed solutions to the localization problem. Further, comparison with the techniques presented in [40] and [91] are also made. We, however, did not compare with the ML estimator, since as discussed earlier, ML estimation requires an initial solution that is close enough to the emitter position and such an initial solution is not available in practical scenarios.

The two scenarios for which the results are presented are shown in Figure 7.2. The 2-D scenario is from [40] and the 3-D scenario is from [91]. In the 2-D scenario there were ten sensors located at (0,0), (-5,8), (4,6), (-2,4), (7,3), (-7,5), (2,5), (-4,2), (3,3), and (1,8), respectively. The emitter was located at (8,22). All the units

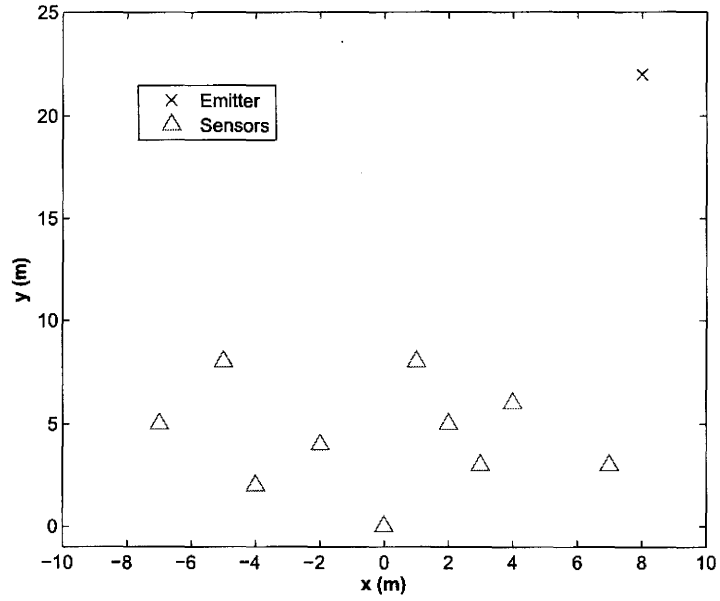

(a) 2-D example scenario.

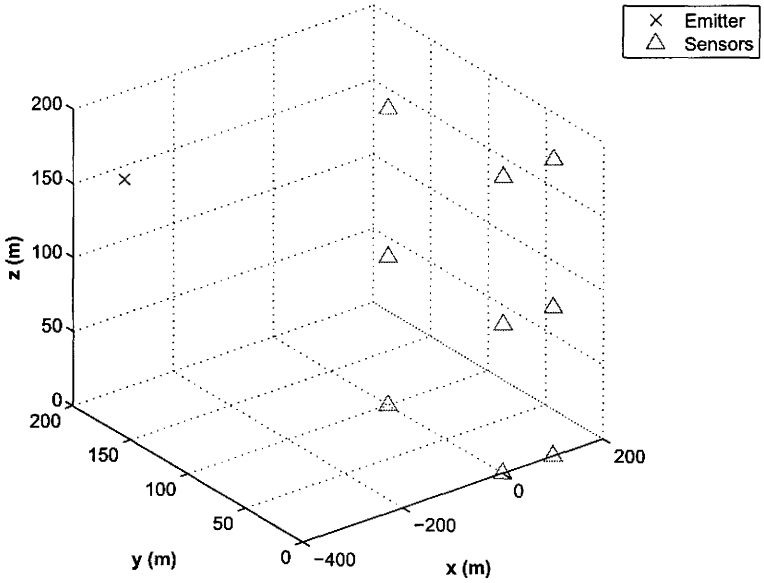

(b) 3-D example scenario.

Figure 7.2: Simulation scenarios.

are in meters.

The simulations were implemented in MATLAB. To solve the SDPs in both the proposed relaxation algorithms, a MATLAB-based software SeDuMi (self-dual minimization) [87] was used. In the randomization step of the technique presented in Section 7.4.1, 100 candidate solutions were generated.

For different range difference standard deviations the root mean square error (RMSE) was calculated in 1000 Monte Carlo runs and the results are shown in Table 7.1. In this table, Relax-A refers to the solution proposed in Section 7.4.1, Relax-B refers to the one described in Section 7.4.2, SI (spherical interpolation) refers to the method proposed in [91], and EEHL refers to the efficient estimator for hyperbolic location discussed in [17]. It can be seen from this table that both the methods proposed in this paper perform comparable to the previously proposed methods. In fact, in the low noise Relax-A outperforms all the other three solution techniques.

Table 7.2 tabulates the localization results for a source far from the sensor array. It was located at (-50,250)m. In this case except in low noise case the RMSEs for all the methods were very high. This is because in (7.14) just the introduction of equation error does not characterize the true nature of the error due to noisy TDOA measurements.

In the 3-D example there were 9 sensors located at (0,0,0), (0,0,100), (0,0,200), (100,0,0), (100,0,100), (100,0,200), (0,100,0), (0,100,100), and (0,100,200)m, respectively. The emitter was located at (-390,160,170)m. Again, the range difference standard deviation was varied and the RMSE results are compared in Table 7.3. The proposed techniques give comparable performance.

The advantage of the proposed techniques, in comparison to the hyperbolic estimator of [17], is that the hyperbolic estimator always produces two solutions to the localization problem. In order to select the correct solution one needs to know the quadrant in which the emitter lies. This requirement will become difficult to satisfy in realistic multitarget scenarios.

The spherical interpolation technique of [91] does not require any prior knowledge as do the proposed techniques. The spherical interpolation technique, however, requires at least four TDOA measurements to localize an emitter[1]. If the spherical interpolation technique were used in the TDOA tracking framework of the previous chapter, it may delay the initialization of a target, since it is not possible to localize an emitter using an S-tuple with three TDOA measurements (or four TOA measurements).

Figure 7.3 gives the reason why we believe that for the QCQP of (7.19) strong duality holds. This figure gives the average duality gap and on average how far the solution, obtained using the technique detailed in Section 7.4.1, violated the constraint. From this figure, it is clear, at least for the scenarios considered, that the duality gap is nearly zero and the equality constraint is nearly satisfied (except, of course, for some numerical errors). We, however, would like to reiterate again that we still do not have analytical proof for strong duality. We would, however, like to note that there are proofs for the strong duality in nonconvex QCQP with two quadratic constraints [7].

[1]Note that three TDOA measurements are adequate to localize an emitter in the three dimensional plane.

Table 7.1: RMSE for different range difference standard deviation for the 2-D case for near source

Method	RMSE (m)		
	$\sigma = 0.01$	$\sigma = 0.05$	$\sigma = 0.1$
Relax-A	0.1213	0.5675	1.1443
Relax-B	0.1249	0.6257	1.2662
SI	0.1249	0.6257	1.2662
EEHL	0.1330	0.6707	1.3918

7.6 Conclusions

Two solution techniques have been presented in this chapter to the localization problem of an emitter using the TDOA measurements. These solutions were based on the sensor-emitter geometry formulation. Extensive simulations were carried out to test the validity of the solutions. The simulation results show that the proposed methods have performed comparable and in some cases better than the methods compared with, namely, the SI and EEHL methods. Unlike the EEHL technique, which requires the quadrant in which the emitter lies to give an unambiguous location estimate (and like SI) both the proposed solutions do not require any prior knowledge.

It has to be noted that the dual-based solution in all the simulations carried out produced a primal feasible solution. Unless strong duality holds, it could possibly produce solutions that are not primal feasible. It would be interesting to determine analytically whether strong duality actually holds.

Table 7.2: RMSE for different range difference standard deviation for the 2-D case for far source

Method	RMSE (m)		
	$\sigma = 0.001$	$\sigma = 0.01$	$\sigma = 0.1$
Relax-A	2.0028	18.6162	230.5973
Relax-B	2.3351	23.6290	214.8745
SI	2.3351	23.6290	214.8745
EEHL	2.4003	26.4740	219.0923

Table 7.3: RMSE for different range difference standard deviation for the 3-D case

Method	RMSE (m)		
	$\sigma = 0.1$	$\sigma = 0.5$	$\sigma = 1$
Relax-A	9.2231	14.0695	25.7781
Relax-B	2.4402	12.6725	24.9360
SI	2.4400	12.6725	24.9361
EEHL	2.4228	12.5692	24.9652

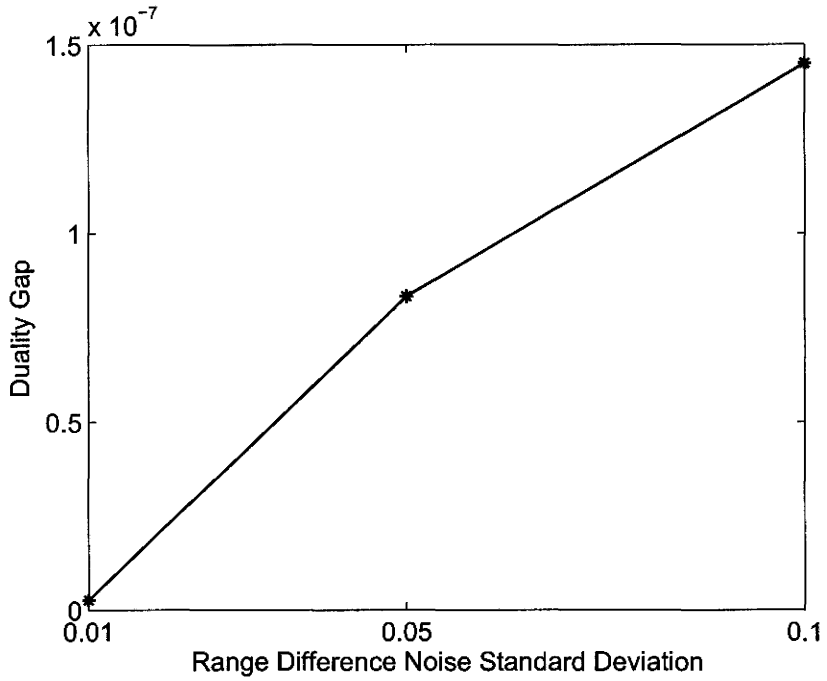

(a) Duality gap

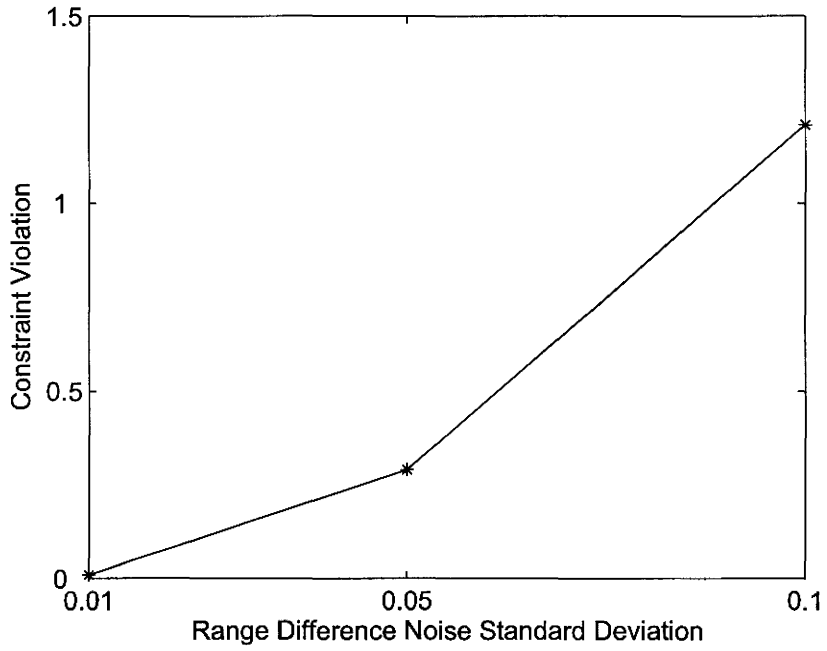

(b) Constraint violation

Figure 7.3: Average duality gap and constraint violation for the 2-D case.

Chapter 8

A New Algorithm to Form Mono Angle Only Tracks

The passive tracking algorithms described in the previous chapters are suitable for centralized tracking. In a centralized tracking system measurements from various sensor platforms are transmitted to a central fusion center where these measurements are processed to perform state estimation. One of the problems with centralized tracking is that when the false alarm rate is high, which typically is the case with passive observations, one needs to transmit a lot of measurements unnecessarily. This will also result in bandwidth requirement.

One approach considered in distributed tracking systems to reduce the bandiwidth requirement is to perform sensor-level processing to form local tracks and transmit the information about these tracks. In the central node, track-to-track association [49] is performed and the associated tracks are fused [18] to form global tracks.

When angle only sensors are deployed at different locations, a stereo track (i.e.,

a track that includes target position) cannot be formed from the measurements of a single sensor. In such cases, one could form mono tracks. Then, only the mono tracks can be sent to the central fusion node for further processing. This reduces the unnecessary measurement transmission and hence, improves bandwidth efficiency. In this chapter, we present an algorithm for the formation of angle only mono tracks from the observations of a uniform linear array (ULA).

We would like to point out an analogy between the formation of the mono tracks and a well-known problem in the signal processing community – the direction of arrival (DOA) estimation/tracking problem [52]. Traditionally, in signal processing the direction from which a signal impinges on an array of sensors is considered as a parameter estimation problem. That is, the DOA is assumed to be fixed. This assumption allowed for high-resolution DOA estimation techniques, such as the maximum likelihood (ML) [69] and MUSIC [85] that used temporal averaging of samples taken over several snapshots.

In practice, however, stationarity assumption of the DOA is questionable since the targets of interest are often moving objects. Further, the number of targets could change dynamically. In such cases, DOA estimation techniques may provide inaccurate estimates. Therefore, recently there has been a great deal of interest in developing DOA tracking algorithms. The algorithms proposed in [37, 48] assumed piece-wise stationarity of the DOAs and also assumed fixed numbers of sources. A particle filtering approach, which did not make such assumptions, for DOA tracking has been proposed in [54, 64]. Particle filtering techniques are generally computationally expensive.

The algorithm presented in this chapter to form angle only mono tracks (or the

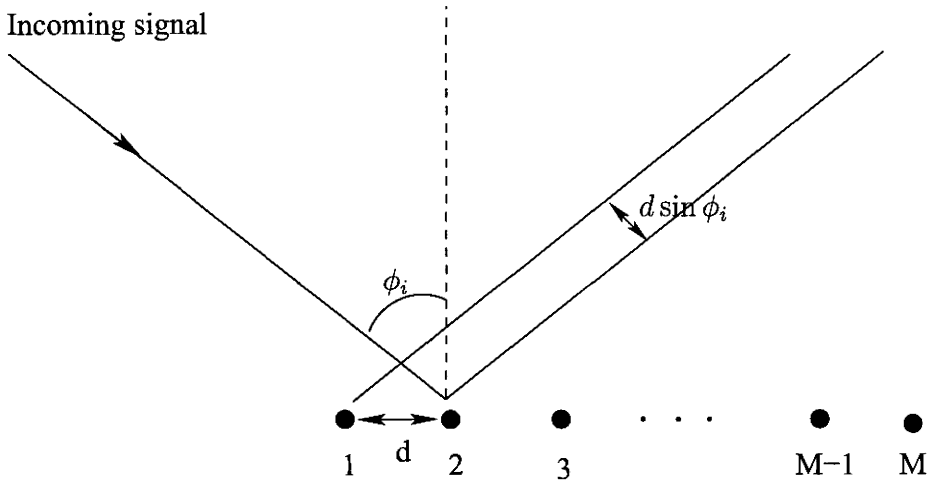

Figure 8.1: ULA with M elements and an interelement spacing of d.

DOA tracking) uses the fast Fourier transform (FFT) to generate the angle measurements from the observations of the sensor array at each scan. Angle measurements from different scans are associated by using the efficient $(S + 1)$-D assignment algorithm to form the mono tracks. Once the association step is over one could send all the associated measurements to the central fusion node. We will now describe this algorithm in detail.

8.1 Uniform linear array — Signal model

A ULA refers to an array of sensors that have equal spacing between different array elements. A ULA, consisting of M array elements, is shown in Figure 8.1. Interelement spacing is denoted by d. The incoming signal arrives at the array at an angle of ϕ_i. For clarity, only one signal is shown in the figure. In the following, however, we assume that there could be an unknown number of signals arriving from different

angles.

We assume that the signals impinging on the array are narrowband. This means that the signal bandwidth is small compared to the carrier frequency. This assumption allows one to approximate the propagation delay of a particular signal between sensor elements with a phase shift [55]. Further, we assume that there are N signals impinging on the array. Note that N could be time varying and we do not assume specific knowledge of it in the algorithm.

The time delay τ between any two successive array elements for a signal arriving from the direction ϕ_i is

$$\tau = \frac{d \sin \phi_i}{c} \tag{8.1}$$

where c is the speed of propagation of the signal. Hence, the delay between the first element and the mth element is given by

$$\tau_m = (m-1)\frac{d \sin \phi_i}{c} \tag{8.2}$$

The response of the mth sensor of a ULA at time k is [55]

$$y_m = \sum_{n=1}^{N} a_n s(\phi_n) + w_m \qquad m = 1, 2, \ldots, M \tag{8.3}$$

In the above a_n is the amplitude of the nth signal, w_m is the additive noise at the mth sensor, and $s(\phi_n)$ is the steering vector corresponding to emitter n. Note that for notational clarity we have omitted the time index k from all the quantities. The

steering vector is given by

$$s(\phi_n) = \begin{bmatrix} 1 \\ \exp\left(-j\frac{2\pi d}{\lambda}\sin\phi_n\right) \\ \vdots \\ \exp\left(-j\frac{2\pi d}{\lambda}\sin\phi_n(M-1)\right) \end{bmatrix} \tag{8.4}$$

where λ is the wavelength of the narrowband signal.

8.2 DOA generation

It is possible to draw a direct correspondence between the spatial samples from a ULA (8.3) and regular temporal sampling [55]. This is because ULA samples a signal uniformly in space on a linear axis. Hence, y_m, $m = 1, 2, \ldots, M$, can be considered equivalent to M discrete-time samples. It is also not difficult to see from (8.3) that the samples y_m consists of N complex exponential signals with *frequencies*

$$\omega_n = \frac{d}{\lambda}\sin\phi_n \tag{8.5}$$

Note that this frequency may become negative since the unambiguous range for ϕ_n is

$$-\pi/2 \leq \phi_n \leq \pi/2 \tag{8.6}$$

With the above definition of frequency it is now possible to define the discrete-time Fourier transform (DTFT) for the discrete sequence y_m ($m = 0, 1, \ldots, M-1$). It is

given by [65]

$$Y(\omega) = \frac{1}{M} \sum_{m=0}^{M-1} y_m \exp(-j\omega m) \tag{8.7}$$

where $Y(\omega)$ are the DTFT coefficients. Note that the frequency range now is

$$-\frac{d}{\lambda} \leq \omega \leq \frac{d}{\lambda} \tag{8.8}$$

Since the sequence y_m are samples of a signal consisting of N complex exponential signals, the DTFT spectrum ideally will consists of N spectral peaks corresponding to the frequencies of these complex exponentials. Hence, if a peak in the DTFT spectrum occurs at ω^*, then the corresponding DOA can be obtained from this peak as

$$\phi = \arcsin\left(\frac{\lambda}{d}\omega^*\right) \tag{8.9}$$

In practice, however, due to the measurement noise and spectral leakage, the number of peaks that appear in the DTFT spectrum may not be equal to the actual number of signals that impinge on the ULA. To eliminate smaller peaks that are primarily due to spectral leakage, we can set a threshold and select only the peaks whose values exceed that threshold as potential measurements.

8.3 Tracking

As discussed before, at each time step by performing DTFT operation on the ULA response one could obtain a set of angle measurements. These measurements can be sent to the central fusion node. Angle measurements from different ULAs can then be used to track the emitter. This, however, would result in high bandwidth requirement, especially, when the false alarm rates are high.

One approach to reduce the bandwidth requirement is to identify the measurements that have originated from targets of interest at the local fusion center and send only those measurements to the central fusion center. Deciding whether a measurement has originated from a particular target or not cannot be performed based on the DOAs obtained from the above step alone. If, however, one forms the angle only mono tracks, i.e., if one tracks the angles that are originated from the same target, then these mono tracks can be transmitted to the central fusion node. The mono tracks received from different ULAs at the central node can then be used to form stereo tracks.

The formation of mono tracks can be achieved through the $(S+1)$-D assignment algorithm developed in Chapter 4 with a simple modification. In the $(S+1)$-D algorithm, the first dimension was the predicted track state and the rest of the S dimensions were measurement lists of various sensors at the same scan. Now, if we assume that the first dimension is the predicted angles from one scan and the rest of the S dimensions are the DOA measurements obtained at successive scans, then we can apply the $(S+1)$-D assignment algorithm to form angle only mono tracks.

Assume that the DOA from a target varies according to the following dynamic model

$$\phi^k = f(\phi^{k-1}) + v^{k-1} \tag{8.10}$$

where f is a mapping between the DOA at time $k-1$ and that at time k, i.e., the state transition function. v is the additive measurement noise. Here, the state is actually the DOA. Further, assume that the mono track at time k is characterized by the mean $\hat{\phi}^k$ and its covariance P^k. And also assume that S lists of angle measurements from scan $k+1$ to $k+S$ are available.

It is now required to find the measurements from each scan that could have

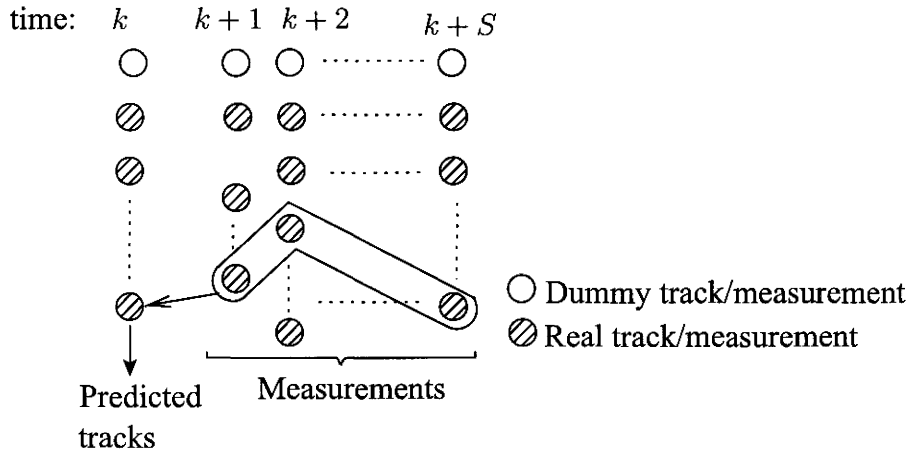

Figure 8.2: $(S+1)$-D assignment in time.

originated from the same target. This data association problem can be solved by considering an $(S+1)$-D assignment as illustrated in Figure 8.2.

This figure is similar to that was shown in Figure 4.2 except that we now have explicitly added the dummy track. The cost of the assignment, i.e., assigning an S-tuple of DOA measurements $(\phi_1, \phi_2, \ldots, \phi_S)$ to a mono track p, is now defined as

$$c_{p\phi_1\phi_2\ldots\phi_S} = -\ln \frac{\psi(p, \phi_1, \phi_2, \ldots, \phi_S)}{\psi(0, \phi_1, \phi_2, \ldots, \phi_S)} \tag{8.11}$$

where $\psi(p, \phi_1, \phi_2, \ldots, \phi_S)$ is the joint likelihood that the S-tuple of measurements originated from the same target represented by track p and $\psi(0, \phi_1, \phi_2, \ldots, \phi_S)$ is likelihood that the S-tuple of measurement originated from an extraneous source.

The multiframe assignment would then be similar to the one given in (3.9) with $S+1$ dimensions. Once a solution to the $(S+1)$-D assignment is obtained one could update the tracks with the corresponding S-tuple of DOA measurements those tracks received. Then with tracks updated up to scan $k+S$, next set of

measurements can be considered for association in a similar manner.

A better approach, however, is to implement the association as a sliding window. This means that after the assignment between the tracks from scan k and measurements from scan $k+1$ to $k+S$, instead of updating the tracks with the S-tuple of measurements they got assigned to, the tracks are updated only with the measurements from scan $k+1$. With the tracks updated to scan $k+1$, an $(S+1)$-D assignment can be performed between these updated tracks and S lists of measurements from scan $k+2$ to $k+S+1$. That is, the algorithm progresses in a sliding window fashion. When implemented in such a sliding window fashion, the multi-frame assignment mimics the optimal multiple hypothesis tracking algorithm [81] within the window.

8.4 Simulations

We apply the proposed algorithm to the DOA tracking scenario similar to the one presented in [54]. There are two targets in the region of interest and their DOA is assumed to obey a random-walk model. That is

$$\phi_n^k = \phi_n^{k-1} + v_n^{k-1} \tag{8.12}$$

where the process noise is assumed to be zero-mean Gaussian process with variance of σ_v^2 for both targets. This creates a nonstationary DOA environment. Further, one of the sources is assumed to leave the scenario at time $k = 25$.

The received signal, i.e., the array response, is the same as (8.3). We assume that the process noise is zero-mean Gaussian distributed with variance σ_w^2. The amplitude a_n varies according to a random-walk model (similar to (8.12)). The

Table 8.1: Simulation parameters

Parameter	σ_v^2	σ_w^2	σ_a^2	$\phi(0)$	a(1)
Value	$5^{\circ 2}$	0.15	0.0707	$[-20°,70°]$	$[2-2j, 4+j]$

amplitude variation is driven by a zero-mean Gaussian process having variance σ_a^2. It is also assumed that the ULA consists of $M = 8$ array elements. Values of various parameters used in the simulation are given in Table 8.1.

In the tracking algorithm we used the $(S+1)$-D data association algorithm with a time depth of three, i.e., $S = 3$. The DOA measurements from the DTFT spectrum will not be exact due to measurement noise and numerical approximations involved in estimating the peaks. We model the error in the DOAs as a zero-mean Gaussian random variable. We used a Kalman filter [6] to track the DOAs since the state-space model is linear.

Figure 8.3 shows the tracking results obtained in a single Monte Carlo run. In this figure, the variation of the DOAs and their estimates are shown. Note that during the entire simulation period the estimates follow the true DOAs closely. Further, the change in the number of targets is detected correctly by the algorithm. The delay in deleting the track corresponding to the target that left the surveillance region is due to the track deletion logic used — a track is considered lost only if it did not receive any measurements for three consecutive scans.

The root mean square error (RMSE) performance of the algorithm is shown in Figure 8.4. Note that there seems to be an improvement in the RMSE after 25th time step. This is because, once the second target has left, the data association problem becomes simpler, and as a result miss association possibilities are reduced.

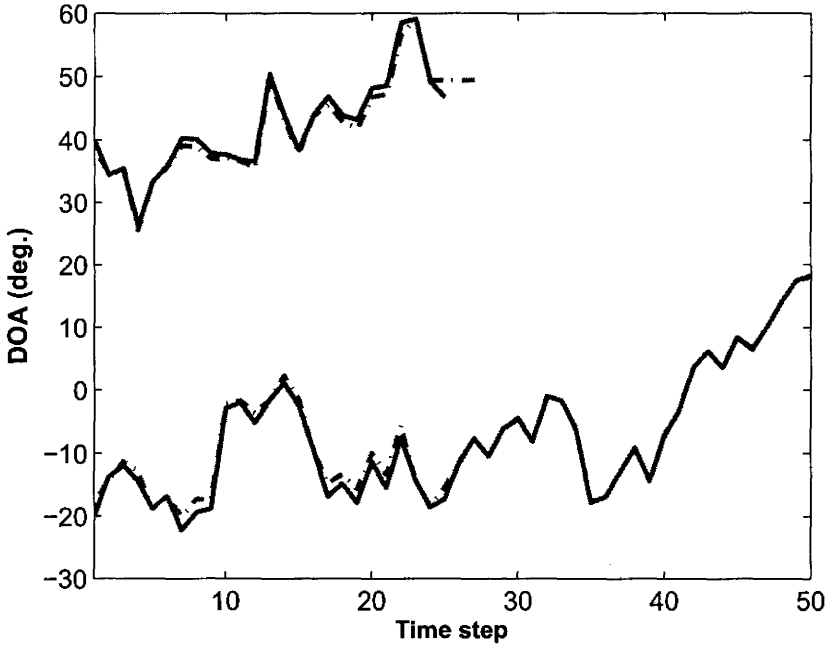

Figure 8.3: True DOA variation and their estimates.

Consequently, the tracking performance improves.

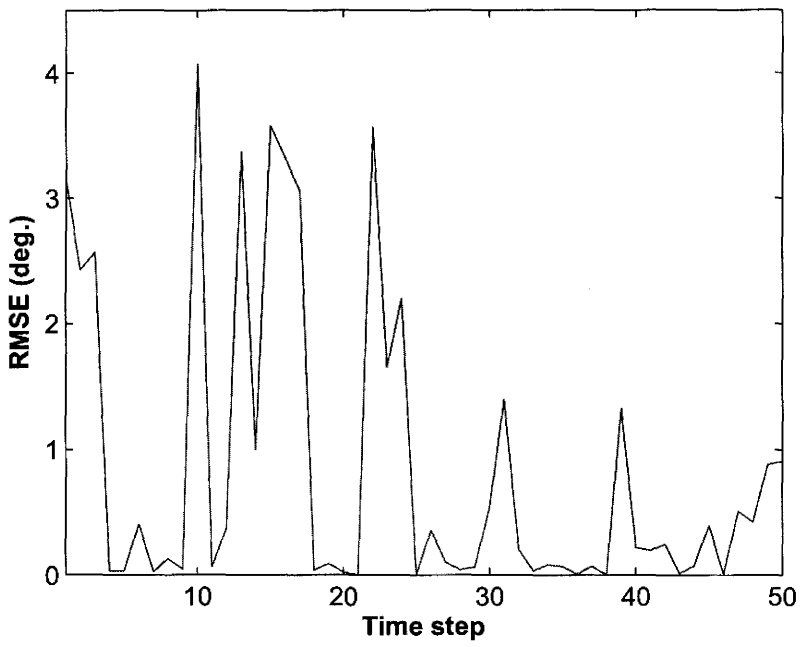

Figure 8.4: RMSE in DOA estimation.

Chapter 9

Summary

This final chapter presents some concluding remarks and provides possible directions for future research.

9.1 Conclusions

This thesis identified several challenging problems in passive localization and tracking and attempted to provide some solutions to these problems. The primary scenario considered is tracking with multiple synchronous passive sensors (i.e., Type 3 initialization and maintenance systems). This typically calls for a centralized tracking architecture and, as a result, presents real computational challenges to any tracking algorithm, since the data association becomes an increasingly complex task.

Two efficient algorithms that are based on a multidimensional assignment formulation were proposed in this thesis to solve the data association in Type 3 systems. The simulation study performed on realistic scenarios (whose results are

presented) showed that the performance of these algorithms is better than the traditional solution, and this performance improvement comes at a significantly reduced computational cost. Also, an approximation to the $(S+1)$-D algorithm, which directly assigns the measurements to the tracks (when sensors are uncorrelated), resulted in a much faster algorithm.

In target tracking, when tracking with passive measurements, most of the studies have only considered uncorrelated measurements. In fact, these studies were restricted to AOA measurements. We presented a framework for tracking with correlated passive measurements with TDOA measurements as the representative example. The data association solution based on assignment algorithm has been modified to account for the correlated TDOA measurements.

The maximum likelihood localization of an emitter using TDOA measurements results in an optimization problem that is highly nonlinear. Hence, obtaining the ML estimate may not be feasible in practical scenarios. Another formulation based on sensor-emitter geometry results in a set of nonlinear equations and the solution of this set of equations localizes the emitter. Our approach to solving this set of equations is to view it as a quadratically controlled quadratic program (QCQP). We proposed two relaxation-based solutions to solve this QCQP. One of them uses direct relaxation of the constrained optimization problem, while the other uses the Lagrangian relaxation. The performances of these algorithms are tested against other well-known solutions. These results suggest that the proposed algorithms perform comparable to those solutions. The advantages and disadvantages of these solutions have also been discussed.

Finally, we also provided an efficient algorithm to form angle only mono tracks when a uniform linear array is used to receive the emissions from the targets. This

algorithm used the DTFT on the received emission to obtain the angle measurements and used assignment based data association to track the angles from the same targets, hence, forming the mono tracks. Formation of the mono tracks usually results in reduced communication load in distributed tracking systems.

9.2 Future work

In this section we identify some extensions to the work that was performed in this thesis to extend the applicability and capability of the proposed algorithms.

As noted earlier, modern tracking systems typically use multiple types of sensors to improve the tracking performance because of the improvements made in sensor technologies and computational capabilities. Hence, it would be worthwhile to study what modifications are needed to these data association algorithms to be used in conjunction with different types of measurements. Also it would be useful to see whether it is efficient to perform the association of these measurements together or to perform the association of the similar types of measurements first to form tracks and then follow this with a track-to-track association.

Also, with regards to the efficient data association algorithms, the simulation study was based on a MATLAB implementation. MATLAB, being a high level language, is not suitable for real-time implementations. Consequently, simulations results presented on computational efficiency of these algorithms are only indicative of the comparative efficiency of these algorithms. These results do not provide any conclusive proof regarding the real-time performance of these algorithms. It would be interesting to see how the computational efficiency of these algorithms would be when implemented in a programming language such as C.

Further, the tracking performance of these algorithms has also been tested on simulated data. Although the data used in the simulations tried to model the real world scenarios (with missed detections and false alarms), it would be an interesting and different exercise to test these algorithms on actual real-world data. The performance of these algorithms may degrade when applied to real-world data since various assumptions, such as Gaussian noise model and Poisson false alarm model that are made may not be met. We, however, believe that the relative performances would remain the same. It has to be noted that the testing of these algorithms with real-world data requires a low level implementation of these algorithms, since such data would have hundreds of targets, and thousands of measurements.

With regards to the optimization solution to the TDOA equations, it would be a challenging proposition to prove or disprove the strong duality of the problem. While proving strong duality will give the optimal localization solution for the TDOA case, disproving it would be helpful in entertaining caution when interpreting the results of this algorithm. In addition, a related problem is the approximation introduced in the TDOA equation through the introduction of the equation error. As seen in the simulation results this equation error did not capture the true nature of the error in some scenarios. One could think about other ways to better approximate the effects of TDOA noise into the error free sensor-emitter equation.

The direction of arrival tracking problem considered only the case where the sensor was a uniform linear array. An interesting problem arises if the array elements are not uniformly placed. It is not clear whether the same steps can be followed to form mono tracks in such a case. Further, it was assumed that the emissions are narrowband signals. An interesting extension would be to consider the case of wideband emissions, with or without uniform linear arrays.

APPENDIX

Here we prove that when the cost of S-D assignment $c_{i_1 i_2 \ldots i_S}$ decomposes, that is, if

$$c_{i_1 i_2 \ldots i_S} = \sum_{s=2}^{S} c_{i_1 i_s} \tag{9.1}$$

then performing the S-D assignment is equivalent to performing a set of 2-D assignments. Consider now the objective function of the S-D assignment defined in (3.9). With the decomposed cost the objective function can be written as

$$\sum_{i_1=0}^{n_1} \sum_{i_2=0}^{n_2} \cdots \sum_{i_S=0}^{n_S} \left(\sum_{s=2}^{S} c_{i_1 i_s} \right) \rho_{i_1 i_2 \ldots i_S} \tag{9.2}$$

It is possible to define the binary indicator variable $\rho_{i_1 i_2 \ldots i_S}$ as

$$\rho_{i_1 i_2 \ldots i_S} = \prod_{s=2}^{S} \gamma_{i_1 i_s} \tag{9.3}$$

where $\gamma_{i_1 i_s}$ is equal to one if an S-tuple containing (i_1, i_s) is added to the solution set, otherwise it is zero. Hence with redefined binary indicator the objective function becomes

$$\sum_{i_1=0}^{n_1} \sum_{i_2=0}^{n_2} \cdots \sum_{i_S=0}^{n_S} \left(\sum_{s=2}^{S} c_{i_1 i_s} \right) \prod_{s=2}^{S} \gamma_{i_1 i_s} \tag{9.4}$$

By rearranging the terms the objective function simplifies to

$$\sum_{i_1=0}^{n_1}\left(\sum_{i_2=0}^{n_2} c_{i_1 i_2}\gamma_{i_1 i_2}\cdots\sum_{i_S=0}^{n_S} c_{i_1 i_S}\gamma_{i_1 i_S}\right) \tag{9.5}$$

Or, the above is equivalent to

$$\sum_{i_1=0}^{n_1}\sum_{i_2=0}^{n_2} c_{i_1 i_2}\gamma_{i_1 i_2}+\ldots+\sum_{i_1=0}^{n_1}\sum_{i_S=0}^{n_S} c_{i_1 i_S}\gamma_{i_1 i_S} \tag{9.6}$$

This means that the when the cost decomposes the objective function of the S-D association also decomposes.

Consider the first set of constraints of the S-D assignment. With the binary indicator variable redefined we can rewrite this constraint as

$$\sum_{i_2=0}^{n_2}\sum_{i_3=0}^{n_3}\cdots\sum_{i_S=0}^{n_S}\prod_{s=2}^{S}\gamma_{i_1 i_s}=1 \qquad i_1=1,2,\ldots,n_1 \tag{9.7}$$

This is equivalent to

$$\left(\sum_{i_2=0}^{n_2}\gamma_{i_1 i_2}\right)\left(\sum_{i_3=0}^{n_3}\gamma_{i_1 i_3}\right)\cdots\left(\sum_{i_S=0}^{n_S}\gamma_{i_1 i_S}\right)=1 \qquad i_1=1,2,\ldots,n_1 \tag{9.8}$$

Since γ is a binary variable that can only assume zero or one, the above equality can happen if and only if the individual sums are equal to one. That is

$$\sum_{i_2=0}^{n_2}\gamma_{i_1 i_2}=1 \quad \sum_{i_3=0}^{n_3}\gamma_{i_1 i_3}=1 \quad \cdots \quad \sum_{i_S=0}^{n_S}\gamma_{i_1 i_S}=1 \qquad i_1=1,2,\ldots,n_1 \tag{9.9}$$

By considering the other constrains of the S-D assignment it is easy to show that

an equivalent set of constraints to (3.9) is

$$\begin{aligned} \sum_{i_1=0}^{n_1} \gamma_{i_1 i_s} &= 1 \quad i_s = 1, 2, \ldots, n_s \\ \sum_{i_s=0}^{n_s} \gamma_{i_1 i_s} &= 1 \quad i_1 = 1, 2, \ldots, n_1 \end{aligned} \tag{9.10}$$

where $s = 2, \ldots, S$.

Therefore, with the objective function decomposing as in (9.6) and the constraints defined in terms of the new binary variable γ it is easy to see that the solution of the S-D is equivalent to the solution of the following $(S-1)$ separate 2-D assignments.

$$\begin{aligned} \min_{\gamma_{i_1 i_s}} \quad & \sum_{i_1=0}^{n_1} \sum_{i_s=0}^{n_s} c_{i_1 i_s} \\ \text{subject to} \quad & \sum_{i_1=0}^{n_1} \gamma_{i_1 i_s} = 1 \quad i_s = 1, 2, \ldots, n_s \\ & \sum_{i_s=0}^{n_s} \gamma_{i_1 i_s} = 1 \quad i_1 = 1, 2, \ldots, n_1 \end{aligned} \tag{9.11}$$

where again $s = 2, \ldots, S$.

Bibliography

[1] M. S. Arulampalam, S. Maskell, N. Gordon, and T. Clapp, "A Tutorial on Particle Filters for Online Nonlinear/Non-Gaussian Bayesian Tracking", *IEEE Transactions on Signal Processing*, Vol. 50, No. 2, pp. 174-188, Feb. 2002.

[2] Y. Bar-Shalom and E. Tse, "Tracking in a Cluttered Environment with Probabilistic Data Association", *Automatica*, Vol. II, pp. 451–460, Sep. 1975.

[3] Y. Bar-Shalom and T. E. Fortmann, *Tracking and Data Association*, Academic Press, Orlando, FL, 1988.

[4] Y. Bar-Shalom, K. C. Chang, and H. A. P. Blom, "Automatic Track Formation in Clutter with a Recursive Algorithm", *Proceedings of the 28th IEEE Conference on Decision and Control*, Vol. 2, pp. 1402–1408, Tampa, FL, Dec. 1989.

[5] Y. Bar-Shalom and X. R. Li, *Multitarget-Multisensor Tracking: Principles and Techniques*, YBS Publishing, Storrs, CT, 1995.

[6] Y. Bar-Shalom, X. R. Li, and T. Kirubarajan, *Estimation with Applications to Tracking and Navigation*, John Wiley & Sons, New York, NY, 2001.

[7] A. Beck and Y. C. Eldar, "Strong Duality in Nonconvex Quadratic ptimization with Two Quadratic Constraints", *SIAM Jorunal on Optimization*, Vol. 17, Issue 3, pp. 844-860, Sep. 2006.

[8] K. Becker, "An Efficient Method for Passive Emitter Location", *IEEE Transactions on Aerospace and Electronic Systems*, Vol. 28, pp. 1091-1104, Oct. 1992.

[9] D. P. Bertsekas, "The Auction Algorithm: A Distributed Relaxation Method for the Assignment Problem", *Annals of Operations Research: Special Issue on Parallel Optimization*, Vol. 14, pp. 105–123, 1988.

[10] D. P. Bertsekas, *Nonlinear Programming*, Athena Scientific, Nashua, NH, 2004.

[11] S. Blackman, *Multiple Target Tracking with Radar Applications*, Artech House, Norwood, MA, 1986.

[12] S. Blackman and R. Papoli, *Design and Analysis of Modern Tracking Systems*, Artech House, Boston, MA, 1999.

[13] W. Blair, G.A.Watson, T. Kriubarajan, and Y. Bar-Shalom, "Benchmark for Radar Resource Allocation and Tracking in the Presence of ECM", *IEEE Transactions on Aerospace and Electronic Systems*, Vol. 34, pp. 1015-1022, Oct. 1998.

[14] E. A. Bloem and H. A. P. Blom, "Joint Probabilistic Data Association Methods Avoding Track Coalescence", *Proceedings of the 34th IEEE Conference on Decision and Control*, New Orleans, LA, pp. 2752-2757, Dec. 1995.

[15] H. A. P. Blom, and Y. Bar-Shalom, "The Interacting Multiple Model Algorithm for Sytems with Markovian Switching Coefficients", *IEEE Transactions on Automatic Control*, Vol. 33, pp. 780-783, Aug. 1988.

[16] S. Boyd and L. Vandenberghe, *Convex Optimization*, Cambridge University Press, Cambridge, UK, 2004.

[17] Y. T. Chan and K. C. Ho, "A Simple and Efficient Estimator for Hyperbolic Location", *IEEE Transactions on Signal Processing*, Vol. 42, pp. 1905–1915, Aug. 1994.

[18] K. C. Chang, R. K. Saha, and Y. Bar-Shalom, "On Optimal Track-to-Track Fusion", *IEEE Transactions on Aerospace and Electronic Systems*, Vol. 33, No. 4, pp. 1271–1276, Oct. 1997.

[19] M. R. Chummun, T. Kirubarajan, K. R. Pattipati, and Y. Bar-Shalom, "Fast Data Association using Multidimensional Assignment with Clustering", *IEEE Transactions on Aerospace and Electronic Systems*, Vol. 37, pp. 898–913, Jul. 2001.

[20] I. Cox and M. Miller, "On Finding the Ranked Assignments with Application to Multitarget Tracking and Motion Correspondence", *IEEE Transactions on Aerospace and Electronic Systems*, Vol. 32, No. 1, pp. 486–489, Jan. 1995.

[21] I. Cox and M. Miller, R. Danchick, and G, Newnam "A Comparison of Two Algorithms for Determining Ranked Assignments with Applicaiton to Multitarget Tracking and Motion Correspondence", *IEEE Transactions*

on Aerospace and Electronic Systems, Vol. 33, No. 1, pp. 295–300, Jan. 1997.

[22] C. R. Drane and C. Rizos, *Positioning Systems in Intelligent Transportation Systems*, Artech House, Norwood, MA, 1998.

[23] R. Danchick and G. Newnam, "A Fast Method for Finding the Exact N-Best Hypotheses for Multitarget Tracking", *IEEE Transactions on Aerospace and Electronic Systems*, Vol. 29, pp. 555–560, Apr. 1993.

[24] S. Deb, K. R. Pattipati, and Y. Bar-Shalom, "A Multisensor-Multitarget Data Association Algorithm for Heterogeneous Sensors", *IEEE Transactions on Aerospace and Electronic Systems*, Vol. 20 No. 2, pp. 560–568, Apr. 1993.

[25] S. Deb, K. R. Pattipati, Y. Bar-Shalom, and M. Yeddanapudi, "A Generalized S-Dimensional Algorithm for Multisensor Multitarget State-Estimation", *Proceeding of the 33rd IEEE Conference Decision and Control*, Vol. 4, pp. 3293–3298, Lake Buena Vista, FL, Dec. 1994.

[26] S. Deb, M. Yeddanapudi, K. R. Pattipati, and Y. Bar-Shalom, "A Generalized S-D Assignment Algorithm for Multisensor-Multitarget State Estimation", *IEEE Transactions on Aerospace and Electronic Systems*, Vol. 33, pp. 523–538, Apr. 1997.

[27] O. E. Drummond and S. S. Blackman, "Challenges of Developing Algorithms for Multiple Sensor, Multiple Target Tracking", *Proceedigs of the SPIE Conf. on Signal and Data Processing of Small Targets*, Vol. 1096, pp. 244–255, Apr. 1989.

[28] O. E. Drummond, "Multiple Target Tracking with Multiple Frame, Probabilistic Data Association", *Proceedings of the SPIE Conference on Signal and Data Processing of Small Targets*, Vol. 1954, pp. 394–408, 1993.

[29] O. E. Drummond, "Multiple Target Tracking with Multiple Frame, Probabilistic Data Association", *Proceedings of the SPIE Conference on Signal and Data Processing of Small Targets*, Vol. 2561, pp. 322–336, 1995.

[30] F. Farina and S. Pardini, "Survey of Radar Data-Processing Techniques in Air-Traffic Control and Surveillance Systems", *Proceedings of IEE*, Vol. 127, Part F, No. 3, pp. 190–204. Jun. 1980.

[31] A. Farina and F. Student, *Radar Data Processing*, Vols. I and II, J. Wiley & Sons and Research Studies Press, Letchworth, Hertfordshire, England, 1985.

[32] R. J. Fitzgerald, "Track Biases and Coalescence with Probabilistic Data Association", *IEEE Tran. Aerospance and Electronic Systems*, Vol. AES-21, No. 6, pp. 822–825, Nov. 1985.

[33] R. J. Fitzgerald, "Development of Practical PDA Logic for Multitarget Tracking by Microprocessor", *Proceedings of the American Control Conference*, Vol. 2, pp. 889–898, 1986.

[34] R. J. Fitzgerald, "Development of Practical PDA Logic for Multitarget Tracking by Microprocessor", *Multisensor-Multitarget Tracking: Advanced Applications*, (Y. Bar-Shalom, ed.), Artech House, Boston, MA, 1990.

[35] T. Fortmann, Y. Bar-Shalom, and M. Scheffe, "Sonar Tracking of Multiple Targets Using Joint Probabilistic Data Association", *IEEE Journal of Oceanic Engineering*, Vol. OE-8, pp. 173–184. Jul. 1983.

[36] W. H. Foy, "Position Location Solution by Taylor Series Estimation", *IEEE Transactions on Aerospace and Electronic Systems*, Vol. 12, pp. 183–198, Mar. 1976.

[37] A. B. Gershman, "Robust Adaptive Beamforming in Sensor Arrays", *International Journal on Electronics Communication*, Vol. 53, No. 6, pp. 305–314, Dec. 1999.

[38] G. Gilbert, "Historical Development of the Air Traffic Control System", *IEEE Transactions on Communications*, Vol. 21, Issue 5, pp. 364–375, May 1973.

[39] N. J. Gordon, D. J. Salmond, A. F. M. Smith, "Novel Approach to Nonlinear/Non-Gaussian Bayesian State Estimation", *IEE Proceedings F - Radar and Signal Processing*, Vol. 140, Issue 2, pp. 107–113, Apr. 1993.

[40] K. C. Ho and Y. T. Chan, "Geolocation of a Known Altitude Object from TDOA and FDOA Measurements", *IEEE Transactions on Signal Processing*, Vol. 33, pp. 770–783, Jul. 1997.

[41] Y. Huang, J. Benesty, G. W. Elko, and R. M. Mersereau, "An Efficient Linear-Correlation Least-Squares Approach to Source Localization", *IEEE Workshop on the Applications of Signal Processing to Audio and Acoustics*, pp. 67–70, Oct. 2001.

[42] R. Jonker and A. Volgenant, "A Shortest Augmenting Path Algorithm for Dense and Sparse Linear Assignment Problems", *Journal of Computing*, Vol. 38, pp. 325–340, 1987.

[43] S. J. Julier and J. K. Uhlmann, "A New Extension of the Kalman Filter to Nonlinear Systems", *Proceedingds of the SPIE Conference Signal Processing, Sensor Fusion, and Target Recognition*, Vol. 3068, pp. 182-193, Orlando, FL, USA, Apr. 1997.

[44] S. J. Julier and J. K. Uhlmann, "Unscented Filtering and Nonlinear Estimation", *Proceedings of the IEEE*, Vol. 92, pp. 401422, Mar. 2004.

[45] I. Kadar, E. Eadan, R. R. Gassner, "Comparison of Robustized Assignment Algorithms", *Proceedings of the SPIE Conference on Signal Processing, Sensor Fusion, and Target Recognition VI*, Vol. 3068, pp. 240–249, Apr. 1997.

[46] R. E. Kalman, "A New Approach to Linear Filtering and Prediction Problem", *Transactions on ASME, Ser. D, J. Basic Eng.*, Vol. 82, pp. 34–45, 1960.

[47] R. E. Kalman and R. S. Bucy, "New Results in Linear Filtering and Prediction Theory", *Transactions on ASME, Ser. D, J. Basic Eng.*, Vol. 83, pp. 95–107, 1961.

[48] V. Katkovnik and A. B. Gershman, "A Local Polynomial Approximation Based Beamforming for Source Localization and Tracking in Nonstationary Environments", *IEEE Signal Processing Letters*, Vol. 7, No. 1, pp. 3–5, Jan. 2000.

[49] A. J. Kanyuck and R. A. Singer, "Correlation of Multiple-Site Track Data", *IEEE Transactions on Aerospace and Electronic Systems*, Vol. AES-6, No. 2, pp. 180–187, Mar. 1970.

[50] T. Kirubarajan and Y. Bar-Shalom, "Kalman Filter vs. IMM Estimator: When do We Need the Latter?", *IEEE Transactions on Aerospace and Electronic Systems*, Vol. 39, Issue 4, pp. 1452–1457, Oct. 2003.

[51] C. H. Knapp and G. C. Carter, "The Generalized Correlation Method for Estimation of Time Delay", *IEEE Transactions on Acoustics, Speech and Signal Processing*, Vol. 24, pp. 320–327, Aug. 1976.

[52] H. Krim and M. Viberg, "Two Decades of Array Signal Processing Research: the Parametric Approach", *IEEE Signal Processing Magazine*, Vol. 13, Issue 4, Jul. 1996.

[53] H. W. Kuhn, "The Hugarian Method for the Assignment Problem", *Naval Research Logistics Quarterly*, No. 2, pp. 83–97, 1955.

[54] J. R. Larocque, J. P. Reilly, and W. Ng, "Particle Filters for Tracking an Unknown Number of Sources", *IEEE Transactions on Signal Processing*, Vol. 50, No. 12, pp. 2926–2937, Dec. 2002.

[55] D. G. Manolakis, V. K. Ingle, and S. M. Kogon, *Statistical and Adaptive Signal Processing*, McGraw-Hill, New York, NY, 2000.

[56] B. McQueen and J. McQueen, *Intelligent Transportation Systems Architectures*, Artech House, Norwood, MA, 1999.

[57] C. L. Morefield, "Application of 0-1 Integer Programming to Multitarget Tracking Problems", *IEEE Transactions onAutomatic Control*, Vol. AC-22, No.3, pp. 302–312, Jun. 1977.

[58] J. Munkers, "Algorithms for the Assignment and Tranportation Problems", *Journal of SIAM*, Vol. 5, pp. 32–38, 1957.

[59] K. Murty, "An Algorithm for Ranking All the Assignment in Order of Increasing Cost", *Operations Research*, Vol. 16, No. 3, pp. 682–687, Jun. 1968.

[60] D. Musicki and R. Evans, "Integrated Probabilistic Data Association in Clutter with Finite Resolution Sensor", *Proceedings of the 32nd IEEE Conference on Decision and Control*, San Antonio, TX, vol. 1, pp. 912–917, Dec. 1993.

[61] D. Musicki, R. Evans, and S. Stankovic, "Integrated Probabilistic Data Association", *IEEE Transactions on Automatic Control*, Vol. 39, No. 6, pp. 1237–1241, Jun. 1994.

[62] D. Musicki and R. Evans, "Joint Integrated Probabilistic Data Association - JIPDA", *Proceedings of the 5th Conference on Information Fusion*, Parkville, Victoria, Australia, vol. 2, pp. 8–11, Jul. 2002.

[63] L. C. Ng and Y. Bar-Shalom, "Multisensor Multitarget Time Delay Vector Estimation", *IEEE Transactions on Acoustic, Speech, and Signal Processing*, Vol. 4, pp. 669–678, Aug. 1986.

[64] W. Ng, J. P. Reilly, T. Kirubarajan, and W. R. Larocque, "Wideband Array Signal Processing Using MCMC Methods", *IEEE Transactions on Signal Processing*, Vol. 50, No. 2, pp. 411–426, Feb. 2005.

[65] A. V. Oppenheim, R. W. Schafer, and J. R. Buck, *Discrete-Time Signal Processing*, Prentice Hall, 1999.

[66] K. R. Pattipati, S. Deb, Y. Bar-Shalom, and R. Washburn, "A New Relaxation Algorithm and Passive Sensor Data Association", *IEEE Transactions on Automatic Control*, Vol. 37, pp. 197–213, Feb. 1992.

[67] K. R. Pattipati, R. L. Popp, and T. Kirubarajan, "Survey of assignment techniques for multitarget tracking", *Multisensor-Multitarget Tracking: Applications and Advances*, Vol. 3, (Y. Bar-Shalom and W. D. Blair, eds.), Artech House, Boston, MA, USA, 2000.

[68] T. S. Perry, "In Search of the Future of Air Traffic Control", *IEEE Spectrum*, Vol. 34, Issue 8, pp. 18–35, Aug. 1997.

[69] M. Pesavento and A. B. Gershman, "Maximum-Likelihood Direction-of-Arrival Estimation in the Presence of Unknown Nonuniform Noise", *IEEE Transactions on Signal Processing*, Vol. 49, No. 7, pp. 1310–1324, 2001.

[70] W. P. Pierskall, "The Multidimensional Assignment Problem", *Operations Research*, Vol. 16, pp. 422–431, 1968.

[71] A. B. Poore and N. Rijavec, "A Lagrangian Relaxation Algorithm for Multidimensional Assignment Problems Arising from Multitarget Tracking", *SIAM J. Optimization*, Vol. 3, pp. 544–563, Aug. 1993.

[72] A. B. Poore, N. Rijavec, T. Barker, and M. Munger, "Data Association Problem Posed As Multidimensional Assignment Problems: Algorithm Development", *Proceedings of the SPIE Conference on Signal Processing, Sensor Fusion, and Target Recognition*, Vol. 1955, pp. 175–183, 1993.

[73] A. B. Poore, N. Rijavec, M. Liggins, and V. C. Vannicola, "Data Association Problems Posed as Multidimensional Assignment Problems: Problem Formulation", *Proceedings of the SPIE Conference on Signal and Data Processing of Small Targets*, Vol. 1954, pp. 552-563, Oct. 1993.

[74] A. B. Poore, N. Rijavec, T. N. Barker, and M. Munger, "Data Association Problems Posed as Multidimensional Assignment Problems: Numerical Simulations", *Proceedings of the SPIE Conference on Signal and Data Processing of Small Targets*, Vol. 1954, pp. 564-573, Oct. 1993.

[75] A. B. Poore, N. Rijavec, T. N. Barker, and M. Munger, "New Multidimensional Data Association Algorithm for Multisensor-Multitarget Tracking", *Proceedigs of the SPIE Conference on Signal and Data Processing of Small Targets*, Vol. 2561, pp. 448-459, Sep. 1995.

[76] R. L. Popp, K. R. Pattipati, Y. Bar-Shalom, and R. R. Gassner, "An Adaptive M-Best S-D Assignment Algorithm and Parallelization for Multitarget Tracking", *Proceedings of the IEEE Aerospace Conference*, Vol. 5, pp. 71–84, Snowmass at Aspen, Colorado, 1998.

[77] R. L. Popp, K. R. Pattipati, Y. Bar-Shalom, "Dynamically Adaptable M-Best 2-D Assignment Algorithm and Multi-Level Parallelization", *IEEE Transactions onAerospace and Electronic Systems*, Vol. 35, pp. , Jan. 1999.

[78] W. H. Press, S. A. Teukolsky, W. T. Vetterling, and B. P. Flannery, *Numerical Recipes in C*, Cambridge University Press, New York, NY, 1992.

[79] T. S. Rappaport, J. H. Reed, and B. D. Woerner, "Position Location Using Wireless Communications on Highways of the Future", *IEEE Communications Magazine*, pp. 33–41, Oct. 1996.

[80] J. H. Reed, K. J. Krizman, B. D. Woerner, and T. S. Rappaport, "An Overview of the Challenges and Progress in Meeting the E-911 Requirement for Location Service", *IEEE Communications Magazine*, pp. 30–37, Apr. 1998.

[81] D. Reid, "An Algorithm for Tracking Multiple Targets", *IEEE Transactions on Automatic Control*, Vol. 6, pp. 423–432, Dec. 1979.

[82] B. Ristic, S. Arulampalam, and N. Gordon, *Beyond the Kalman Filter: Particle Filters for Tracking Applications*, Artech House, Boston, MA, 2004.

[83] J. A. Roecker, "Multiple Scan Joint Probabilistic Data Association", *IEEE Transactions onAerospace and Electronic Systems*, Vol. AES-31, No. 3, pp. 1204–1210, Jul. 1995.

[84] R. L. Rothrock and O. E. Drummond, "Performance Metrics for Multiple-Sensor, Multiple-Target Tracking", *Proceedings of the SPIE Conference on Signal and Data Processing of Small Targets*, Vol. 4048, pp. 521–531, Jul. 2000.

[85] R. Schmidt, "Multiple Emitter Location and Signal Parameter Estimation", *IEEE Transactions on Antennas and Propagation*, Vol. 34, No. 3, pp. 276–280, Mar. 1986.

[86] R. O. Schmidt, "Least Squares Range Difference Location", *IEEE Transactions onAerospace and Electronic Systems*, Vol. 32, pp. 234–242, Jan. 1996.

[87] "SeDuMi", *http://sedumi.mcmaster.ca*.

[88] R. Singer, R. Sea, K. Housewright, "Derivation and Evaluation of Improved Tracking Filter for Use in Dense Multitarget Environments", *IEEE Transactions on Information Theory*, Vol. 20, pp. 423–432, Jul. 1974.

[89] R. W. Sittler, "An Optimal Data Association Problem in Surveillance Theory", *IEEE Transactions onMil. Electron.*, Vol. 8, pp. 125–139, Apr. 1964.

[90] M. I. Skolnik, *Introduction to Radar Systems*, McGraw-Hill, New York, NY, 2002.

[91] J. O. Smith and J. S. Abel, "Closed Form Least Squares Source Location Estimation from Range Difference Measurements", *IEEE Transactions onAcoustics, Speech and Signal Processing*, Vol. 35, pp. 1661–1669, Dec. 1987.

[92] D. J. Torrieri, "Statistical Theory of Passive Location Systems", *IEEE Transactions onAerospace and Electronic Systems*, Vol. 26, pp. 183–198, Mar. 1984.

[93] H. L. Van Trees, *Detection, Estimation, and Modulation Theory, Part I*, John Wiley & Sons, 2001.

[94] A. D. Waite, *Sonar for Practising Engineers*, John Wiley & Sons, West Sussex, England, 2002.

[95] E. A. Wan and R. van der Merwe, "The Unscented Kalman Filter", in *Kalman Filtering and Neural Networks*, (S. Haykin, ed.), pp. 1210–1217, Wiley & Sons, New York, NY, USA, Oct. 2001.

[96] H. Wang, T. Kirubarajan, and Y. Bar-Shalom, "Precision Large Scale Air Traffic Surveillance Using IMM/Assignment Estimators", *IEEE Transactions Aerospace and Electronic Systems*, Vol. 35, pp. 255–266, Jan. 1999.

[97] M. Wax and T. Kailath, "Optimum Localization of Multiple Sources by Passive Arrays", *IEEE Transactions on Acoustics, Speech and Signal Processing*, Vol. 31, pp. 1210–1217, Oct. 1983.

[98] R. G. Wiley, *Electronic Intelligence: The Analysis of Radar Signals*, 2nd Ed., Artech House, Norwood, MA, 1993.

[99] H. Wolkowicz, L. Vandenberghe, and R. Saigal (editors), *Handbook of Semidefinite Programming — Theory, Algorithms, and Applications*, Springer, Berlin, Germany, 2005.

[100] M. Yeddanapudi, Y. Bar-Shalom, and K. R. Pattipati, "IMM Estimation for Multitarget Multisensor Air Traffic Surveillance", *Proceeding of IEEE*, Vol. 85, No. 1, pp. 80–94, Jan. 1997.

[101] F. Zhang, "The Schur Complement and its Applications", Springer, New York, NY, 2005.

[102] B. Zhou and N. K. Bose, "An Efficient Algorithm for Data Association in Multitarget Tracking", *IEEE Transactions on Aerospace and Electronic Systems*, vol. 31, no. 1, pp. 458–468, Jan. 1995.